"SOLAR PLASMA I:
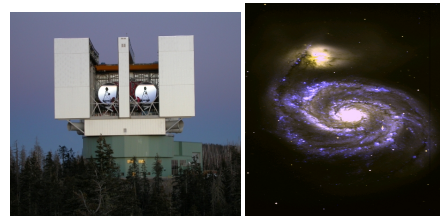# PLASMA, ATOMIC STRUCTURE, SPECTROSCOPY"

SULTANA N. NAHAR

Astronomy, Ohio State University, Columbus, Ohio, USA
Email: nahar.1@osu.edu

ISYA
INTERNATIONAL SCHOOL
FOR YOUNG ASTRONOMERS

International School for Young Astronomers 2018

Lecture Course: Mar 25 - April 11, 2018

Venue: NRIAG, Helwan, Egypt

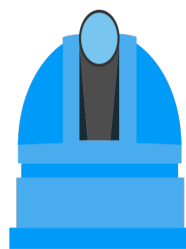## Topics for "The Sun and Atomic Physics"

- Prof. Sultana N. Nahar,

Astronomy Dept, The Ohio State University, USA

• Textbook: "Atomic Astrophysics and Spectroscopy"

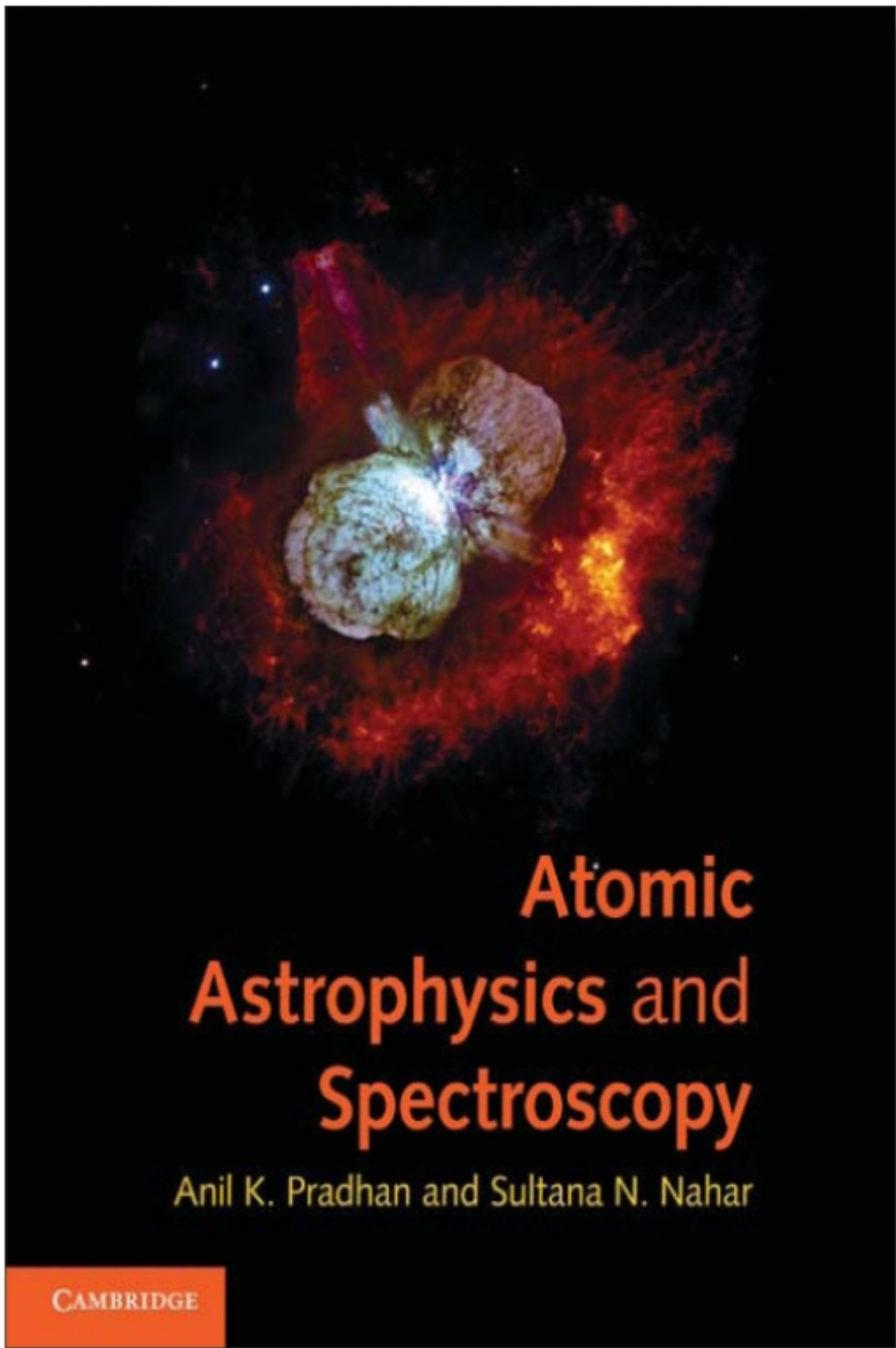(A.K. Pradhan and S.N. Nahar, Cambridge U Press, 2011)

SYLLABUS

Lecture 1:

i) Radiation, the medium to study Astronomical objects

ii) Atomic Structure, Spectrum, Plasma Opacity

iii) Radiative and Collisional Processes in Astrophysical Plasmas

Lecture 2:

i) The Sun and x-ray diagnostics

ii) The Solar System

iii) Exoplanets

Lecture 3:

i) Solar Abundances, the Z-bump

ii) Problem with the boundary of radiative and convection zones

iii) X-ray opacity and solar abundances

Atomic Astrophysics and Spectroscopy

Anil K. Pradhan and Sultana N. Nahar

CAMBRIDGE

Table of Contents

Invite to APS membership:

AMERICAN PHYSICAL SOCIETY

Membership (free for 4 - 6 years) info:

Contact for details: Sultana Nahar

Email: nahar.1@osu.edu Web:

http://www.astronomy.ohio-state.edu/ ~nahar/fip.html

• Fill out simple form and email with your resume

After becoming member (will recieve ID from APS),

- become a member of your division & of APS unit FIP:

Forum of International Physics

- Submit abstracts for APS conferences

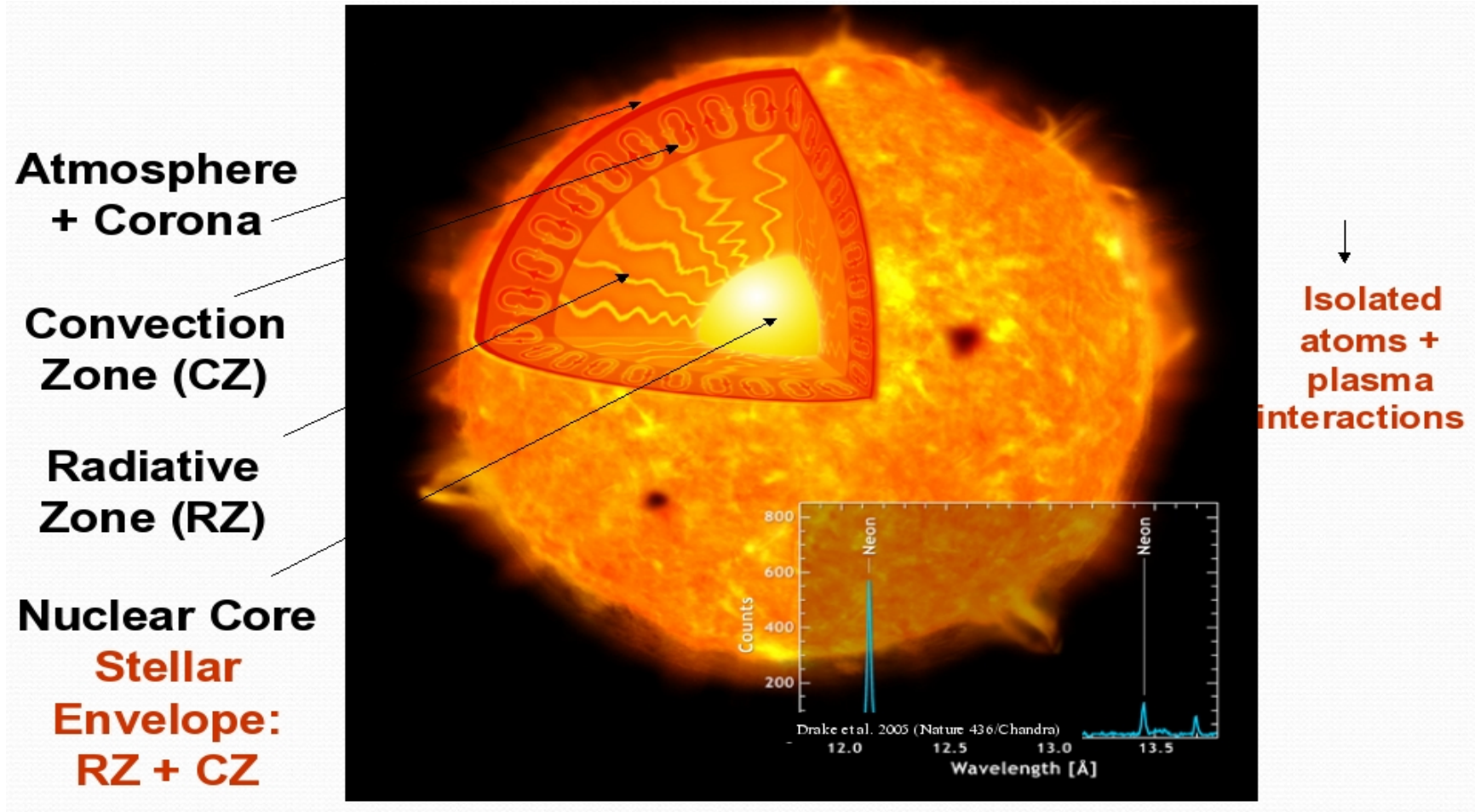- Apply for travel grant

- Check many other activities and benefits, such as,

free isses of Physics today, newsletters, calendar, research

alerts, application notices for various recognition

- Post your resume

- Sign up for job alerts and apply online

THE SUN

Atmosphere + Corona

Convection Zone (CZ)

Radiative Zone (RZ)

Nuclear Core

Stellar Envelope: RZ + CZ

Isolated atoms + plasma interactions

Drake et al. 2005 (Nature 436/Chandra)
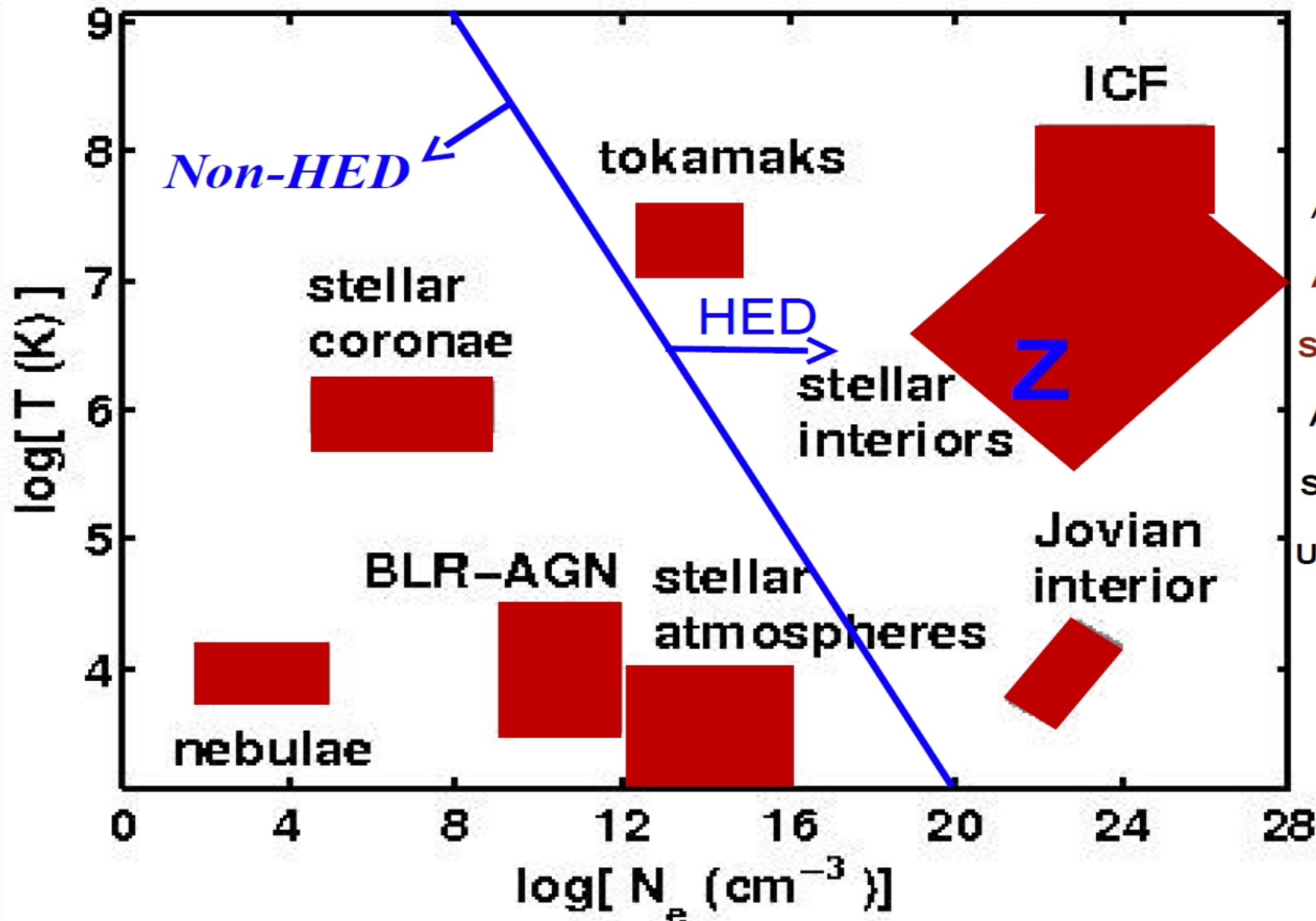
- Core: 100g/cc - more dense than any solid, superhot 15 MK plasma: Nuclear fusion → Gamma rays
- Radiation, as it travels outward, is repeatedly absorbed & emitted by atoms and molecules, and looses energy to become visible photons - measures opacity
- Takes over a million years for radiation created in the core to travel to surface: Reason - OPACITY
- Region of study: Convection zone

PLASMA COVERS 99% OF REGION IN T-ρ PHASE SPACE

Temperature-Density In HED Environments

- BLR-AGN (broad-line regions in active galactic nuclei), where many spectral features are associated with the central massive black hole
- Laboratory plasmas - tokamaks (magnetic confinement fusion devices), Z-pinch machines (inertial confinement fusion (ICF) devices)

Hydrogen phase diagram
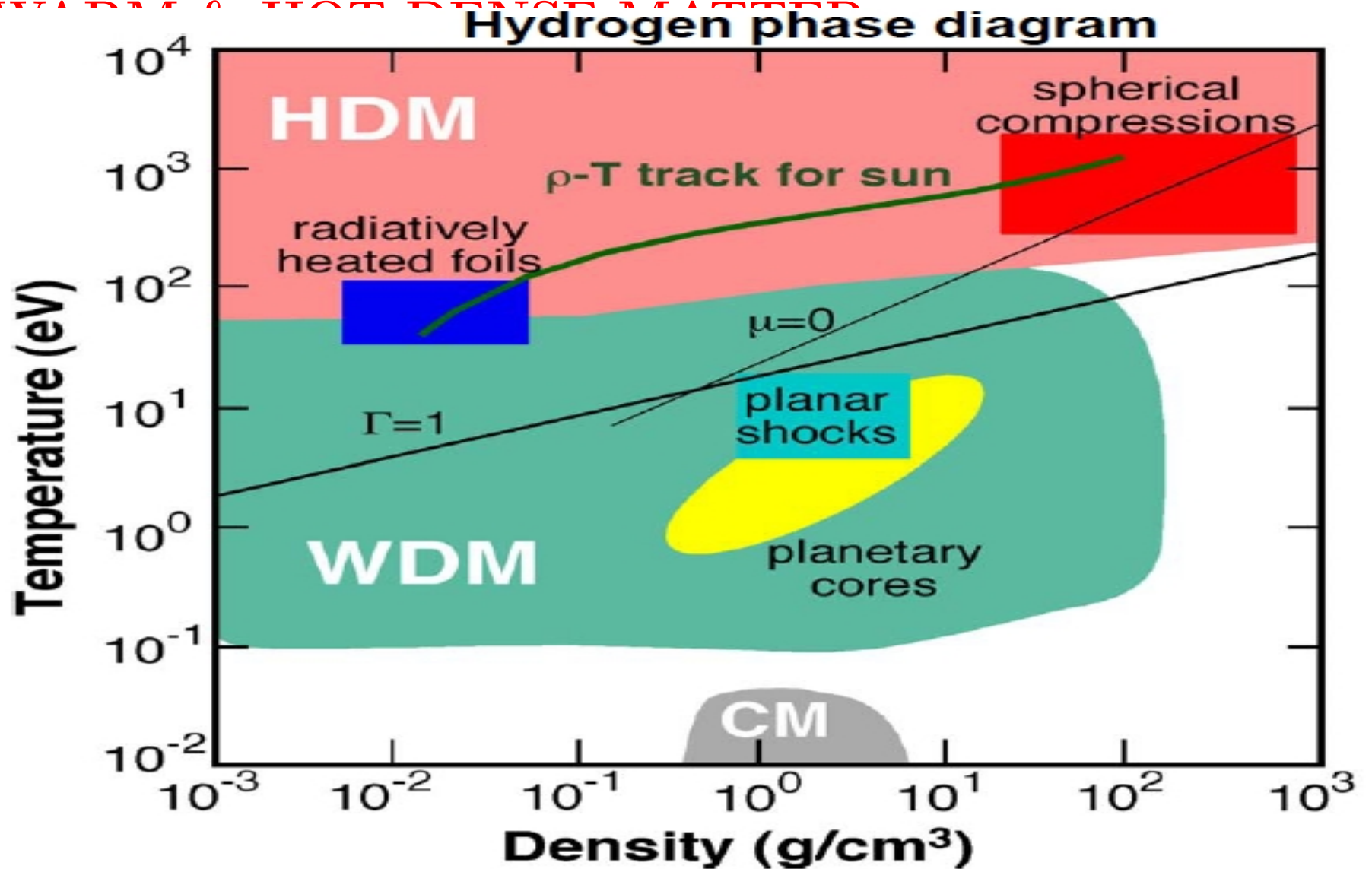
- **Hot Dense Matter (HDM):** - Sun's ρ-T track, Supernovae, Stellar Interiors, Accretion Disks, Blackhole environments - Lab plasmas in fusion devices: inertial confinement - laser produced (NIF) & Z pinches (e.g. Sandia), magnetic confinement (tokamaks)
- **Warm Dense Matter (WDM):** - cores of large gaseous planets

UNIVERSE through RADIATION: Most Complete 3D Map
(Created by 2MASS maping over 3 decades)
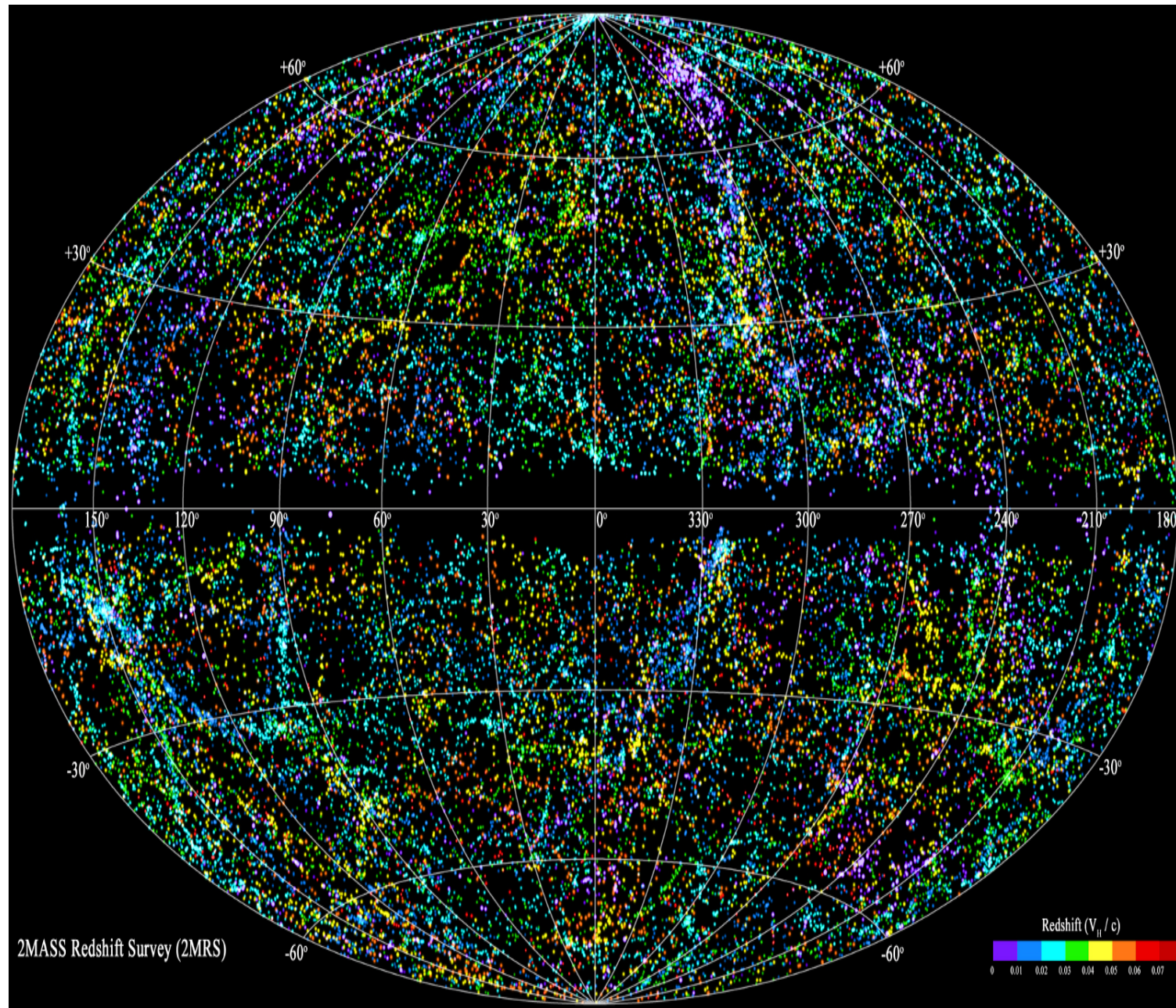
- The 2-Micron All-Sky Survey includes 43,000 galaxies within 380 million Ly
- Missing black band in the middle because of invisibility behind the Milky Way

The MILKY WAY, Our Galaxy

- Has 200-400 billion stars

Astronomical Objects: Anything beyond our earth

- How do we study them? - Analyzing the light coming from them
- Light is emitted by excited or "HOT" atoms, molecules in them

THE 1ST OBSERVATORY, SAMARKAND, 1420, BY MUS-LIM RULER ULUGH BEG

- Ulugh Beg built the madrasa in 1420 in Samarkand and extended it to an observatory
- Beg himself recorded of many astronomical objects.

EX: GROUND AND SPACE BASED TELESCOPES, LABS

Large Binocular Telescope in Arizona

L: Hubble space telescope, R: International Space station of NASA

ATMOSPHERIC OPACITY & TELESCOPES
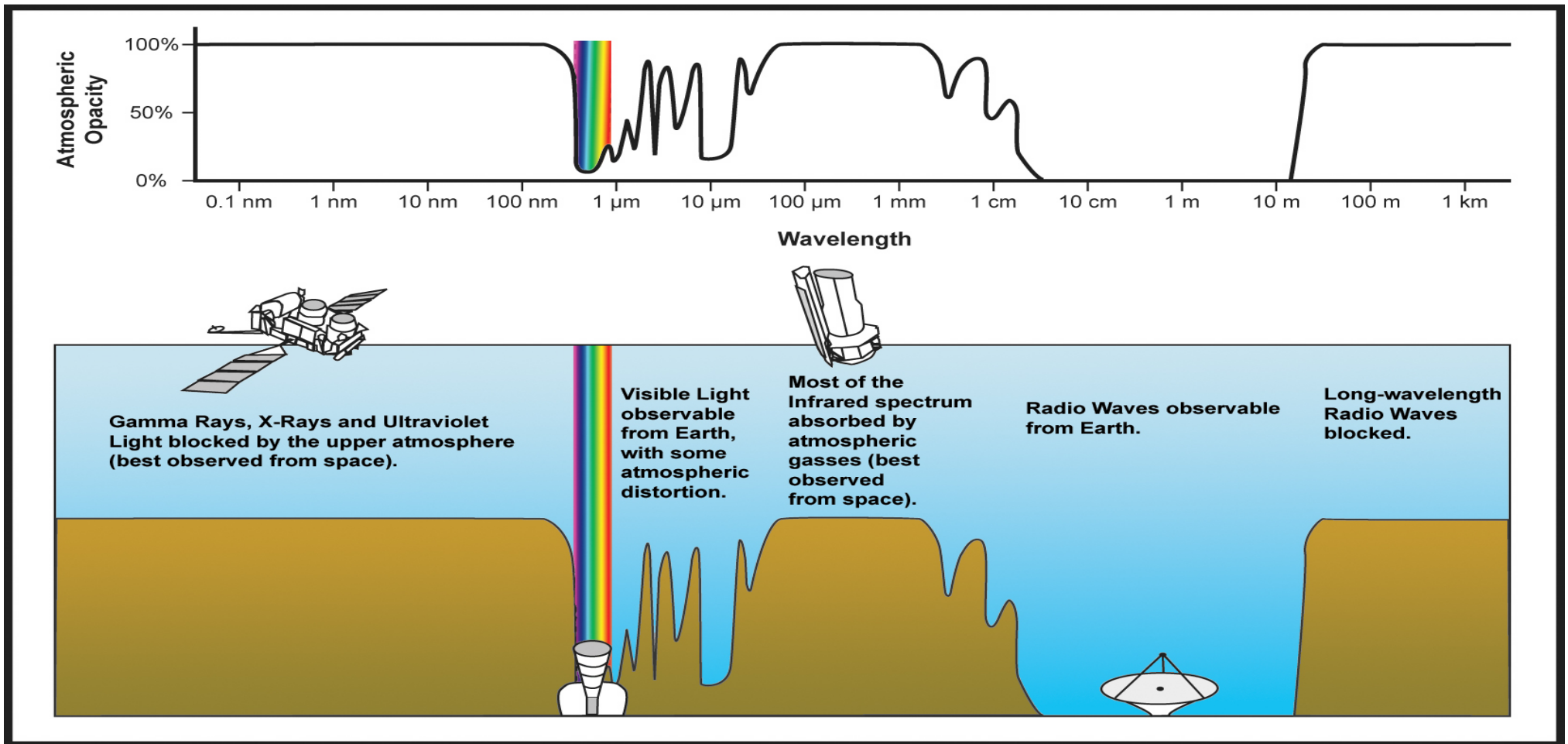
- Higher opacity -less radiation, lower opacity - more radiation reaching earths surface
- Opacity determines types of telescopes - earth based or space based
- Gamma, X-ray, UV are blocked while visible light passes through
- CO_2, H_2O vapor, other gases absorb most of the infrared frequencies
- Part of radio frequencies is absorbed by H_2O and O_2, and part passes through

STUDYING ASTRONOMICAL OBJECTS

ASTRONOMICAL objects are studied in three ways:

- **Imaging:**
- Beautiful pictures of astronomical objects, Stars, Nebulae, Active Galactic Nuclei, Blackhole Environments, etc
$\rightarrow$ Provides information of size and location of the objects

- **Photometry:**
- Low resolution spectroscopy - Bands of Electromagnetic Waves - Colors ranging from X-ray to Radio waves
$\rightarrow$ macroscopic information

- **Spectroscopy:**
- Taken by spectrometer - Provides most of the detailed knowledge: temperature, density, abundances, chemical composition, etc. of astronomical objects

Spectroscopy is underpinned by Atomic & Molecular Physics

ETA CARINAE: Photometric image
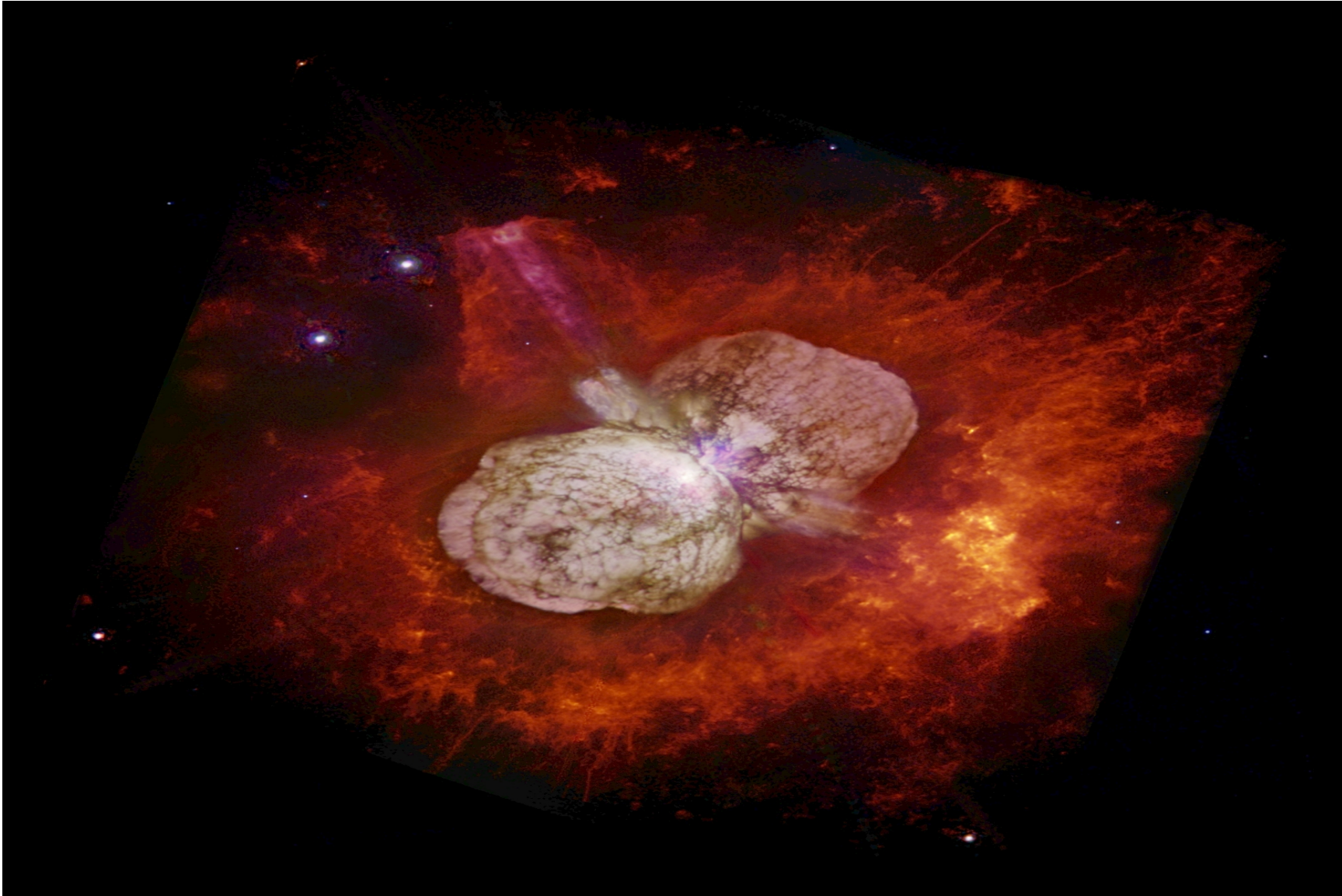
- Consists of 2 massive bright (5M times the sun) stars, heavier one went under a near supernova explosion
- Explosion produced two polar lobes, and a large but thin equatorial disk, all moving outward at 670 km/s. Mass indicates future eruptions
- HST image shows the bipolar Homunculus Nebula surrounds it

SUPERNOVA REMNANT CASSIOPIA A
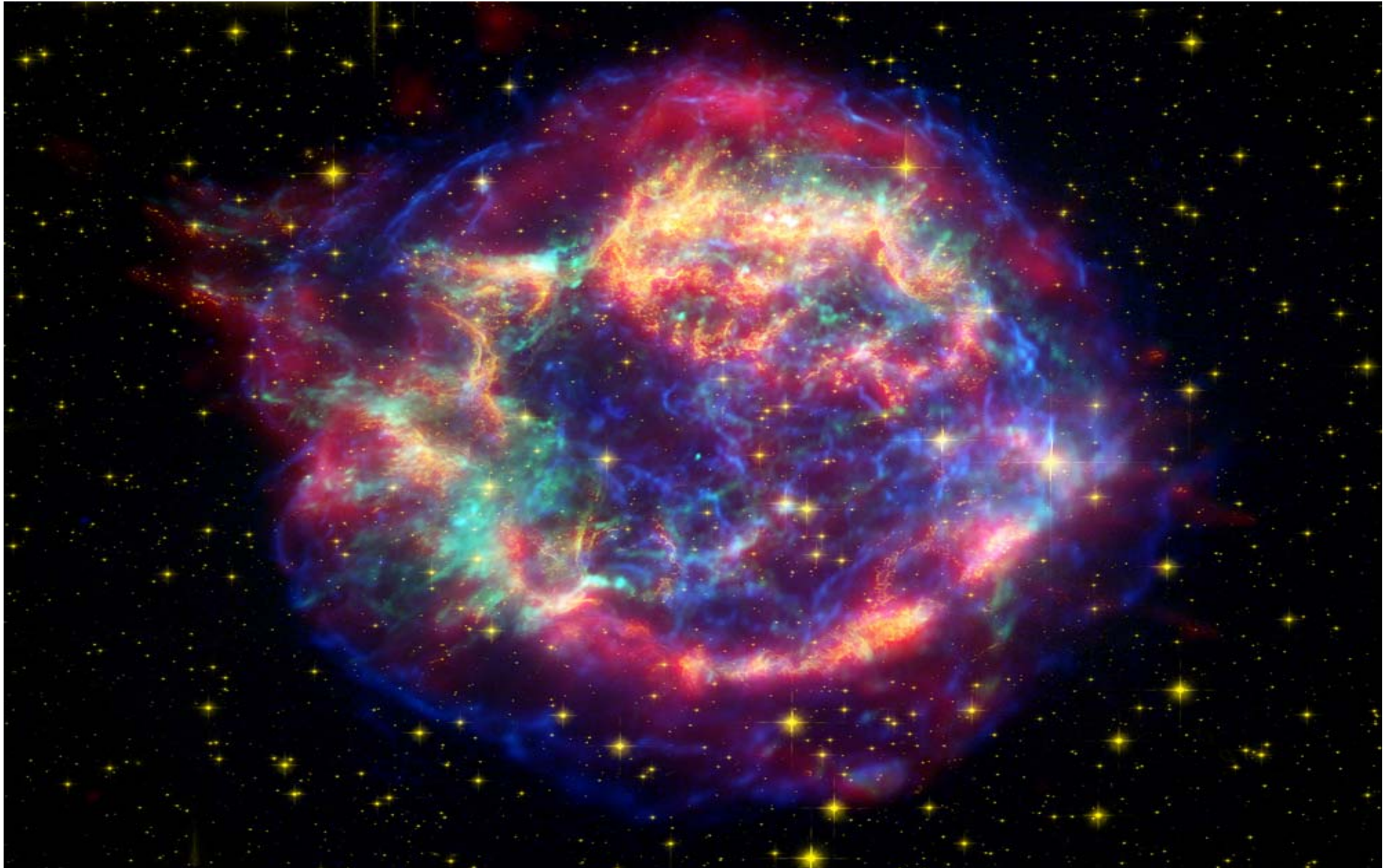
- Photometric Observation: Spitzer (Infrared - red), Hubble (Visible - yellow), Chandra (X-ray - green & blue)
- Heavier elements - Supernova explosion
- Solar system made from debris of supernova explosions

SPECTRUM OF THE WIND NEAR BLACK HOLE: GRO J1655-40 BINARY STAR SYSTEM
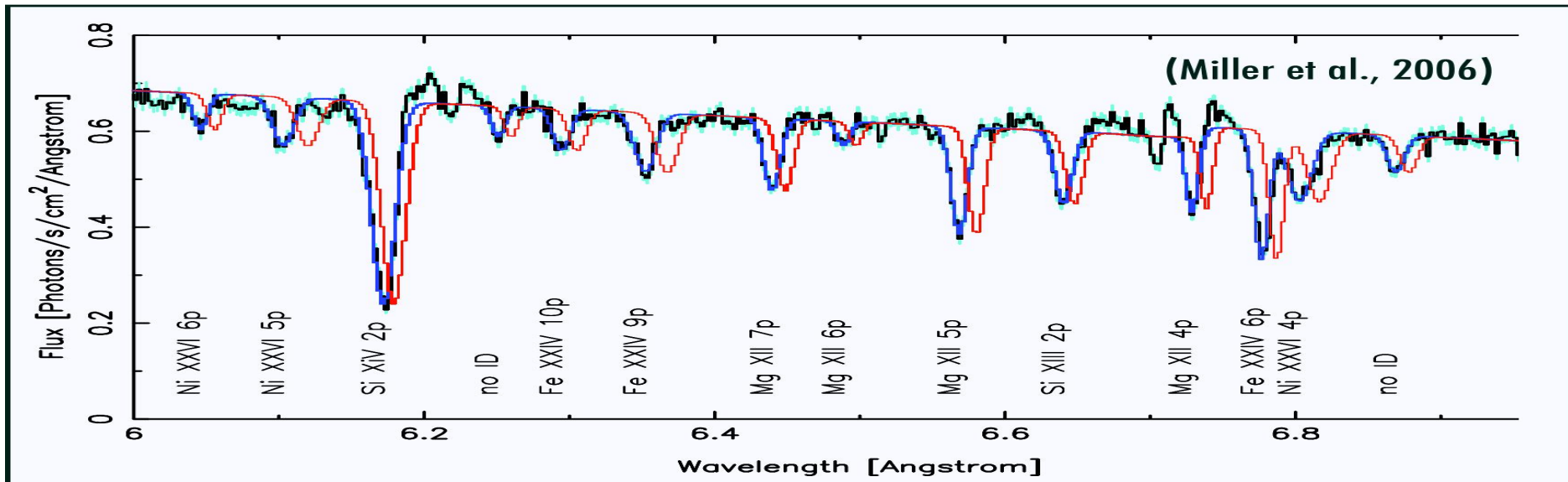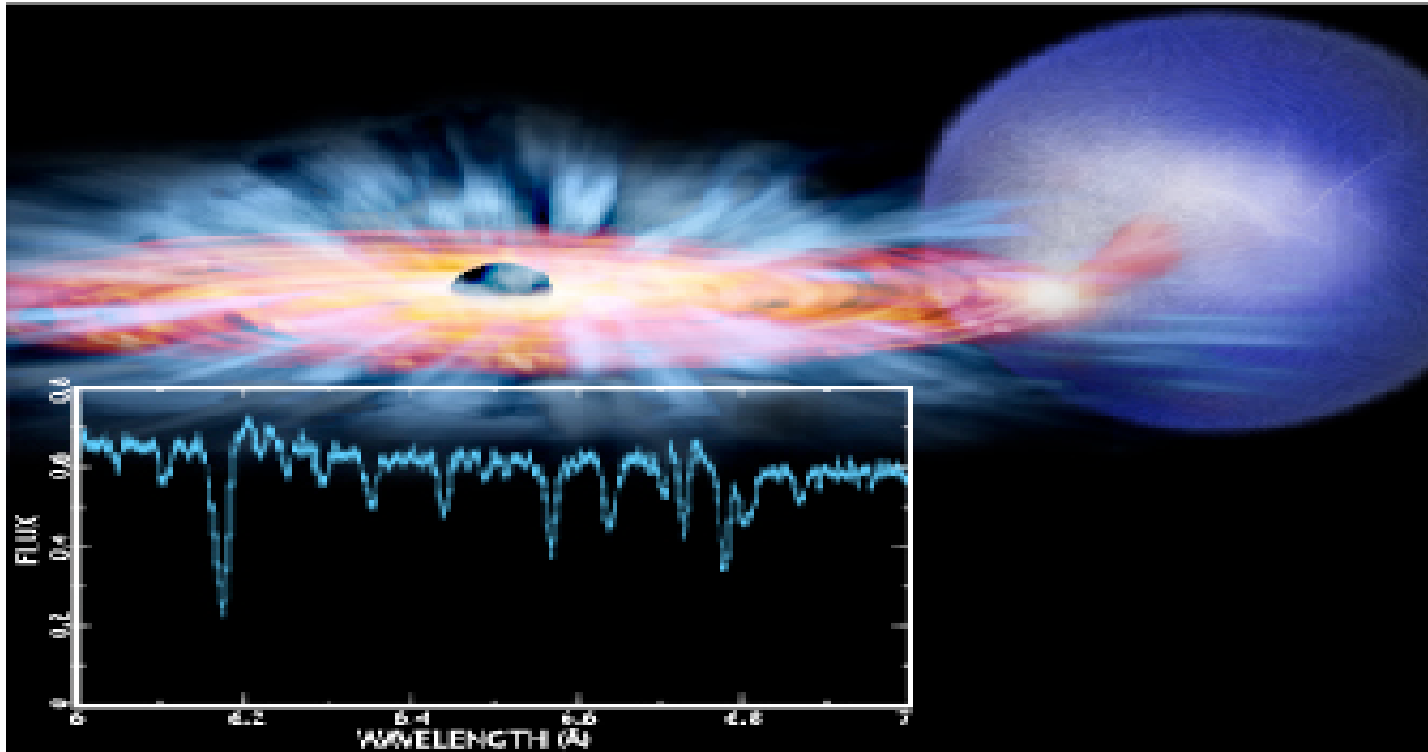
• Spectrum (BH - blue, Theory - red): Highly charged Mg, Si, Fe, Ni lines. Doppler Blue Shift - Wind is blowing toward us

SOLAR SPECTRA: ABSORPTION & EMISSION LINES

- Absorption line - forms as an electron absorbs a photon to jump to a higher energy level
- Emission line - forms as a photon is emitted due to the electron dropping to a lower energy level
- For the same transition levels, lines form at the same energy position
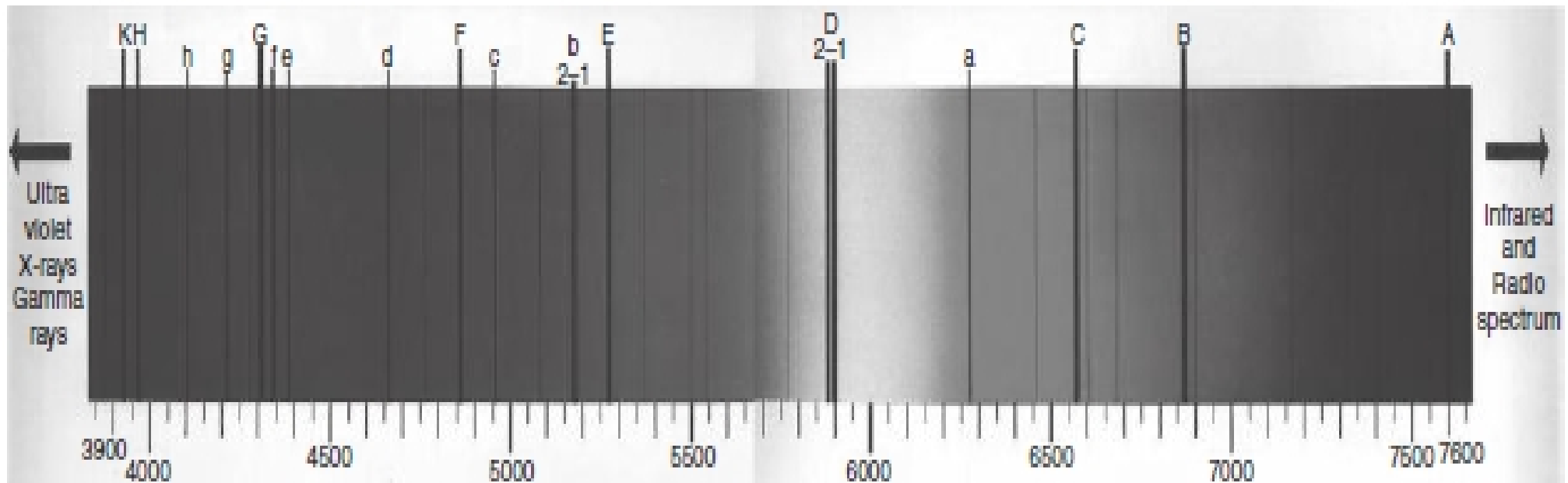
- Fraunhofer (1815) observed lines in the solar spectrum & used alphabet for designation
- Later spectoscopy with quantum mechanics identified them: A (7594 Å,O), B (6867 Å,O) (air), C (6563 Å H), D1 & D2 (5896, 5890 Å Na, yellow sun), E(5270 Å, Fe I), F (4861 Å, H), G(4300 Å, CH), H & K (3968, 3934 Å, Ca II)
- Russel and Saunders (1925) introduced LS coupling designation

MATTER IN THE UNIVERSE
(WMAP-Wilkinson Microwave Anisotropy Probe
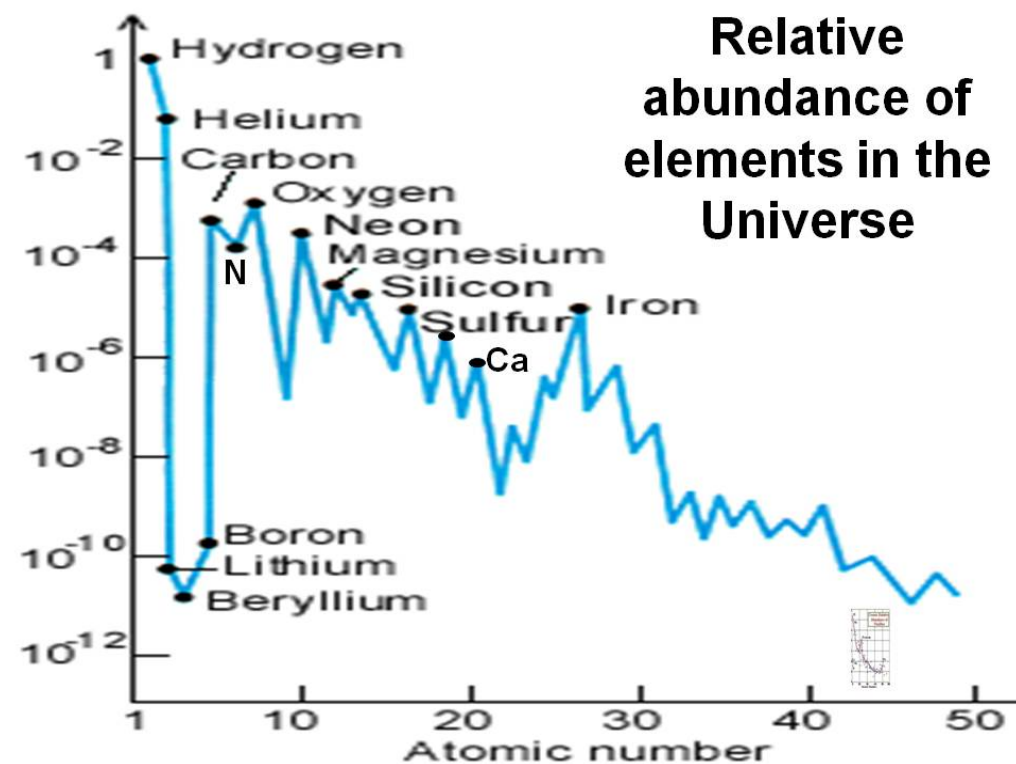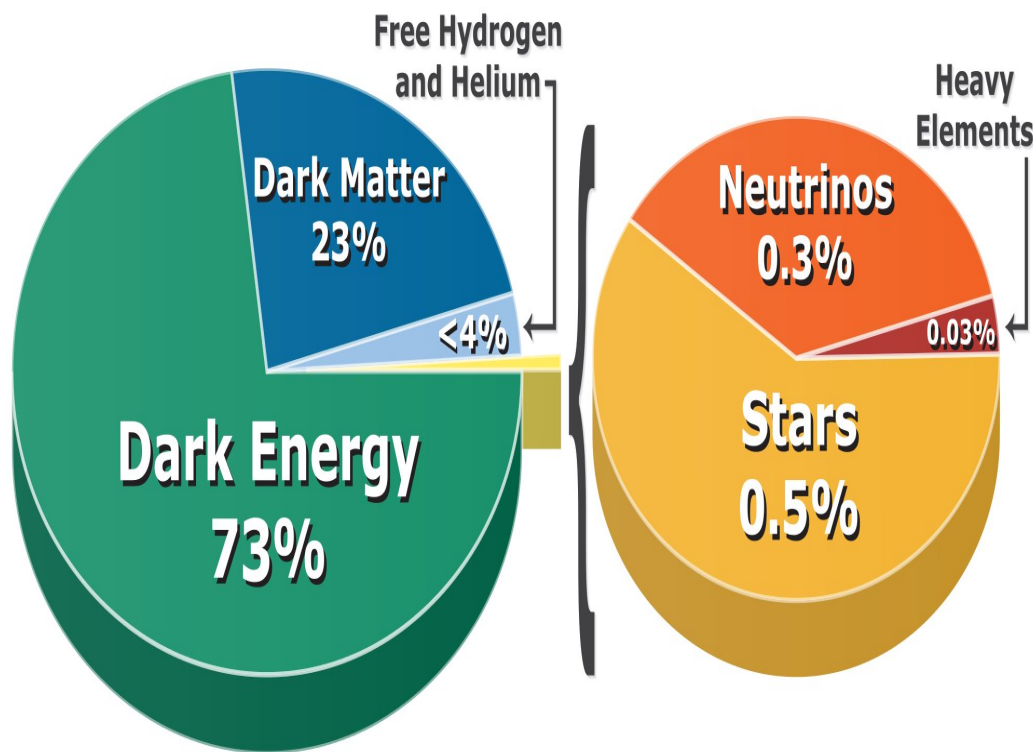
- Gravity of dark matter slows expansion and dark energy pushes out for expansion
- H (X - 90%, mass: 70%), He (Y - 7%, mass: 28%)
- Metals: Li, Be, B, C, N, O, F, Ne, Na, Mg, Al, Si, S, Ar, Ca, Ti, Cr, Fe, Ni
- Although constitute only 3% of the plasma, the metals are responsible for most of the spectral features
- Study elements through spectroscopy

Atomic Structure: ELEMENTS (key information) and SPECTROSCOPY:

PERIODIC TABLE
Atomic Properties of the Elements

NIST — National Institute of Standards and Technology, U.S. Department of Commerce

Physical Measurement Laboratory — www.nist.gov/pml
Standard Reference Data — www.nist.gov/srd

Frequently used fundamental physical constants

For the most accurate values of these and other constants, visit physics.nist.gov/constants
1 second = 9 192 631 770 periods of radiation corresponding to the transition between the two hyperfine levels of the ground state of ^{133}Cs
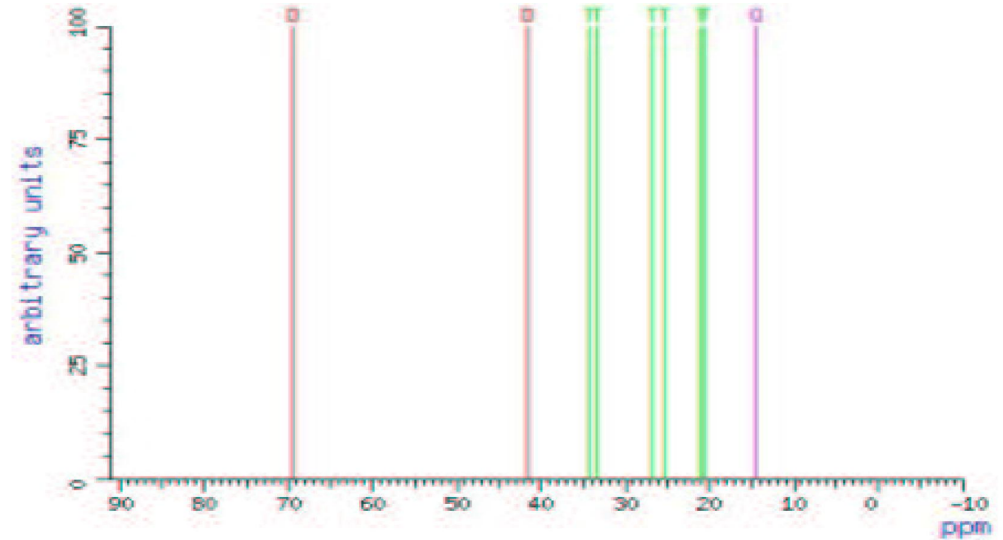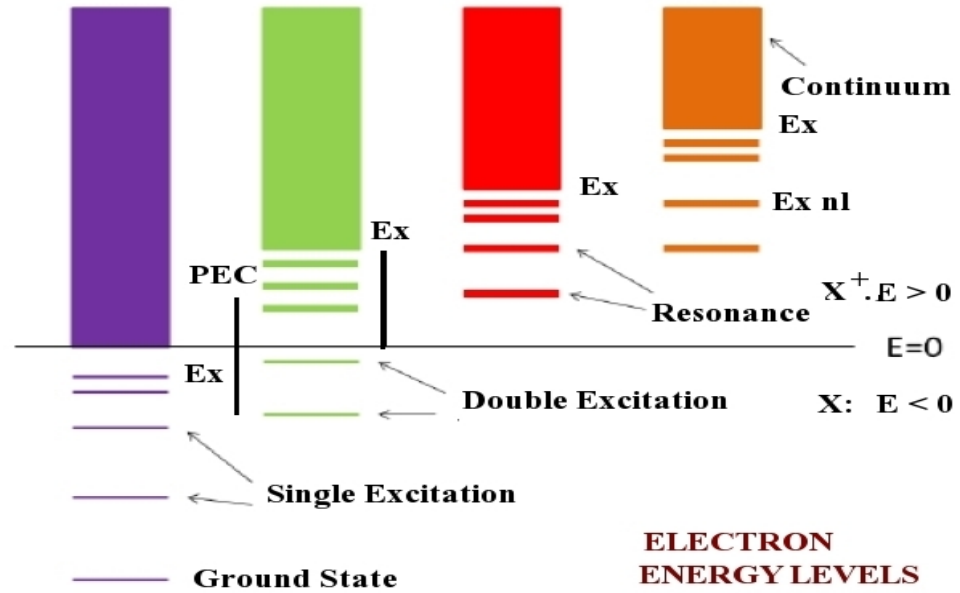
speed of light in vacuum	c	299 792 458 m s^{-1}	(exact)
Planck constant	h	6.626 07 x 10^{-34} J s	($\hbar = h/2\pi$)
elementary charge	e	1.602 177 x 10^{-19} C	
electron mass	m_e	9.109 38 x 10^{-31} kg	
	$m_e c^2$	0.510 999 MeV	
proton mass	m_p	1.672 622 x 10^{-27} kg	
fine-structure constant	α	1/137.035 999	
Rydberg constant	R_∞	10 973 731.569 m^{-1}	
	$R_\infty c$	3.289 841 960 x 10^{15} Hz	
	$R_\infty hc$	13.605 69 eV	
Boltzmann constant	k	1.380 6 x 10^{-23} J K^{-1}	

Solids (white) | Liquids (blue) | Gases (pink) | Artificially Prepared (yellow)

*IUPAC conventional atomic weights; standard atomic weights for these elements are expressed in intervals; see iupac.org for an explanation and values.

†Based upon ^{12}C. ( ) indicates the mass number of the longest-lived isotope.

For a description of the data, visit physics.nist.gov/data
NIST SP 966 (September 2014)

- **Elements: Gases (pink), Solids (white), Liquids (blue), Artificially Prepared (yellow)**
- **Nuclear fusion ends at Fe (strongest nuclear force)**
- **Heavier elements - Supernova explosion (r-process), some through neutrino capture (s-process)**

DETECTION OF GRAVITATIONAL WAVES FROM MERGER OF BLACK HOLES & HEAVY ELEMENTS
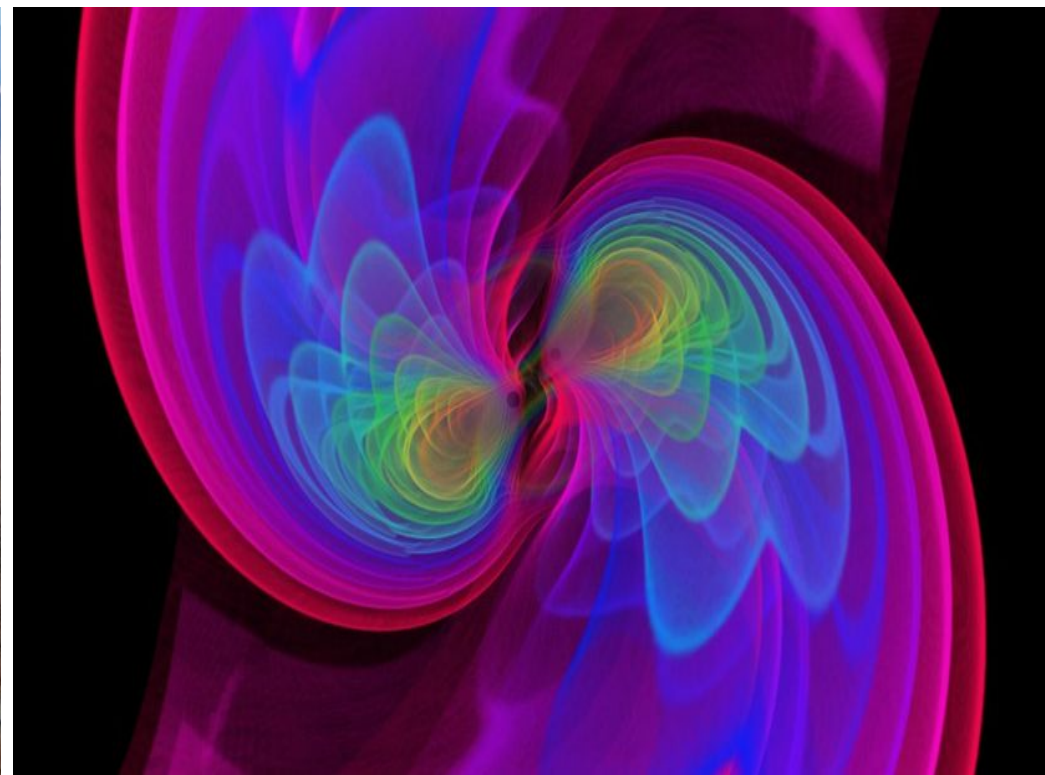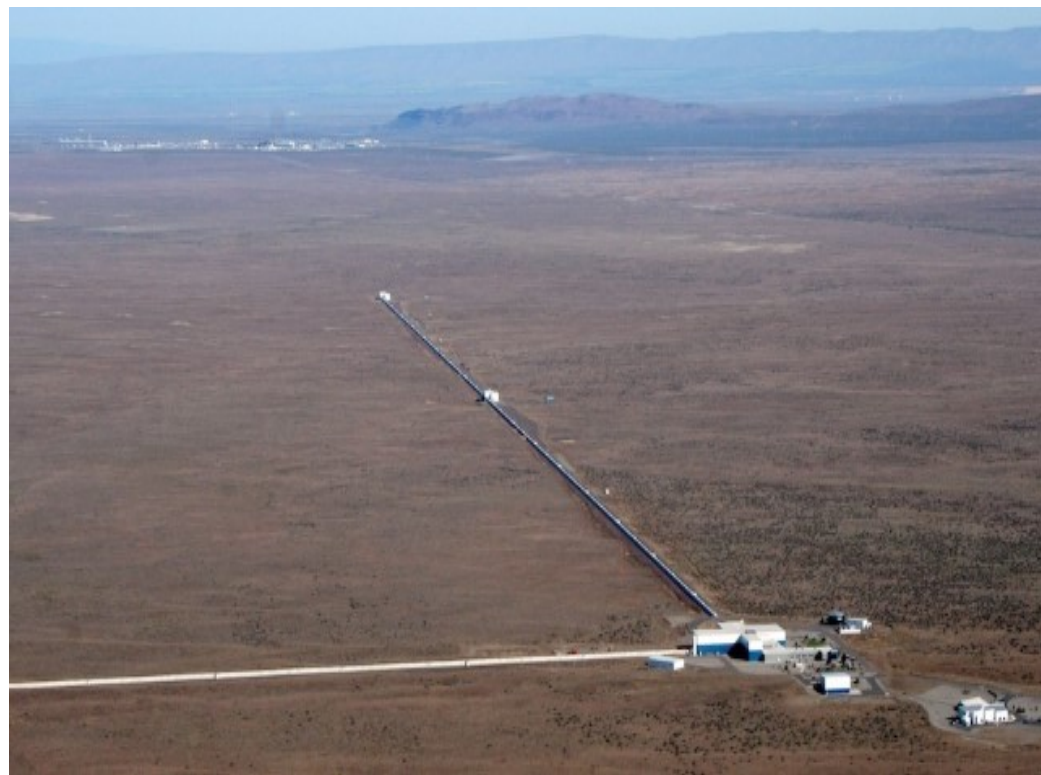
- Einstein: Moving objects generate gravitational wave traveling at the spped of light - extremely weak to detect except those from mergers of black holes or neutron stars when part of the mass converts to strong gravitational waves

- R. A computer simulation of gravitational waves radiating from two merging black holes • Since 2015 Detected 4 black hole merger mergers and one neutron stars megers

- New finding: They also detected electromagnetic waves of heavy elements

RADIATION FROM ATOMS & SPECTRUM

Continuum
Ex
Ex
Ex nl
Ex
Ex
PEC
Resonance
$X^+ . E > 0$
E = 0
Ex
Double Excitation
X: E < 0
Single Excitation
Ground State

ELECTRON ENERGY LEVELS
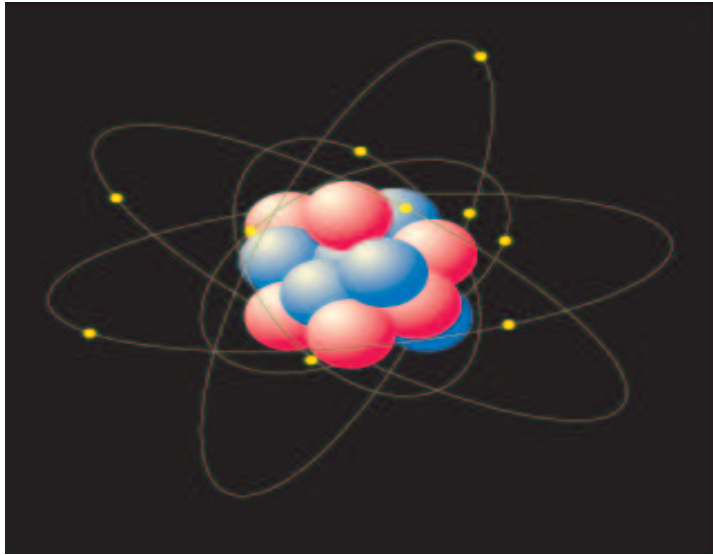
- Energy levels are quantized
- An electron can be excited to higher levels. While dropping down, it gives out a photon. Radiation contains photons of many energies
- SPECTURM: Splitting the radiation in to its colors: Rainbow, C lines

ATOMIC STRUCTURE

- Atomic structure - i) Organization of electrons in various shells and subshells, ii) Determinations of electron energies and wave functions
- As Fermions, unlike Bosons, electrons form *structured* arrangements bound by the attractive nuclear potential
- Different atomic states arise from quantization of motion, orbital and spin angular momenta of all electrons. Transitions among those states involve photons which are seen as lines in observed spectra
- The combination of orbital angular momentun L and spin angular momentum S follow strict coupling rules, known as selection rules, that determine the stationary energy states and expectation values, such as, mean radius.
- The dynamic state of an atom - described by a Schrodinger equation
- HYDROGEN ATOM - only atomic system that can be treated exactly
- Approximation begins from 2-electrons systems

HYDROGEN ATOM

Schrodinger equation of hydrogen, with $\mathbf{KE = P^2/(2m)}$ and nuclear potential energy $\mathbf{V(r)}$, is

$$\left[-\frac{\hbar^2}{2m}\left(\nabla^2\right) \quad + \quad V(r) \right]\Psi \;=\; E\,\Psi \qquad (1)$$

$$or, \quad \left[-\frac{\hbar^2}{2m}\left(\nabla_r^2 + \nabla_\perp^2\right) \quad + \quad V(r) \right]\Psi \;=\; E\,\Psi$$

$$V(r) = -\frac{Ze^2}{r} = -\frac{2Z}{r/a_0}\,\mathrm{Ry}$$

In spherical coordinates

$$\nabla_{\mathbf{r}}^{\mathbf{2}} = \frac{1}{r^2}\frac{\partial}{\partial r}\left(r^2\frac{\partial}{\partial r}\right) \qquad (2)$$

$$\nabla_\perp^2 = \frac{1}{r^2\sin\vartheta}\frac{\partial}{\partial\vartheta}\left(\sin\vartheta\frac{\partial}{\partial\vartheta}\right) + \frac{1}{r^2\sin^2\vartheta}\frac{\partial^2}{\partial\varphi^2}$$

The solution or wavefunction has independent variables r, θ, ϕ, each will correspond to a quantum number,

$$\Psi(\mathbf{r},\vartheta,\varphi) = R(r)\,Y(\vartheta,\varphi)$$

ANGULAR EQUATION & m QUANTUM NUMBER

The angular equation is separated with constant λ as

$$\frac{1}{\sin\vartheta}\frac{\partial}{\partial\vartheta}\left(\sin\vartheta\frac{\partial\mathbf{Y}}{\partial\vartheta}\right) + \frac{1}{\sin^2\vartheta}\frac{\partial^2\mathbf{Y}}{\partial\phi^2} + \lambda\mathbf{Y} = 0 \qquad (3)$$

The solutions are spherical harmonics,

$$\mathbf{Y}(\vartheta,\varphi) = \Theta(\vartheta)\ \Phi(\varphi) \qquad (4)$$

The equation can be expressed in the form

$$\mathbf{L^2Y}(\vartheta,\varphi) = \left[-\frac{\hbar^2}{2m}\left(\nabla^2\right)\right]\mathbf{Y}(\vartheta,\varphi) = \lambda\mathbf{Y}(\vartheta,\varphi), \qquad (5)$$

L is an angular momentum operator. Substituting Y,

$$\frac{d^2\Phi}{d\varphi^2} + \nu\Phi = 0, \qquad (6)$$

$$\frac{1}{\sin\vartheta}\frac{d}{d\vartheta}\left(\sin\vartheta\frac{d\Theta}{d\vartheta}\right) + \left(\lambda - \frac{\nu}{\sin^2\vartheta}\right)\Theta = 0\,,$$

where $\nu = m^2$, and $\Phi(\varphi) = (2\pi)^{-1/2}\,e^{im\varphi}$. $m =$*magnetic angular quantum number* and equals to $0, \pm1, \pm2, \ldots$

Replacing ϑ by $w = \cos\vartheta$ the Θ equation is

$$\frac{d}{dw}\left[(1-w^2)\frac{d\Theta}{dw}\right] + \left[\lambda - \frac{m^2}{1-w^2}\right]\Theta(w) = 0. \qquad (7)$$

A finite solution Θ requires $\lambda = l(l+1)$, where $l = 0, 1, 2\ldots$ The solutions are associated Legendre polynomials of order l and m,

$$P_l^m(w) = (1-w^2)^{|m|/2}\frac{d^{|m|}}{dw^{|m|}}P_l(w), \qquad (8)$$

$m = l, l-1, \ldots -l$. $m = 0 \rightarrow P_l(w) =$ Legendre polynomial of order l. The angular solution of normalized spherical harmonic:

$$Y_{lm}(\vartheta, \varphi) = N_{lm}\, P_l^m(\cos\vartheta)\, e^{im\varphi} \qquad (9)$$

where

$$N_{lm} = \epsilon\left[\frac{2l+1}{4\pi}\frac{(l-|m|)!}{(l+|m|)!}\right]^{1/2}, \qquad (10)$$

$\epsilon = (-1)^m$ **for $m > 0$ and $\epsilon = 1$ for $m \leq 0$.**

THE RADIAL EQUATION

The radial equation representing the dynamical motion of the electron is

$$\left[\frac{1}{r^2} \frac{d}{dr} \left(r^2 \frac{d}{dr} \right) + \frac{2m}{\hbar^2} \left(E - V(r) \right) - \frac{\lambda}{r^2} \right] R(r) = 0 \,, \quad (11)$$

Substituting $R(r) = P(r)/r$, it is reduced to

$$\left[\frac{\hbar^2}{2m} \frac{d^2}{dr^2} - V(r) - \frac{l(l+1)\hbar^2}{2mr^2} + E \right] P(r) = 0 \,. \quad (12)$$

The equation shows motion of a particle in a potential

$$V(r) + \frac{l(l+1)\hbar^2}{2mr^2} \,, \quad (13)$$

We switch to Rydberg unit for the Schrodinger equation,

$$\left[\frac{d^2}{d(r/a_0)^2} + \frac{2Z}{r/a_0} - \frac{l(l+1)}{(r/a_0)^2} + E/\mathrm{Ry} \right] P(r) = 0 \quad (14)$$

$$\text{or,} \quad \left[\frac{d^2}{dr^2} - V(r) - \frac{l(l+1)}{r^2} + E \right] P(r) = 0 \,, \quad (15)$$

SOLVING RADIAL EQUATION

• The radial equation can be solved on specifying boundary conditions, (i) r at ∞, and (ii) r near $r = 0$

• The bound electron moves in the nuclear attractive potential: $\lim_{r\to\infty} V(r) = 0$. Hence for case (i) for $r \to \infty$

$$\left[\frac{d^2}{dr^2} + E \right] P(r) = 0 , \tag{16}$$

which has solutions

$$P(r) = e^{\pm ar}, \qquad a = \sqrt{-E} . \tag{17}$$

Taking $E < 0$ for bound states, $\lim_{r\to\infty} e^{-ar}$ is a possible solution. It is also valid for $E > 0$, when a becomes imaginary. Hence, the asymptotic behavior suggests

$$P(r) = e^{-ar} f(r) \tag{18}$$

subject to $\lim_{r\to 0} f(r) = 0$. On substitution,

$$\frac{d^2 f}{dr^2} - 2a\frac{df}{dr} + \left[\frac{2Z}{r} - \frac{l(l+1)}{r^2} \right] f(r) = 0 \tag{19}$$

WAVEFUNCTION & n QUANTUM NUMBER

- For $r << 1$, the solution $f(r)$ is expressed as a power series

$$f(r) = r^s[A_0 + A_1 r + A_2 r^2 + \ \ldots \ ]$$

Finite f as $r \to 0$ requires $s > 0$ for consistent behavior of a bound electron. The possible radial wave function is

$$P(r) = f(r)e^{-ar} \approx r^{l+1}e^{-ar} \tag{20}$$

at large distances r. This again diverges at infinity, unless the series for f terminates at a point where the energy is

$$E = -(Z^2/n^2) \times \text{Ry}; \tag{21}$$

n is a positive integer & defined as the *principal quantum number*. Full $P(r)$ in Laguerre polynomial L is,

$$P_{nl}(r) = \sqrt{\frac{(n-l-1)!Z}{n^2[(n+l)!]^3 a_0}} \left[\frac{2Zr}{na_0}\right]^{l+1} e^{\frac{-Zr}{na_0}} \times L_{n+l}^{2l+1}\left(\frac{2Zr}{na_0}\right),$$

where

$$L_{n+l}^{2l+1}(\rho) = \sum_{k=0}^{n-l-1} \frac{(-1)^{k+2l+1}[(n+l)!]^2 \rho^k}{(n-l-1-k)!(2l+1+k)!k!} . \tag{22}$$

QUANTUM DESIGNATION OF A STATE

- Atomic Shells: n = 1,2,3,4 .. = K,L,M,N
- No of electrons = $2n^2$ - Closed shell, $< 2n^2$ - Open Shell
- Orbital angular momentum: l=0,1,2,3,4...(n-1) = s,p,d,f,.
- No of nodes in a wavefunction= n-l-1
- Total Angular Momentum: L=0,1,2,3,4, ... , = S,P,D,F,..
- Magnetic angular momentum: m_l = 0,±1,±2,±3,4 ..±l
  (2l+1) values → angular momentum multiplicity = 2L+1
- Spin angular momentun S was introduced due to electron spin. It is inherent in Dirac equation. S = integer or 1/2 integer depending on number of electrons with spin s=1/2
- Spin magnetic angular momentum = m_s = ±S - (2S+1) values - spin multiplicity
- Spin multiplicity = 1,2,3, .. =singlet, doublet, triplet ..
- Total angular momentum: J = |L±S|, J_M = 0,±1,±2,±3,4 ..±J, J multiplicity = 2J+1
- Parity (introduced from wavefunction) = π = $(-1)^l$ = +1 (even) or -1 (odd)
- Symmetry of a state: $^{(2S+1)}L^\pi$ (LS), $^{(2S+1)}L_J^\pi$ (LSJ)

SPECTRAL LINES & RYDBERG FORMULA

Hydrogen spectral line - Photon emitted or absorbed is of energy

$$\Delta\mathcal{E}_{n,n'} = \mathcal{R}_H \left[\frac{1}{n^2} - \frac{1}{n'^2} \right] \quad (n' > n), \tag{23}$$

where $\mathcal{R}_H = 109,677.576\,/\text{cm} = 911.76\,/\text{Å}$ is the Rydberg constant. Energy in wavelength in Ångström units:

$$\lambda = \frac{911.76\,\text{Å}}{\Delta E/\text{Ry}}. \tag{24}$$

• $\Delta\mathcal{E}_{n,n'}$ yields series of spectral lines,

$\mathcal{R}_H \left[1 - \frac{1}{n'^2} \right], \ n' = 2, 3, 4, \ldots$ **Lyman (Ly)**

$\mathcal{R}_H \left[\frac{1}{2^2} - \frac{1}{n'^2} \right], \ n' = 3, 4, 5, \ldots$ **Balmer (Ba)**

$\mathcal{R}_H \left[\frac{1}{3^2} - \frac{1}{n'^2} \right], \ n' = 4, 5, 6, \ldots$ **Paschen (Pa)**

$\mathcal{R}_H \left[\frac{1}{4^2} - \frac{1}{n'^2} \right], \ n' = 5, 6, 7, \ldots$ **Brackett (Br)**

$\mathcal{R}_H \left[\frac{1}{5^2} - \frac{1}{n'^2} \right], \ n' = 6, 7, 8, \ldots$ **Pfund (Pf)**

HYDROGEN SPECTRUM & EI
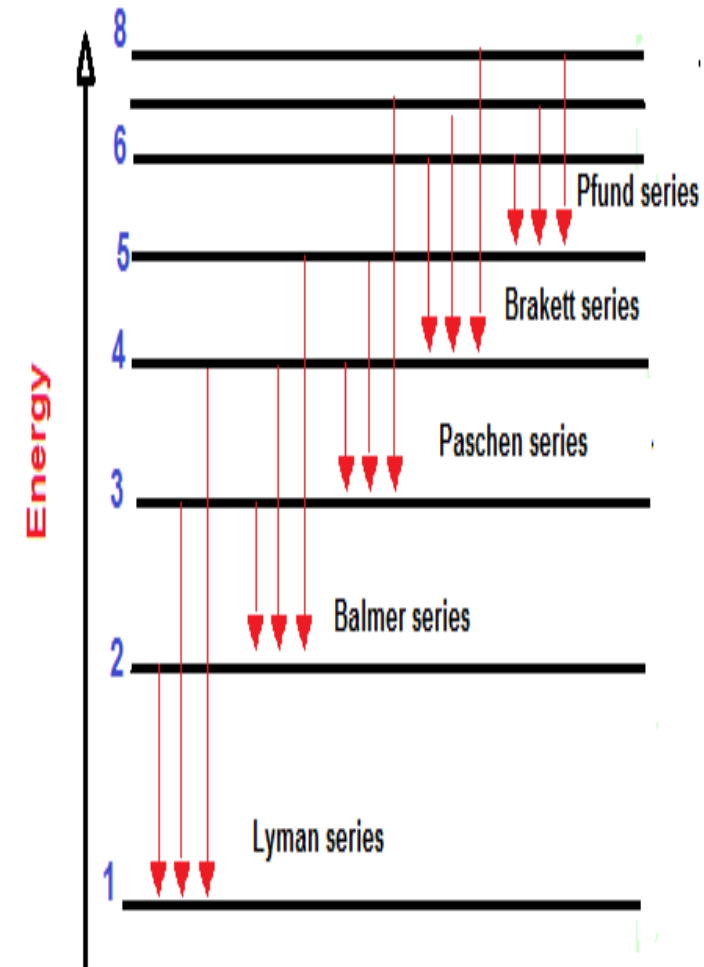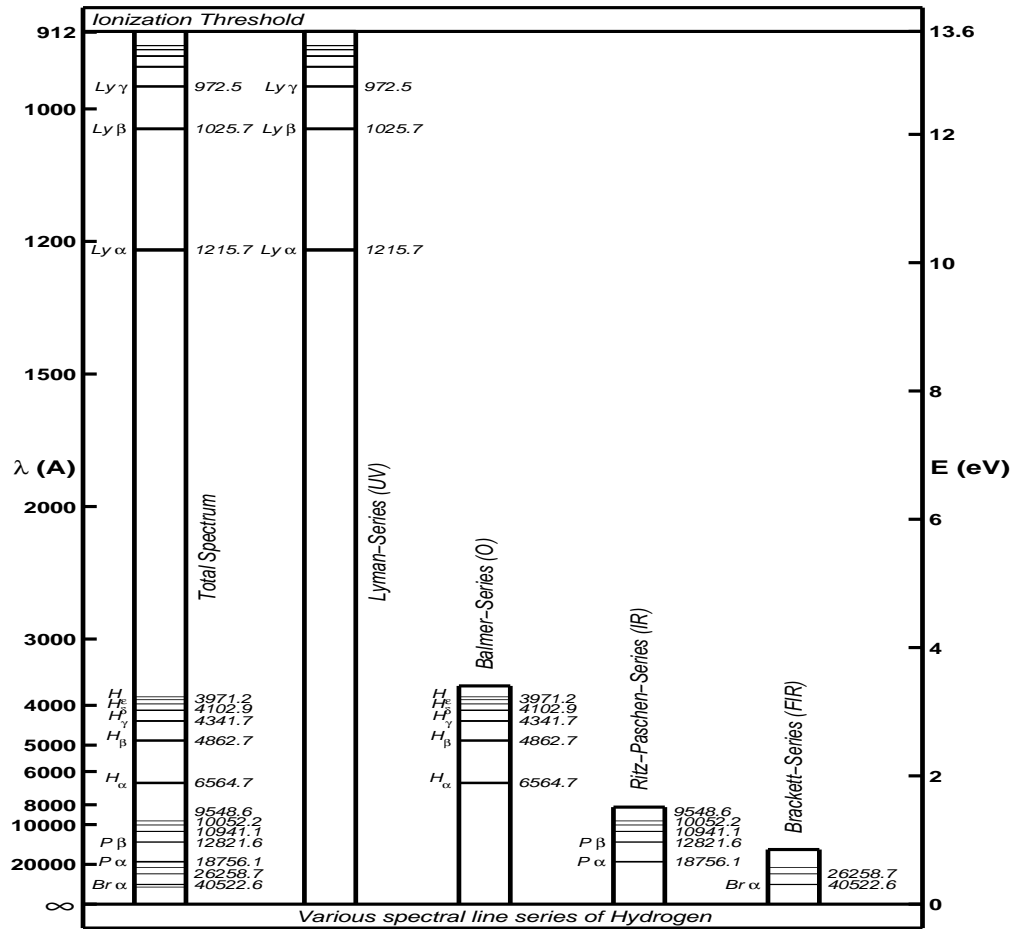
- **Lyman series:** 1215 − 912 Å (Far ultra-violet FUV), **Balmer series:** 6564 − 3646 Å (Optical O & Near UV), **Paschen series:** 18751 − 8204 Å (Near IR NIR), **Brackett series:** Far IR (FIR)
- For each series, Δn sequence is defined with α, β, γ, δ, etc., **Ex: Lyman series:** Ly α (1215.67 Å), Ly β (1025.72 Å), Ly γ (972.537 Å)..., Ly$_\infty$ (911.76 Å)
- Lyα - (1s-2p) is "the resonance line"

MULTI-ELECTRON ATOM

A many-electron system requires to sum over (i) all one-electron operators, that is KE & attractive nuclear Z/r potential, (ii) two-electron Coulomb repulsion potentials

$$\mathbf{H}\Psi = [H_0 + H_1]\Psi, \tag{25}$$

$$H_0 = \sum_{i=1}^{N}\left[-\nabla_i^2 - \frac{2Z}{r_i}\right], H_1 = \sum_{j<i}\frac{2}{r_{ij}} \tag{26}$$

$$H = \sum_i f_i + \sum_{j\neq i} g_{ij} \equiv F + G \tag{27}$$

- H_0: one-body term, stronger, H_1: two-body term, weaker, can be treated perturbatively
- Start with a trial wave function Ψ^{t} in some parametric form, Slater Type Orbitals

$$\mathbf{P}_{\mathbf{nl}}^{\mathrm{STO}}(\mathbf{r}) = \mathbf{r}^{\mathbf{l+1}}\mathbf{e}^{-\mathbf{ar}}$$

- A trial function should satisfy variational principle that through optimization an upper bound of energy eigenvalue is obtained in the Schrödinger equation.

MULTI-ELECTRON SYSTEM CONFIGURATIONS

- Determination of Configuration - Arranging electrons in to various orbits
- Orbitals fill up normally up to Ar $(3p^6)$
- No particular rule applies for the ground configurations or lowest energy state
- For large n all subshells exist, but they become excited states as higher orbitals may become lower states. Ex. For the next elements K (Z=19) and Ca (Z=20), 4s fills up instead of 3d. Two general rules:
- **Rule 1'**: A *subshell which gives lower* $(n+\ell)$ *value is filled in first* [K, Ca: $(n + \ell) = 4$ with 4s, but $= 5$ with 3d]
- **Rule 2'**: For the same $(n + \ell)$, higher ℓ is filled up first. Ex: Fe-group elements from Ca to Zn $(Z = 20 - 30)$ - 3d fills up after 4s instead of 4p as they have $(n + \ell) = 5$
- However, for configuration with Z > Fe (Z=26), $(n + \ell)$-first rule deviates, & no particular rule is followed as states are mixed with overlapped wavefunctions
- Electron-electron interactions introduce multiplet structures & levels

ANGULAR MOMENTA COUPLINGS

- **Total L and S angular momenta may couple differently for the total angular momentum J - depends on Z**
- **Multi-electron elements may be divided as, 'light' ($Z \leq 18$) and 'heavy' ($Z > 18$) (although not precise)**
- **LS coupling (typically $Z \leq 18$): Vector summation of orbital and spin angular momenta is done separately**
  $L = |L_2 - L_1|$, ..., $|L_2 + L_1|$, L Multiplicity $= 2L+1$
  $S = |S_2 - S_1|$, ..., $|S_2 + S_1|$, S Multiplicity $= 2S+1$
  Then the *total angular momentum quantum numbers*:
  $J = |L - S|$, ..., $|L + S|$, J Multiplicity $= 2J+1$
- **The *J*-values $\rightarrow$ finestructure levels. Each *LS* can correspond to several finestructure J levels**
- **The symmetry of a state is Jπ or $^{(2S+1)}L_J^{\pi}$**
- **Coulomb force between an electron and nucleus becomes stronger for large Z and highly charged ions and can increase the velocity of the electron to relativistic level. Angular coupling changes**
- **Intermediate or *LSJ* coupling (typically $19 \leq Z \leq 40$): Consideration of full relativistic effects is not necessary**

ANGULAR MOMENTA COUPLINGS

- **For the total angular momentum J, the angular momenta** l **and** $s = 1/2$ **of an interacting electron are added to the total orbital & spin angular momenta,** J_1 **of all other electrons, as:**

$$\mathbf{J_1} = \sum_i \mathbf{l_i} + \sum_i \mathbf{s_i}, \qquad \mathbf{K} = \mathbf{J_1} + \mathbf{l}, \quad \mathbf{J} = \mathbf{K} + \mathbf{s},$$

- jj **coupling (typically for Z >40): When relativistic effect is more prominent, the total J is obtained from sum of individual electron total angular momentum** j_i **from its angular & spin angular momenta:**

$$\mathbf{j_i} = \mathbf{l_i} + \mathbf{s_i}, \quad \mathbf{J} = \sum_i \mathbf{j_i}, \tag{28}$$

For any 2 electrons, J ranges from $|\mathbf{j_1 + j_2}|$ to $|\mathbf{j_1 - j_2}|$

- **States designation=** $(j_i j_2)_J$ **Ex;** (pd) **configuration-** $.j_1(1 \pm 1/2)$**=1/2, 3/2, and** $j_2(2 \pm 1/2)$**=3/2, 5/2. The states are:**
$.(\mathbf{1/2\ 3/2})_{\mathbf{2,1}}, (\mathbf{1/2\ 5/2})_{\mathbf{3,2}}, .(\mathbf{3/2\ 3/2})_{\mathbf{3,2,1,0}}, (\mathbf{3/2\ 5/2})_{\mathbf{4,3,2,1}}$

ANGULAR MOMENTA COUPLINGS

● **Hyperfine structure:** Form when finestructure levels J split further via vector addition with nuclear spin I $\rightarrow$ quantum state $J + I = F$

Configuration   Term Structure   Fine Structure   H

$\{n_i\ l_i\}$

$L = l_1 + l_2$
$S = s_1 + s_2$

$J = L + S$

L S Terms   LSJ Levels
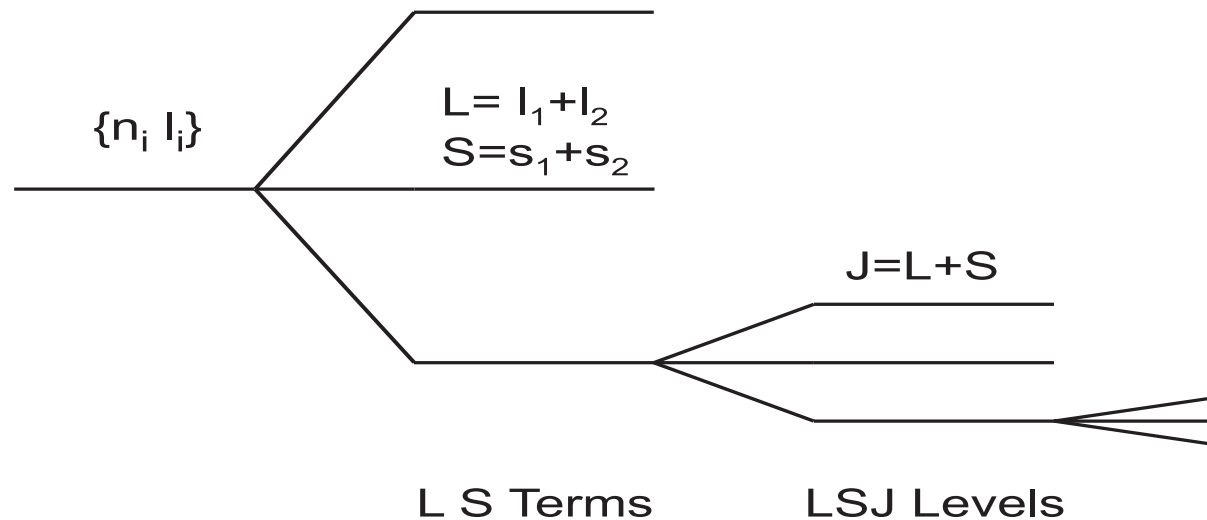
NON-EQUIVALENT & EQUIVALENT ELECTRON STATES

- **Number of valence electrons in the outer orbit: $> 1 \rightarrow$ Equivalent electron state**

  $= 1 \rightarrow$ **Non-equivalent electron state**

- **<u>Non-equivalent electron states</u>: All possible states the vectorial sum allows. Ex. States of 3-electron configuration: nsn'pn''d:**

$$ns\ n'\mathrm{p}\ (^{1}P^{o})\ n''\mathrm{d} \longrightarrow {}^{2}P^{o},\ {}^{2}D^{o},\ {}^{2}F^{o}$$

$$ns\ n'\mathrm{p}\ (^{3}P^{o})\ n''\mathrm{d} \longrightarrow {}^{(2,4)}(P, D, F)^{o}.$$

- **<u>Equivalent electron state</u>: Less number of LS states. Ex: configuration, np^{2}. If the configuration is npn'p, 6 possible states are: $^{1,3}\mathrm{S}, ^{1,3}\mathrm{P}, ^{1,3}\mathrm{D}$. However, for n=n', Pauli exclusion principle will eliminate some -reducing 6 to 3 states, $^{1}\mathrm{S}, ^{3}\mathrm{P}, ^{1}\mathrm{D}$, as follows**

- **Possible m_{l} and m_{s} values of a p electron**

  m_{l} = 1, 0, -1; m_{s} = 1/2, -1/2

  Six possible designation of a p electron are:

  $m_{l}\ m_{s}$: 1 1/2(1^{+}), 0 1/2(0^{+}), -1 1/2(-1^{+}),

  1 -1/2(1^{-}), 0 -1/2(0^{-}), -1 -1/2(-1^{-})

Vector addition for two p-electrons

$$M_L = \sum_i m_l = \mathbf{0}, \pm 1, \pm 2; \quad M_S = \sum_i m_s = \mathbf{0}, \pm 1$$

Possible combinations of np^2

M_S/ M_L=	2	1	0	-1	-2
0	1^+1^-	1^+0^-	$1^+\text{-}1^-$	$\text{-}1^+0^-$	$\text{-}1^+\text{-}1^-$
1		1^+0^+	$1^+\text{-}1^+$	$\text{-}1^+0^+$	
0		1^-0^+	$1^-\text{-}1^+$	$\text{-}1^-0^+$	
-1		1^-0^-	$1^-\text{-}1^-$	$\text{-}1^-0^-$	
0			0^+0^-		

- **The highest value of $M_L = |2|$ associates only with $M_S = 0$, & hence can only be ^1D. ^1D includes all 5 entries of M_L= 0,±1,±2**
- **Next highest value of $M_L = |1|$ associates with 3 $M_S = 0,\pm 1$ belong to ^3P and takes out the 9 entries**
- **The single remaining entry with M_L=0 and $M_S = 0$ corresponds to ^1S**
- **For np³: ⁴Sᵒ, ²Dᵒ, ²Pᵒ**

HUND'S RULE FOR ATOMIC STATES

- It governs the energy positions of states from spin multiplicity (2S + 1), orbital L, total J angular momenta
- S-rule: An LS term with the highest spin multiplicity (2S + 1) $\rightarrow$ lowest in energy - relates to exchange effect where electrons with like spin spatially avoid one another Ex: np^3 ($^4S^o$, $^2D^o$, $^2P^o$) for N I, OII, P I, S II: ground state is $^4S^o$
- L-rule: States of the same (2S+1), larger total L lies lower, again due to less electron repulsion Ex: np^3 above, $^2D^o$ term lies lower than the $^2P^o$
- J-rule: For fine-structure levels L+S =J
- For < half-filled subshells, the lowest J -level lies lowest
- For > half-filled, the highest J -level lies lowest in energy Ex: $^3P_{0,1,2}$ of ground configuration $(2p^2)$ of O III and $(2p^4)$ of Ne III. Order of fine-structure energy levels: J = 0,1,2 for OIII, J =2, 1,0 for Ne III.

RYDBERG FORMULA FOR ENERGIES & QUANTUM DEFECT

- General Rydberg formula is similar to that of H-like ions, but accounts for the screening effect on the valence electron by the core electrons
- The outer electron sees an *effective charge* $z = Z - N + 1$, $N =$ no of electrons
- Departure from a pure Coulomb form effectively *reduces* the principal quantum numbers n in Rydberg formula as

$$E(nl) = \frac{z^2}{(n - \mu)^2}$$

where $\mu \geq 0 =$ *quantum defect*
- The amount of screening (μ) depends on the orbital angular momentum ℓ. μ is a constant for each ℓ. We can write,

$$E(nl) = \frac{z^2}{(n - \mu_\ell)^2}$$

- Excited energy levels described by the Rydberg formula → "Rydberg levels"
- $\mu_s > \mu_p > \mu_d \ldots$

RYDBERG FORMULA FOR ENERGIES & QUANTUM DEFECT

- For light elements, such as C, with increasing l the valence electron sees a constant Coulomb potential. Hence $\mu_\ell \approx 0$ for any $\ell \geq f$, that is, there is no departure from n an f-electron onwards
- For heavier elements, e.g. Fe, f-orbitals may be occupied causing screening effect for the f-electron. Hence, the $\mu \approx 0$ for $\ell > f$
- Formula holds for all atoms & ions when the outer electron is in high-n state, i.e. sufficiently far away from inner electrons to experience only the residual charge z
- It can be used to obtain energy of any large n-level up to series limit at $n = \infty$ for any given l
- Define $\nu \equiv n - \mu = $ *effective quantum number*

$$E_n = -\frac{z^2}{\nu^2}$$

As $n \to \infty$, $E \to 0$ & the bound electron becomes free
- ν increases approximately by unity. However, it is often a decimal number

HARTREE-FOCK EQUATION
(AAS: Pradhan and Nahar 2011)

Optimize Schrodinger equation, $H\Psi = E\Psi$ for minimum E,

$$\delta\langle\Psi|H|\Psi\rangle = 0,$$

• E is stationary to the variations of the spin-orbitals, ψ_i subject to N^2 orthonormality conditions (N= number of electrons) $\rightarrow N^2$ Lagrange multipliers λ_{IJ}

$$\delta E - \sum_k \sum_l \lambda_{kl}\, \delta\langle\psi_k|\psi_l\rangle = 0$$

• Matrix of Lagrange multipler λ_{kl} is diagonal with elements $E_k\delta_{kl}$, that is,

$$\delta E - \sum_k E_k\delta\langle\psi_k|\psi_k\rangle = 0.$$

• Since each electron moves in a potential created by all other electrons, construct the potential $V(r_i)$ for the ith electron *self-consistently* $\rightarrow$ self-consistent iterative scheme of Hartree-Fock equations
• $H_1(r_1)$ depends on $\psi(r_2)$, implying $\psi(r_2)$ must be known before solving $H_1(r_1)$. Hence a trial $\psi(r_2)$ is adopted to obtain $\psi(r_1)$ using the variational criterion

HARTREE-FOCK EQUATION

• Since the form of $\psi(\mathbf{r_1})$ and $\psi(\mathbf{r_2})$ are identical, the new $\psi(\mathbf{r_2})$ is used again to obtain $\psi(\mathbf{r_1})$. This continues until the desired accuracy is attained. The scheme is often called Hartree-Fock Self-Consistent Field method.

• Hartree approx: total atomic wavefunction - product of one-electron spin orbitals

$$\psi_{\mathbf{n,l,m_l,m_s}}(\mathbf{r}, \theta, \phi, \mathbf{m_s}) = \prod_{i=1}^{N} \psi_{\mathbf{n_i}, \ell_i, \mathbf{m}_{\ell_i}, \mathbf{m}_{s_i}} \tag{29}$$

• But this lacks anti-symmetrization - manifestation of Pauli principle that wavefuntion changes sign on electron exchange of position

• Fock introduced anti-symmetrization, through the determinant form, to Hartree method → Hartree-Fock method Ex: He atom:

$$\mathbf{\Psi(1,2)} = \frac{1}{\sqrt{2}} \left[\psi_1(1)\psi_2(2) - \psi_1(2)\psi_2(1) \right]$$

This can be written in determinant form:

HARTREE-FOCK EQUATION

He wavefunction is then:

$$\Psi = \frac{1}{\sqrt{2}} \begin{vmatrix} \psi_1(1) & \psi_1(2) \\ \psi_2(1) & \psi_2(2) \end{vmatrix} \tag{30}$$

Ψ vanishes if coordinates of both electrons are the same

• The N-electron wavefunction in the determinantal representation

$$\Psi = \frac{1}{\sqrt{N}} \begin{vmatrix} \psi_1(1) & \psi_1(2) & \dots & \psi_1(N) \\ \psi_2(1) & \psi_2(2) & \dots & \psi_2(N) \\ \dots & \dots & \dots & \dots \\ \psi_N(1) & \psi_N(2) & \dots & \psi_N(N) \end{vmatrix} \tag{31}$$

This is called the *Slater determinant.* Substitution in Hartree-Fock equation gives set of one-electron radial equations,

$$\left[-\nabla_i^2 - \frac{2Z}{r_i}\right] u_k(r_i) + \left[\sum_l \int u_l^*(r_j) \frac{2}{r_{ij}} u_l(r_j) dr_j\right] u_k(r_i) \tag{32}$$

$$- \sum_l \delta_{m_L^k, m_L^l} \left[\int u_l^*(r_j) \frac{2}{r_{ij}} u_k(r_j) dr_j\right] u_l(r_i) = E_k u_k(r_i).$$

1st term= 1-body term, 2nd term= Direct term, 3rd term= Exchange term. • The total energy is given by

$$E[\Psi] = \sum_i I_i + \frac{1}{2} \sum_i \sum_j [J_{ij} - K_{ij}]. \tag{33}$$

CENTRAL FIELD Approximation for a Multi-Electron System

• H_1 consists of non-central forces between electrons which contains a large spherically symmetric component

• We assume that each electron is acted upon by the averaged charge distribution of all the other electrons and construct a potential energy function $V(r_i)$ with one-electron operator. When summed over all electrons, this charge distribution is spherically symmetric and is a good approximation to actual potenial. Neglecting non-radial part,

$$H = -\sum_{i=1}^{N} \frac{\hbar^2}{2m}\nabla_i^2 + V(\mathbf{r}).$$

where

$$V(\mathbf{r}) = -\sum_{i=1}^{N} \frac{e^2 Z}{r_i} + \left\langle \sum_{i\neq j}^{N} \frac{e^2}{r_{ij}} \right\rangle. \tag{34}$$

A short range excahnge potential with spherical charge distribution is often added to it.

• $V(\mathbf{r})$ is the *central-field potential* with boundary conditions

$$V(\mathbf{r}) = -\frac{Z}{r} \quad \text{if } r \to 0, \quad = -\frac{z}{r} \text{ if } \mathbf{r} \to \infty \tag{35}$$

CONFIGURATION INTERACTION

- **A multi-electron system is described by its configuration and a defined spectroscopic state.**
- **All states of the same SLπ, with different configurations, interact with one another - configuration interaction. Hence the wavefunction of the SLπ may be represented by a linear combination of configurations giving the state.**
- **Example, the ground state of Si II is $[1s^2 2s^2 2p^6] 3s^2 3p\,(^2P^o)$. $^2P^o$ state can also be formed from $3s^2 4p\,(^2P^o)$, $3s3p3d\,(\ldots,^2P^o)$. $3p^3(^2P^o)$ and so on. These 4 configurations contribute with different amplitudes or mixing coefficients (a_i) to form the four state vectors $^2P^o$ of a $4{\times}4$ Hamiltonian matrix. Hence for the optimized energy and wavefunction for each $^2P^o$ state all 4 configurations should be included,**

$$\Psi(^2P^o) = \sum_{i=1}^{4} a_i \psi[C_i(^2P^o)] = \left[a_1 \psi(3s^2 3p) + a_2 \psi(3s^2 4p) \right.$$
$$\left. + a_3 \psi(3p^3) + a_3 \psi(3s3p3d) \right]$$

Relativistic Breit-Pauli Approximatiom

Hamiltonian: For a multi-electron system, the relativistic Breit-Pauli Hamiltonian is:

$$H_{BP} = H_{NR} + H_{mass} + H_{Dar} + H_{so} +$$

$$\frac{1}{2} \sum_{i \neq j}^{N} [g_{ij}(so + so') + g_{ij}(ss') + g_{ij}(css') + g_{ij}(d) + g_{ij}(oo')]$$

where the non-relativistic Hamiltonian is

$$H_{NR} = \left[\sum_{i=1}^{N} \left\{ -\nabla_i^2 - \frac{2Z}{r_i} + \sum_{j>i}^{N} \frac{2}{r_{ij}} \right\} \right]$$

the Breit interaction is

$$H_B = \sum_{i>j} [g_{ij}(so + so') + g_{ij}(ss')]$$

and one-body correction terms are

$$H_{mass} = -\frac{\alpha^2}{4} \sum_i p_i^4, \ H_{Dar} = \frac{\alpha^2}{4} \sum_i \nabla^2 \left(\frac{Z}{r_i} \right), \ H_{so} = \frac{Ze^2\hbar^2}{2m^2c^2r^3} L.S$$

Wave functions and energies are obtained solving:

$$H\Psi = E\Psi$$

1. "PHOTO-EXCITATION"

Photo-Excitation & De-excitation:

$$X^{+Z} + h\nu \rightleftharpoons X^{+Z*}$$
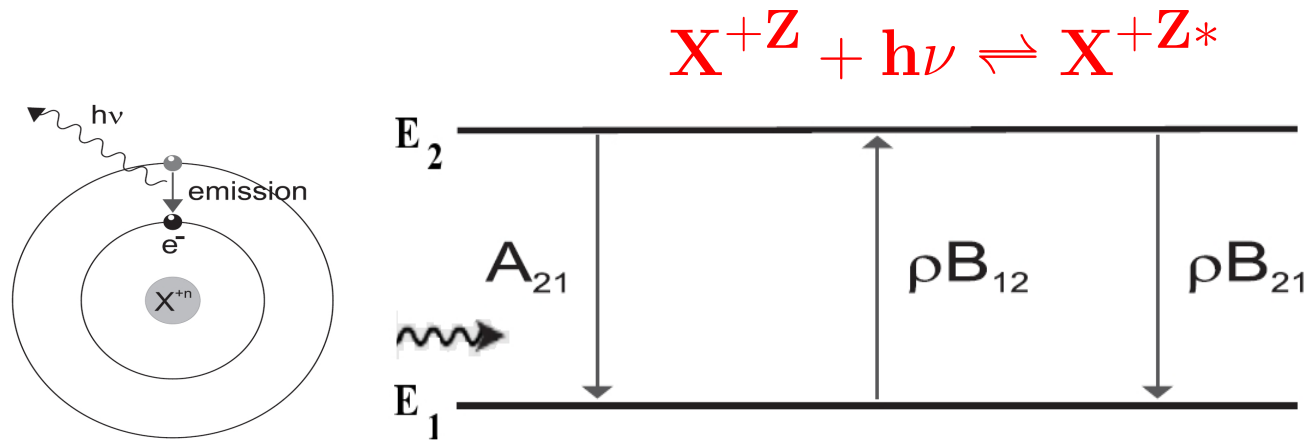
- **Atomic quantities**

B_{12} - **Photo-excitation, Oscillator Strength (f)**

A_{21}- **Spontaneous Decay, - Radiative Decay Rate (A-value)**

B_{21}- **Stimulated Decay with a radiation field**

- P_{ij}, **transition probability,**

$$P_{ij} = 2\pi \frac{c^2}{h^2 \nu_{ji}^2} | <j| \frac{e}{mc} \hat{e}.pe^{ik.r}|i> |^2 \rho(\nu_{ji}). \qquad (36)$$

$$e^{ik.r} = 1 + ik.r + [ik.r]^2/2! + \ldots,$$

- **Various terms in $e^{ik.r} \rightarrow$ various transitions 1st term E1, 2nd term E2 and M1, ...**

TRANSITION MATRIX ELEMENTS WITH A PHOTON

- 1st term: Dipole operator: $\mathbf{D} = \sum_i \mathbf{r}_i$:
- Transition matrix for Photo-excitation & Deexcitation:

$$< \boldsymbol{\Psi}_{\mathbf{B}} || \mathbf{D} || \boldsymbol{\Psi}_{\mathbf{B}'} >$$

Matrix element is reduced to generalized line strength (length form):

$$\mathbf{S} = \left| \left\langle \varPsi_{\mathbf{f}} \left| \sum_{\mathbf{j=1}}^{\mathbf{N+1}} \mathbf{r_j} \right| \varPsi_{\mathbf{i}} \right\rangle \right|^2 \tag{37}$$

- There are also "Velocity" & "Acceleration" forms

Allowed electric dipole (E1) transititions

The oscillator strength (f_{ij}) and radiative decay rate (A_{ji}) for the bound-bound transition are

$$\mathbf{f_{ij}} = \left[\frac{\mathbf{E_{ji}}}{\mathbf{3g_i}} \right] \mathbf{S},$$

$$\mathbf{A_{ji}(sec^{-1})} = \left[0.8032 \times 10^{10} \frac{\mathbf{E_{ji}^3}}{\mathbf{3g_j}} \right] \mathbf{S}$$

ALLOWED & FORBIDDEN TRANSITIONS

Angular momentum integrals introduce the selection rules

i) <u>Allowed:</u> Electric Dipole (E1) transitions - same-spin & intercombination (different spin) transition
($\triangle$ J = 0,$\pm$1, $\triangle$ L = 0,$\pm$1,$\pm$2; parity changes)

<u>Forbidden:</u>
ii) Electric quadrupole (E2) transitions
($\triangle$ J = 0,$\pm$1,$\pm$2, parity does not change)

iii) Magnetic dipole (M1) transitions
($\triangle$ J = 0,$\pm$1, parity does not change)

iv) Electric octupole (E3) transitions
($\triangle$ J= $\pm$2, $\pm$3, parity changes)

v) Magnetic quadrupole (M2) transitions
($\triangle$ J = $\pm$2, parity changes)

Allowed transitions are much strongher than Forbidden transitions

FORBIDDEN TRANSITIONS

i) Electric quadrupole (E2) transitions ($\Delta J = 0, \pm 1, \pm 2$, π - same)

$$A_{ji}^{E2} = 2.6733 \times 10^3 \frac{E_{ij}^5}{g_j} S^{E2}(i,j) \text{ s}^{-1}, \tag{38}$$

ii) Magnetic dipole (M1) transitions ($\Delta J = 0, \pm 1$, π - same)

$$A_{ji}^{M1} = 3.5644 \times 10^4 \frac{E_{ij}^3}{g_j} S^{M1}(i,j) \text{ s}^{-1}, \tag{39}$$

iii) Electric octupole (E3) transitions ($\Delta J = \pm 2, \pm 3$, π changes)

$$A_{ji}^{E3} = 1.2050 \times 10^{-3} \frac{E_{ij}^7}{g_j} S^{E3}(i,j) \text{ s}^{-1}, \tag{40}$$

iv) Magnetic quadrupole (M2) transitions ($\Delta J = \pm 2$, π changes)

$$A_{ji}^{M2} = 2.3727 \times 10^{-2} \text{s}^{-1} \frac{E_{ij}^5}{g_j} S^{M2}(i,j) \,. \tag{41}$$

LIFETIME:

$$\tau_k(s) = \frac{1}{\sum_i A_{ki}(s^{-1})}.$$

Monochromatic Opacity (κ_ν): $\quad \kappa_\nu(i \to j) = \frac{\pi e^2}{mc} N_i f_{ij} \phi_\nu$

EX: ALLOWED & FORBIDDEN TRANSITIONS

Diagnostic Lines of He-like Ions: w,x,y,z

$w(E1):\ 1s2p(^1P_1^o) - 1s^2(^1S_0)$ (Allowed Resonant)

$x(M2):\ 1s2p(^3P_2^o) - 1s^2(^1S_0)$ (Forbidden)

$y(E1):\ 1s2p(^3P_1^o) - 1s^2(^1S_0)$ (Intercombination)

$z(M1):\ 1s2s(^3S_1) - 1s^2(^1S_0)$ (Forbidden)

NOTE: 1s-2p are the K_α transitions
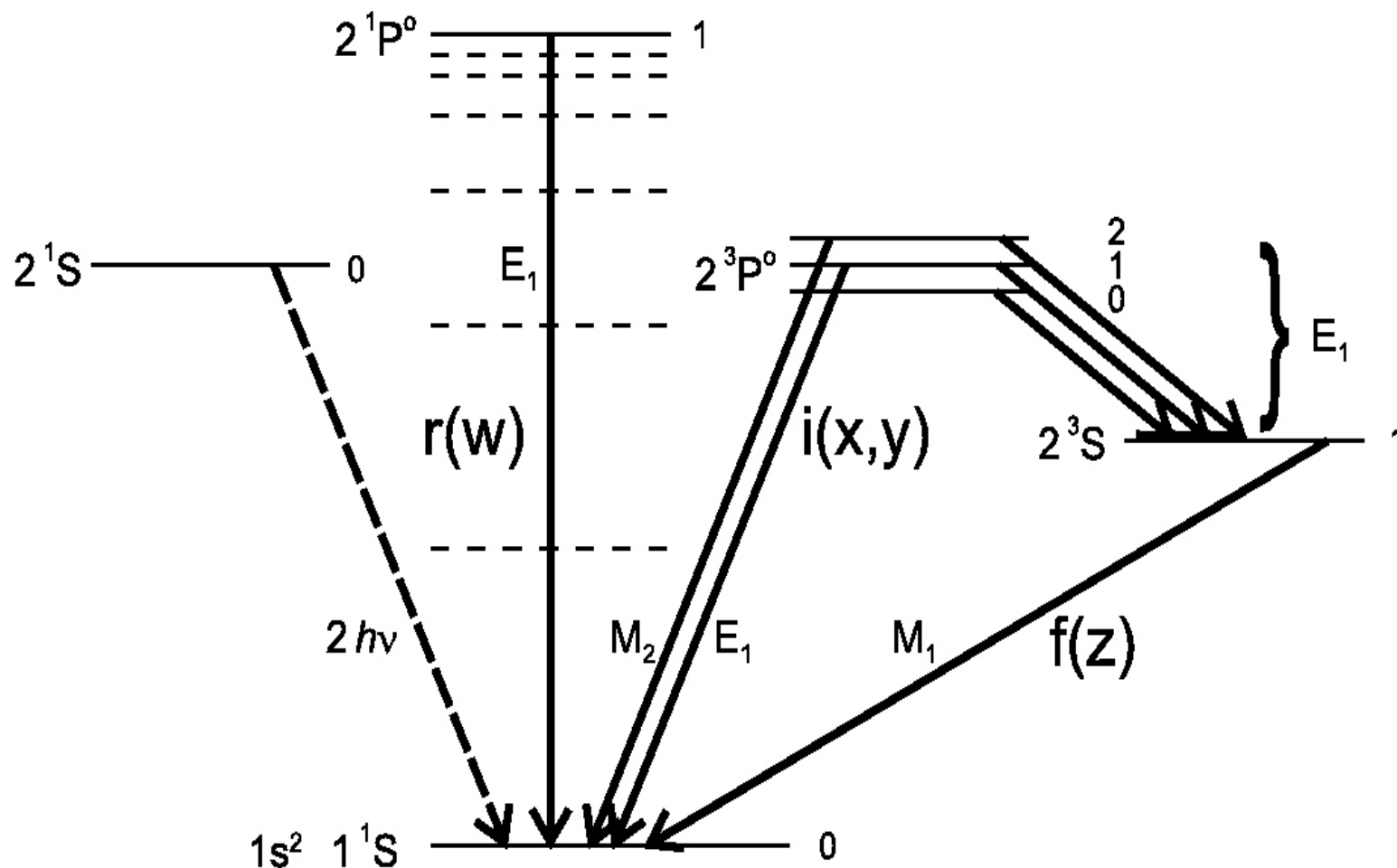
O VII w,x,y,z LINES IN ASTROPHYSICAL SPECTRA
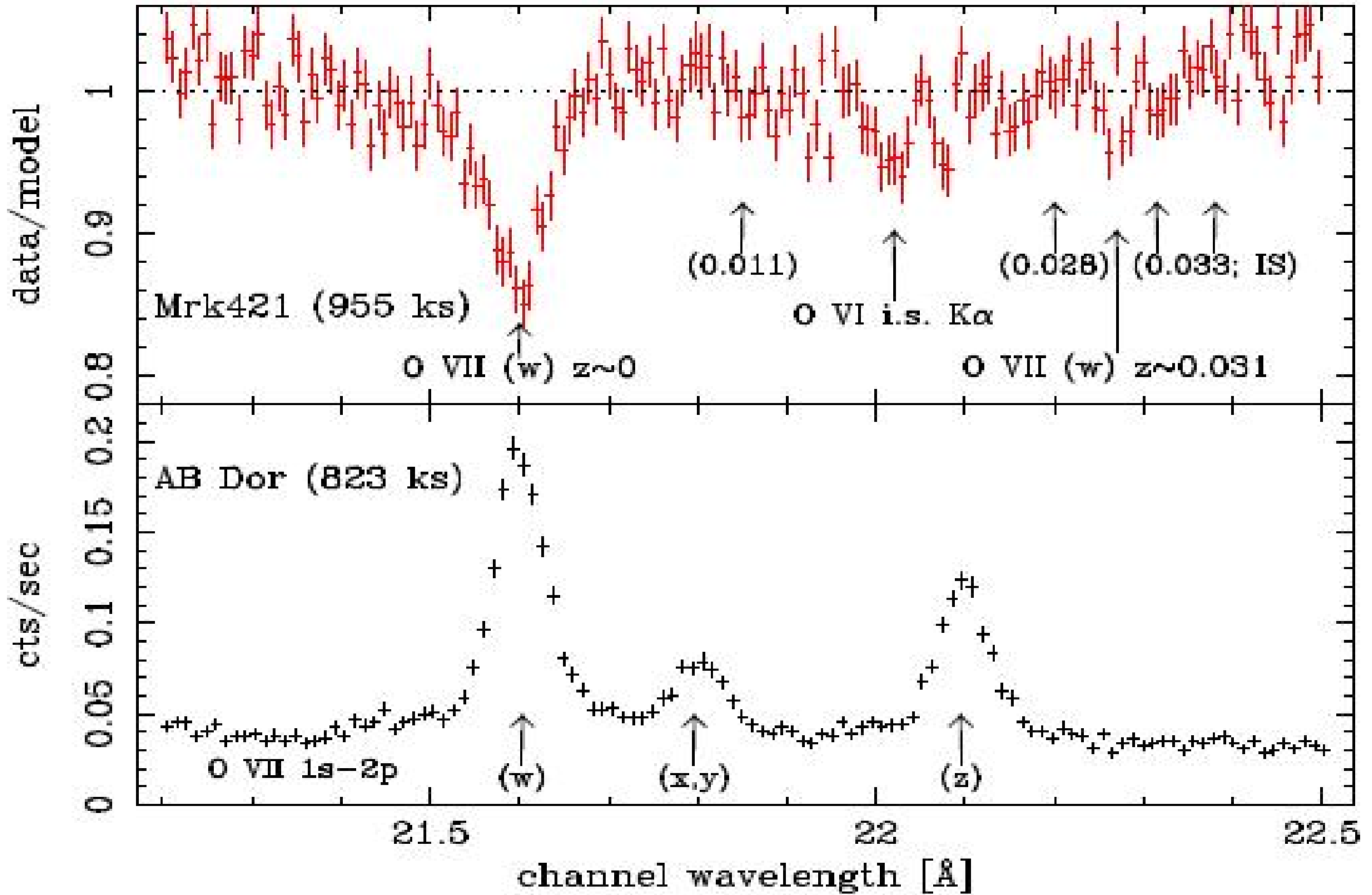
- These lines are detected in the X-ray spectra of Mrk 421 observed by XMM-Newton (Rasmussen et al 2007)

SOLAR SPECTRUM AS SEEN FROM THE EARTH

KITT PEAK SOLAR FLUX ATLAS   (KURUCZ, FURENLID, BRAULT, AND TESTERMAN 1984)
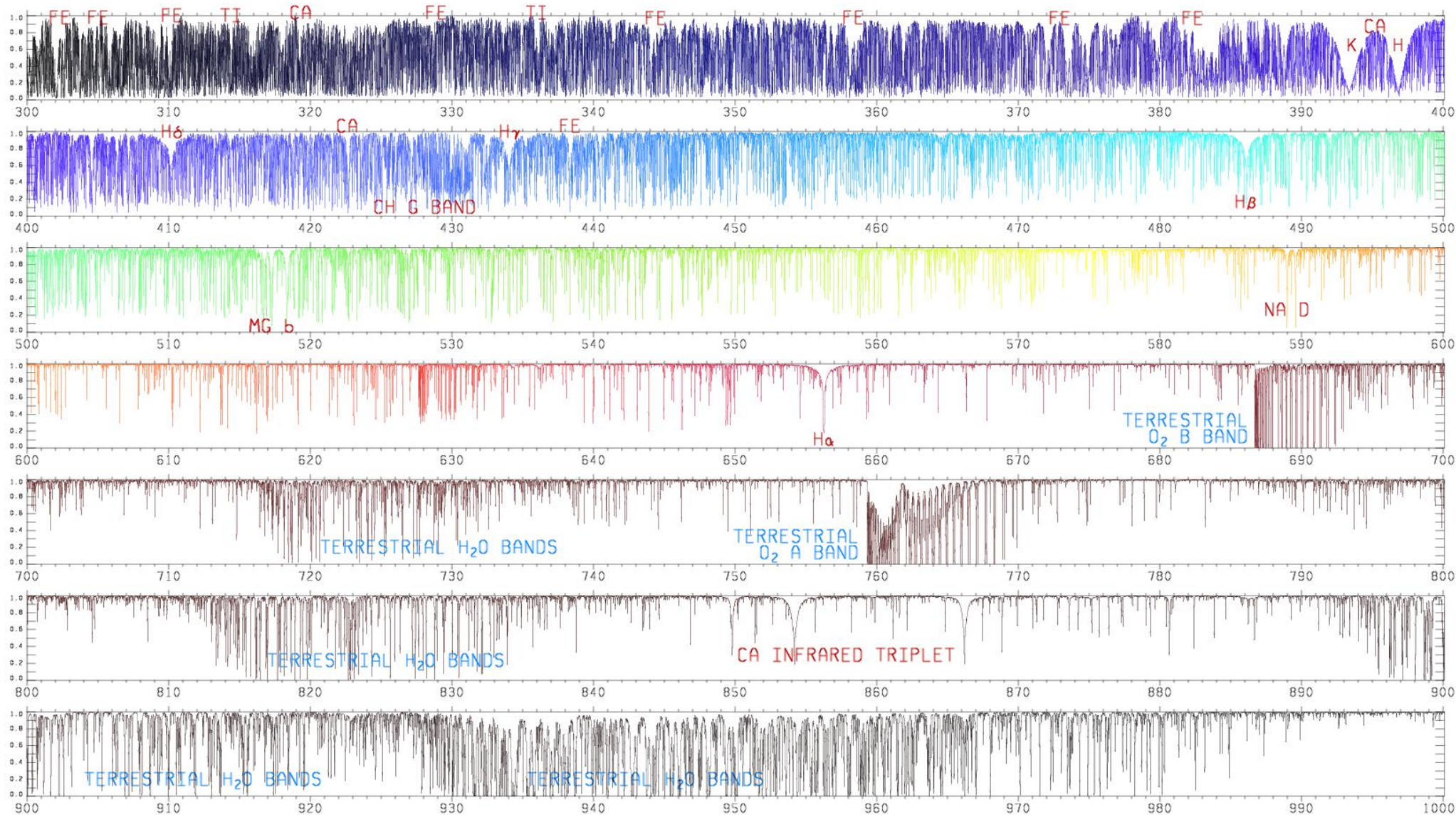
• Solar spectrum by Kurucz. The short wavelength region is mainly from Fe I, Fe II with large absorption or high opacity. - Less opacity in the yellow region, peak in the black body distribution function - reaonson for the yellow sun.

Electron & Photon Distribution Functions in Plasmas

- Temperature 'T' is defined differently for a radiation (photon) or the particle (electron) *kinetic energy distribution:*

$$E = h\nu \sim kT \text{ (photon), or } E = 1/2mv^2 = 3/2kT \text{ (electron)}$$

- Consider a star ionizing a molecular cloud into a gaseous nebula - They two objects, the star & the nebula, have different T distribution functions

- Energy of the radiation emitted by the star - Planck distribution function
- Energies of electrons in the surrounding ionized gas heated by the star - Maxwell distribution
- total energy per m^2sec emitted by an object at temperature T is given by Stefan-Boltzmann Law,

$$E = \sigma T^4 \tag{42}$$

$\sigma = 5.67 \times 10^{-8}$ Watts/(m^2 K^4)= Stefan constant

PLANCK DISTRIBUTION FUNCTION

● Radiation of a star, a blackbody, is given by the Planck distribution function

$$B_\nu(T_*) = \frac{2h\nu^3}{c^2} \frac{1}{\exp(h\nu/kT_*) - 1},\qquad(43)$$

$T_* = $ *radiation temperature*, $\nu = $ frequency of the photons.

MAXWELL DISTRIBUTION FUNCTION

The charged particles in the plasma ionized by a star in an H II region has an electron temperature T_e associated with the mean kinetic energy of the electrons kT_e

$$\frac{1}{2}mv^2 = \frac{3}{2}kT_e. \qquad(44)$$

The velocity (or energy) distribution of electrons is characterized by a Maxwellian function at temperature T_e,

$$f(v) = \frac{4}{\sqrt{\pi}} \left(\frac{m}{2kT}\right)^{3/2} v^2 \exp\left(-\frac{mv^2}{2kT}\right). \qquad(45)$$

PLANCK & MAXWELL DISTRIBUTION FUCNTIONS
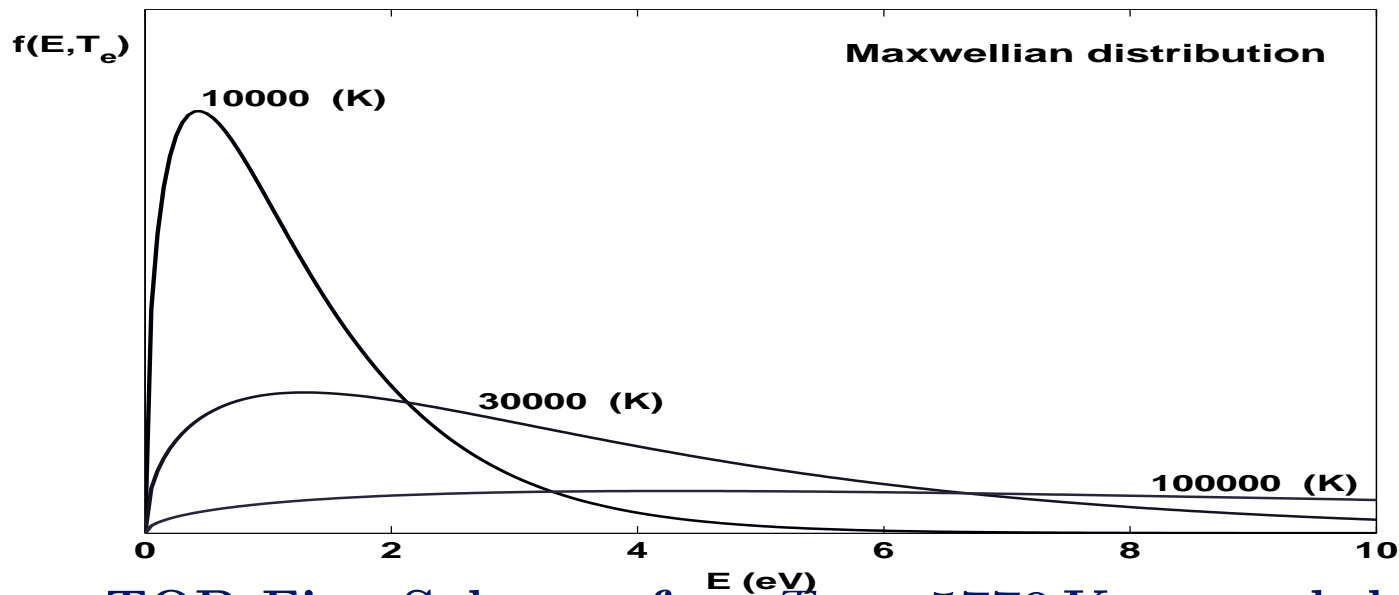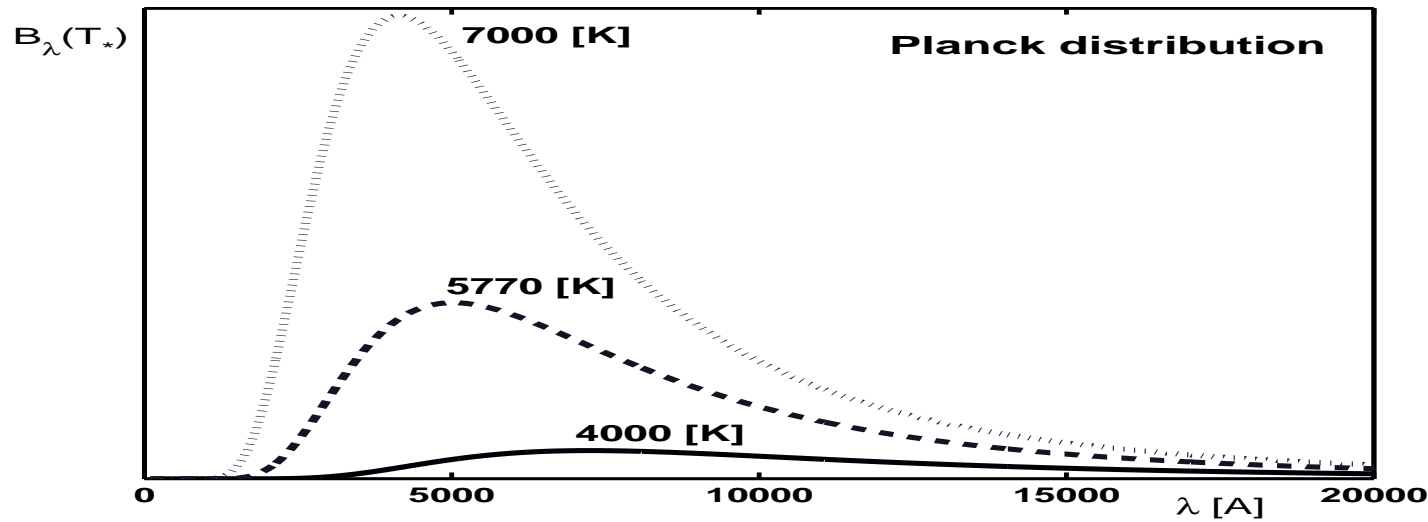
- **TOP Fig:** Solar surface $T_* = 5770\,\mathrm{K} \rightarrow$ peak blackbody emission - yellow $\sim 5500\,\text{Å}$.
- **Bottom Fig:** H II region (nebula): Ionized by star blackbody radiation of $T \sim 30000$ - $40000\,\mathrm{K}$, electron KE of Maxwellian distribution - $T_e \approx 10000 - 20000\,\mathrm{K}$

Monochromatic Opacity κ_ν of Fe II (Nahar & Pradhan 1993)
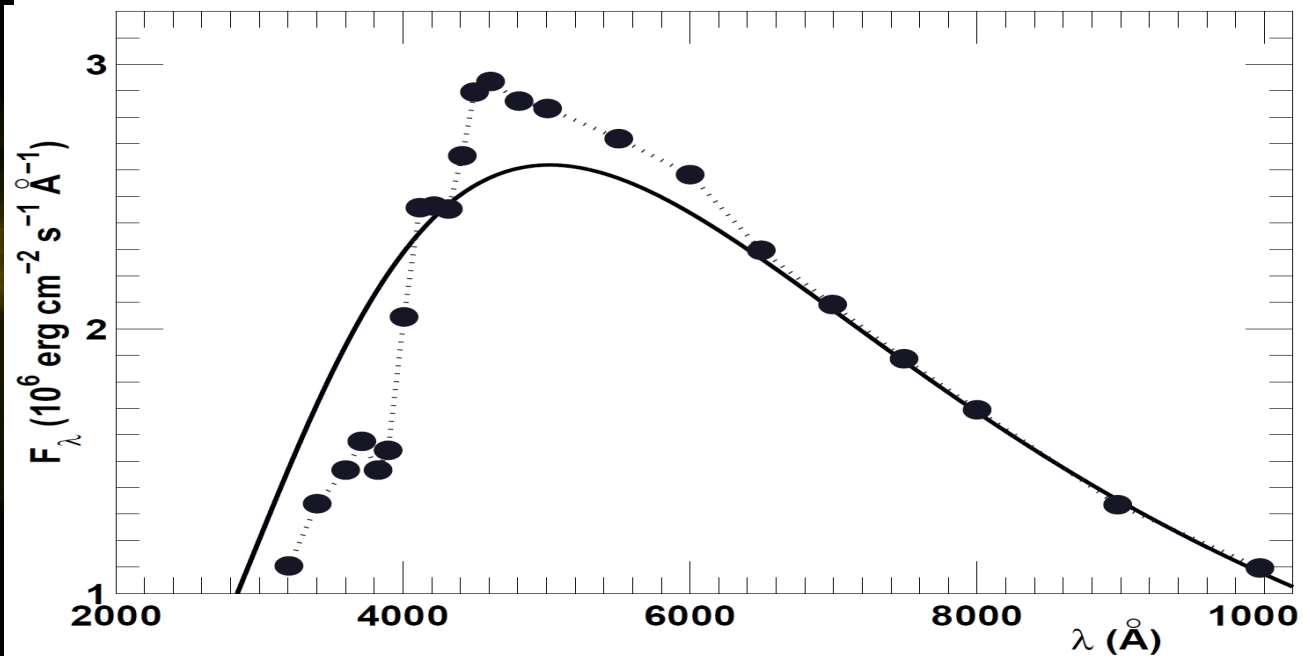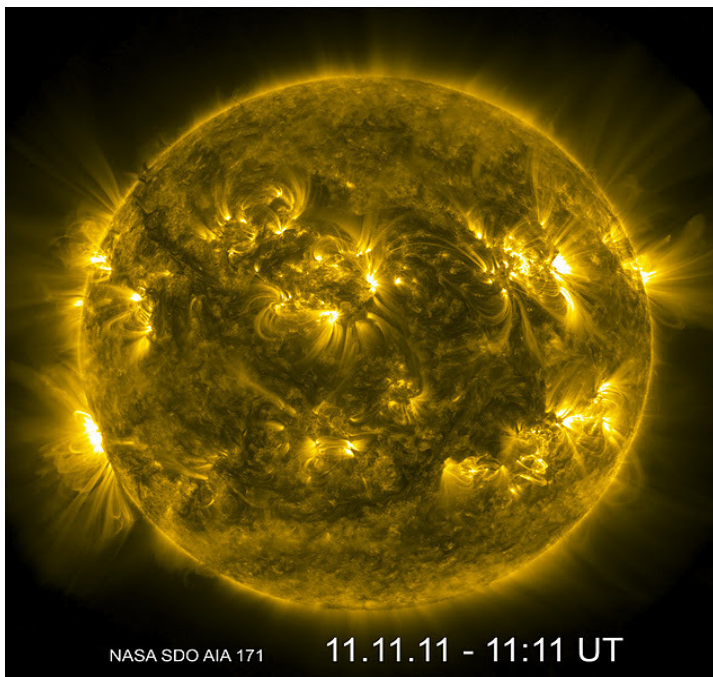
TOP: Flux distribution on solar surface - the discrepancy below 4000 $\mathring{A}$.

BOTTOM: Theory: High radiation absorption (opacity) by Fe II on surface
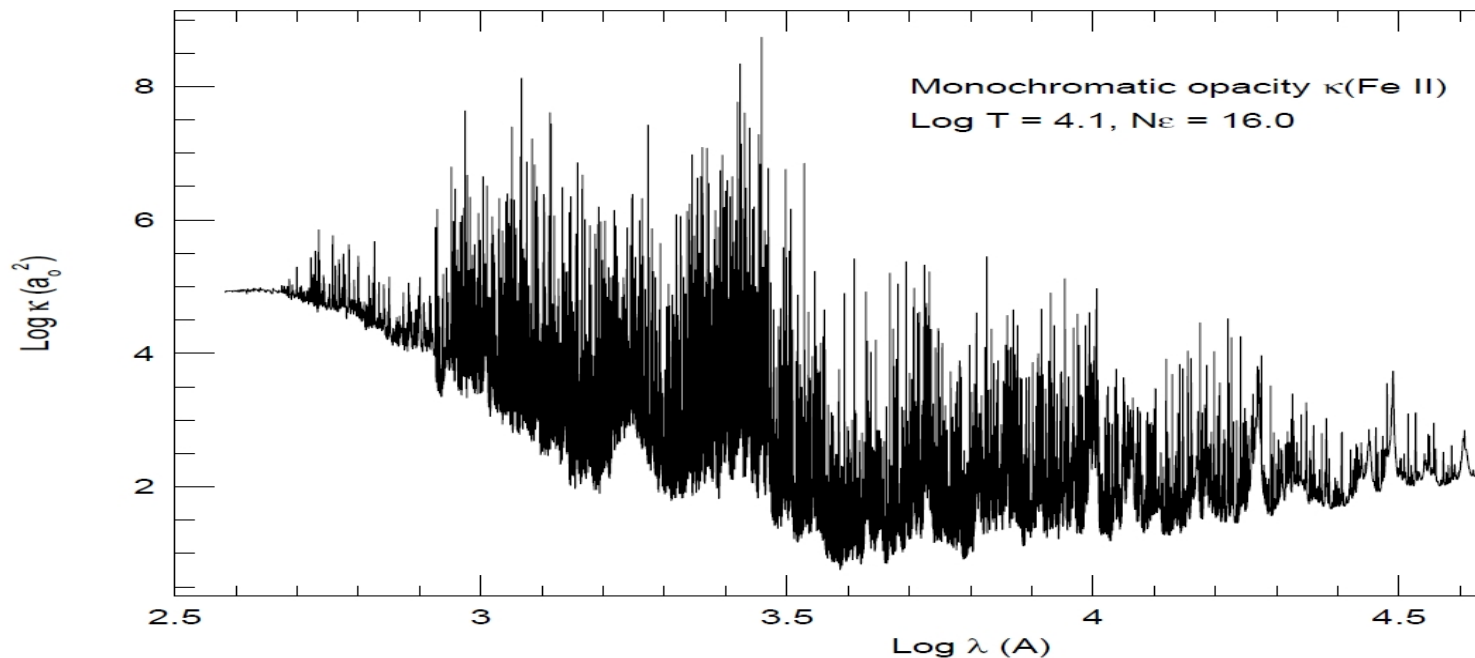
OBSERVATION OF Ti I LINES:

- Ti I in LMC Spectra: PHOENIX, Gemini South
- 157 ly away - a prime target to probe the chemical evolution of stars

LMC 2.3256

Relative Flux vs Wavelength (Å)

Fe I, Fe I, OH, Ti I, OH, CN, OH, OH
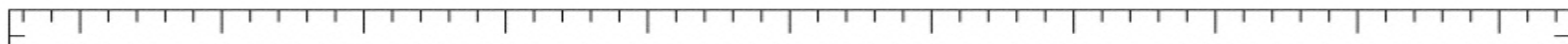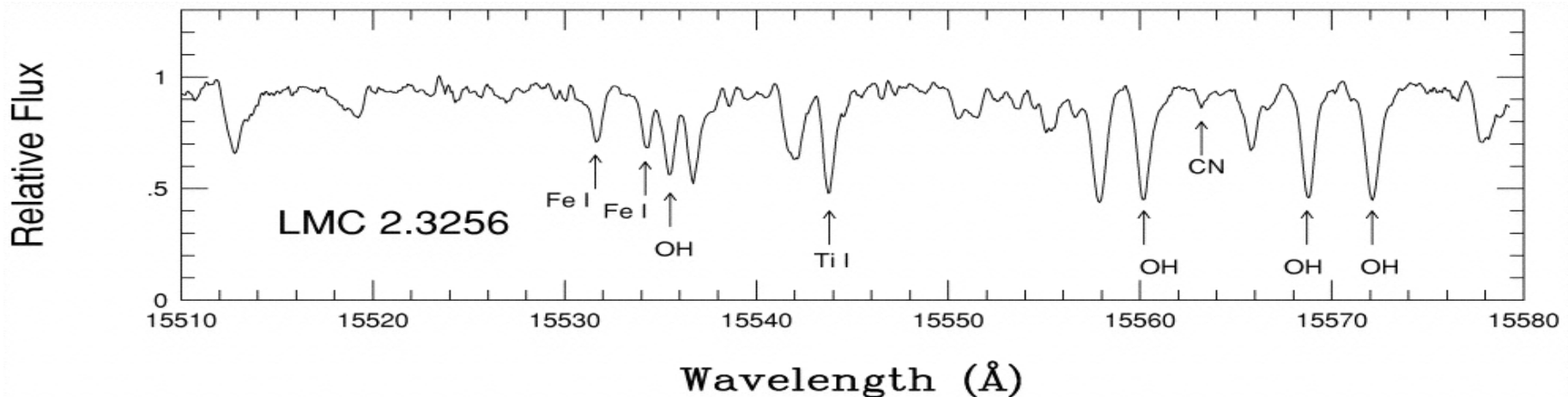
OBSERVATION OF Ti LINES:
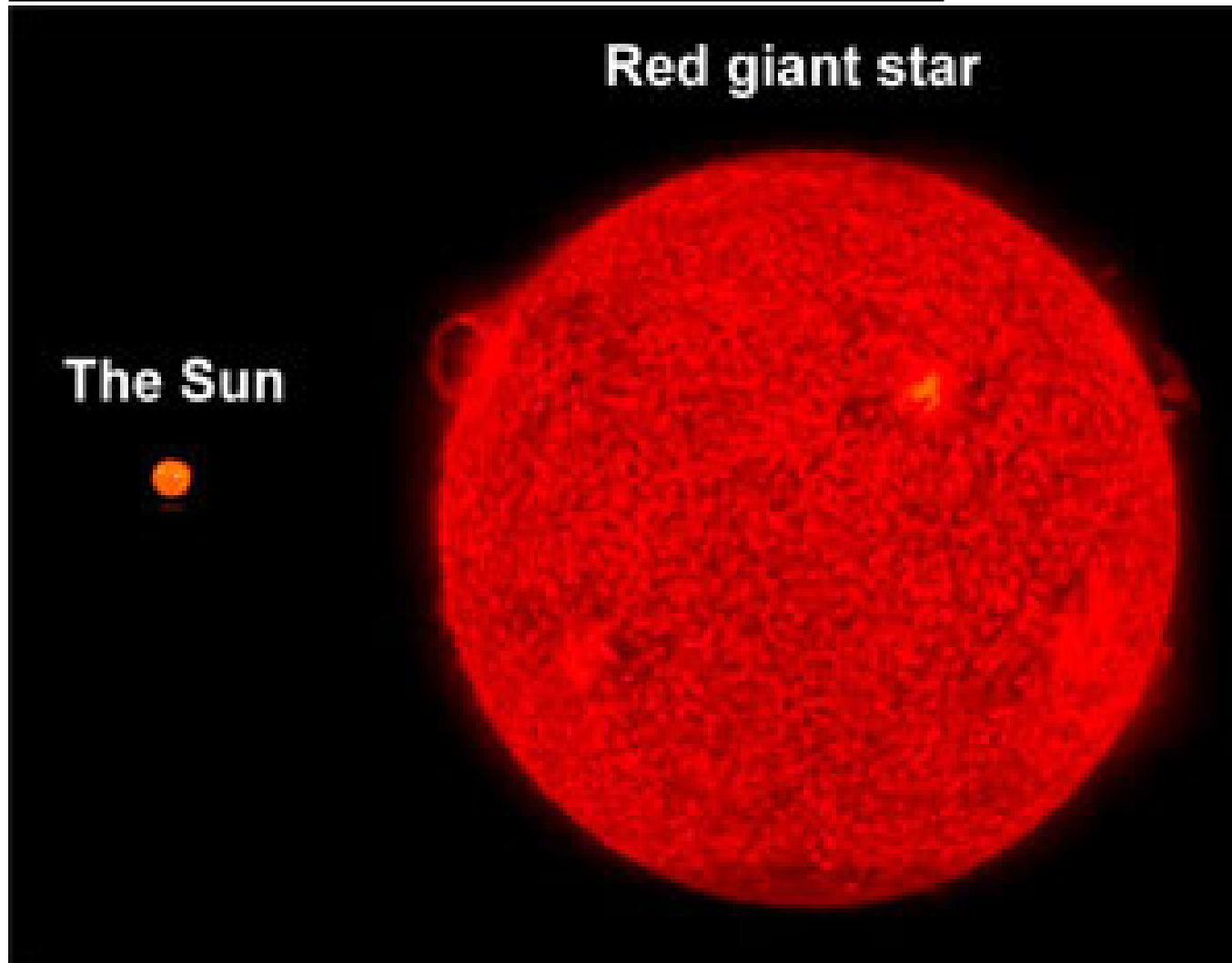
- TiO absorption lines see in spectra of red supergiants. A red giant star is a dying star, the last stages of stellar evolution. The outer atmosphere is inflated and tenuous, the surface temperature low, from 5,000 K and lower.
- Figure shows sun's fate in 6-7 billion years
- Amount of Ti I locked in TiO affect fluxes, spectral energy distributions $\rightarrow$ determination of fundamental stellar parameters & abun-

PHOTOABSORPTION SPECTRUM OF Ti I (Nahar 2016)

- Obtained from **270,423** fine structure transitions
- Dominant absorption from optical to far-infrared (4000$\mathring{A}$ - 100 micron) region - typical for cool stars

Photo-Absorption Spectrum of Ti I

ELECTRON-IMPACT EXCITATION (EIE)

$$e + X^{+Z} \rightarrow e' + X^{+Z*} \rightarrow e' + X^{+Z} + h\nu$$
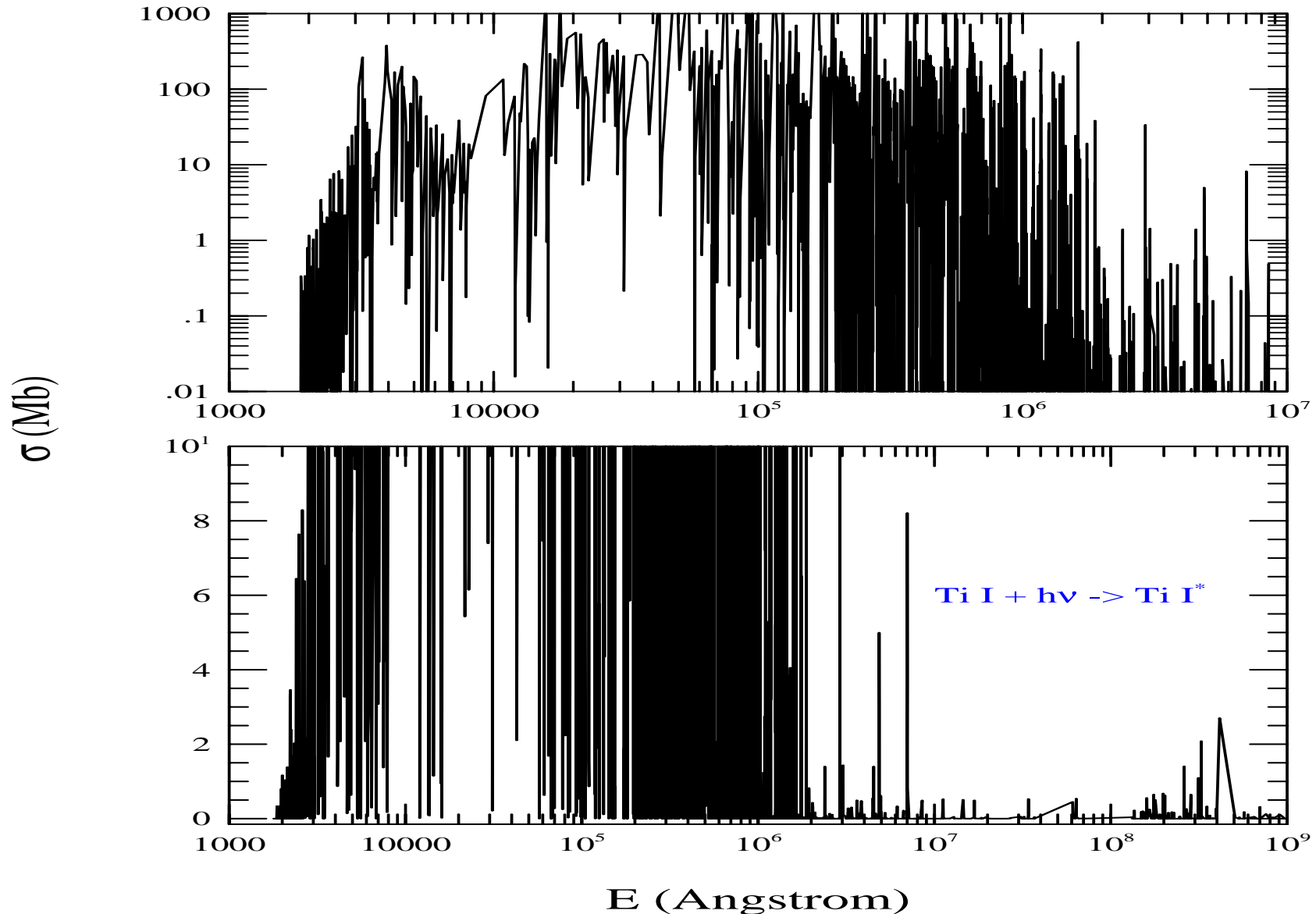
- Light is emitted as the excitation decays
- seen as most common lines in astrophysical spectra
- mostly diagnostic forbidden lines
- Scattered electron shows features with energy & can have autoionizing resonances
- Atomic quantity: *Collision Strength (Ω)*

Fig. Excitation by electron impact:
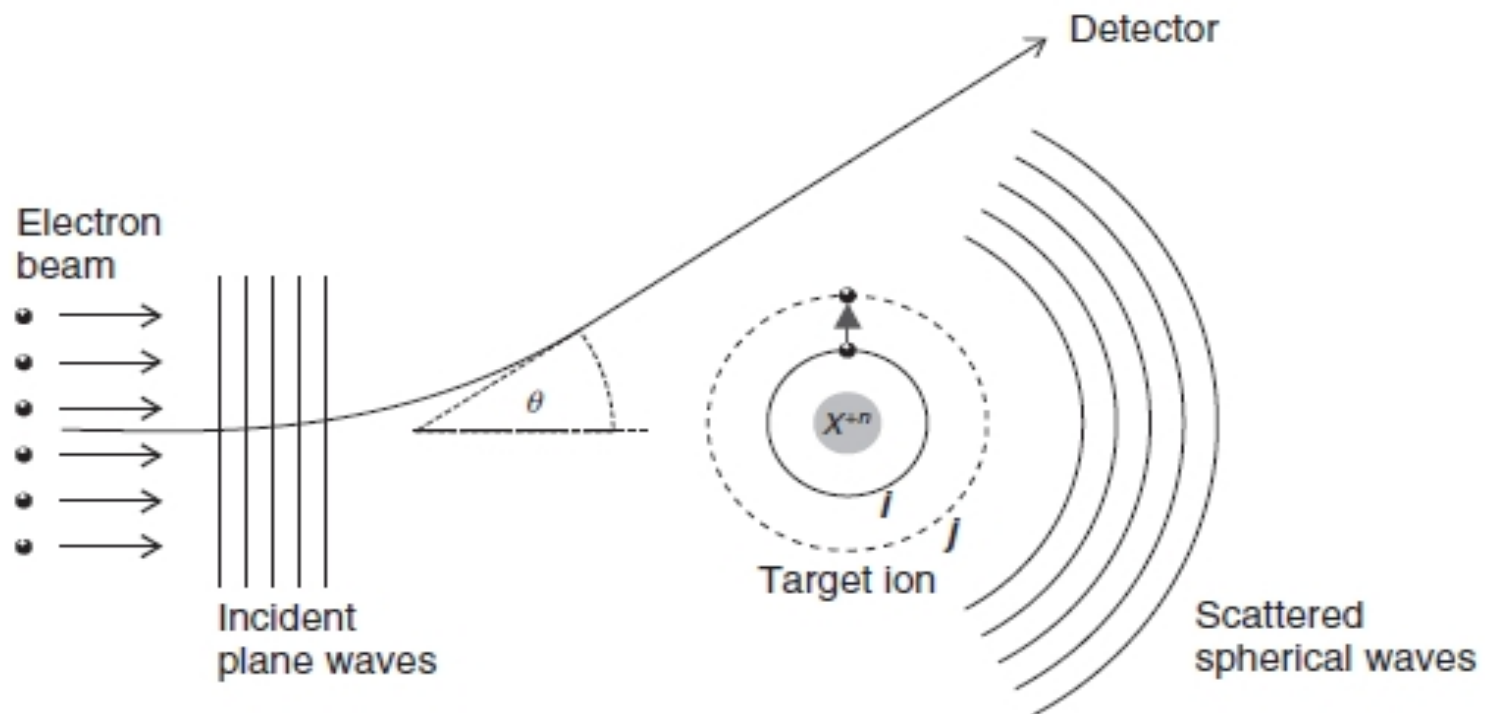
ULTRA-LUMINOUS INFRA-RED GALAXY (ULIRG) IRAS-19297-0406: STUDY THROUGH FORBIDDEN LINES

- ULIRG - emits more than 10^{11} solar luminosities in IR (as stars are born), heavily dust obscured

- Only far-infrared photons (e.g. forbidden lines of Ne V) escape from absorption, observed at high redshift (by SPITZER, HERSCHEL, SOFIA) - provides information on chemical evolution of the galaxy.

ELECTRON IMPACT EXCITATION (EIE)

- EIE Scattering matrix $S_{SL\pi}(i,j)$ is obtained from the wave function phase shift. The EIE collision strength is

$$\Omega(S_iL_i - S_jL_j) = \frac{1}{2}\sum_{SL\pi}\sum_{l_il_j}(2S+1)(2L+1)|S_{SL\pi}(S_iL_il_i - S_jL_jl_j)|^2$$

Ω is a dimensionless quantity, introduced by Seaton. It does not diverge like the cross section, σ_{EIE} at origin,

$$\sigma_{EIE} = \pi/(g_ik^2)\Omega a_o^2,$$

- The quantity used in models is **effective collision strength** $\Upsilon(T)$, the Maxwellian averaged collision strength:

$$\Upsilon(T) = \int_0^\infty \Omega_{ij}(\epsilon_j)e^{-\epsilon_j/kT}d(\epsilon_j/kT)$$

- The **excitation rate coefficient** $q_{ij}(T)$ is given by

$$q_{ij}(T) = \frac{8.63\times10^{-6}}{g_iT^{1/2}}e^{-E_{ij}/kT}\Upsilon(T) \text{ cm}^3\text{s}^{-1}$$

$E_{ij} = E_j - E_i$ in Ry, T in K, $(1/kT = 157885/T)$

ENERGY LEVELS

• Bound energy levels are negative, electron is free at zero energy. Ex: C I and C II levels

<div align="center">Energy Levels</div>

Configuration $^{2S+1}L^\pi$

- -
- -
- -

———————————————— ^2P
———————————————— ^2S
———————————————— ^2D

$2s2p^2$ ———————————————— ^4P

C II: $2s^2 2p$ ———————————————————— $^2P^o$

- -
- -
- -

———————————————— $^1P^o$
———————————————— $^3P^o$
———————————————— $^1D^o$
———————————————— $^3D^o$
———————————————— $^3S^o$

$2s2p^3$ ———————————————— $^5S^o$

———————————————— ^1S
———————————————— ^1D

C I: $2s^2 2p^2$ ———————————————————— ^3P
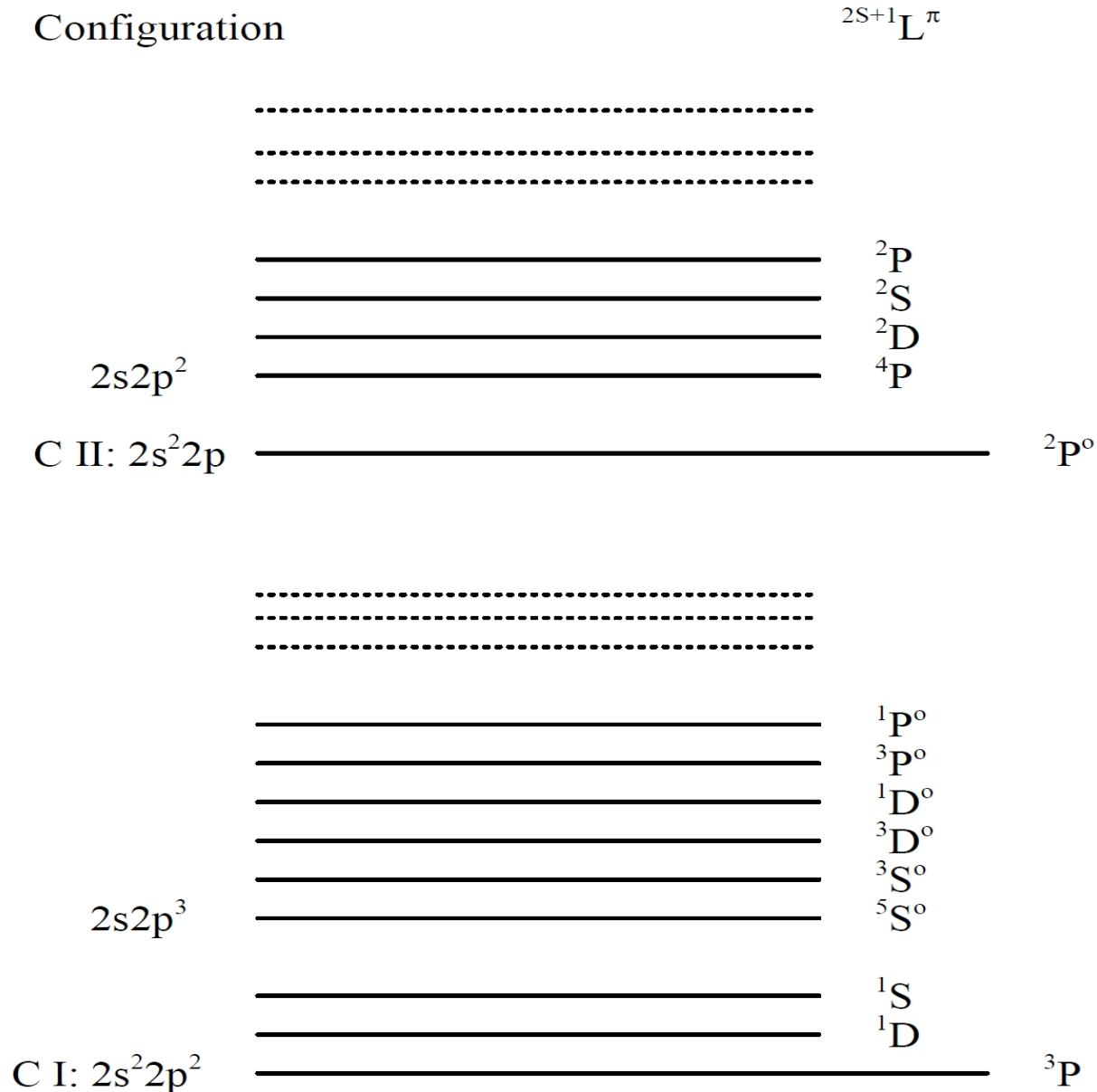
RESONANCES AT AUTOIONIZING RYDBERG STATES $E_x nl$
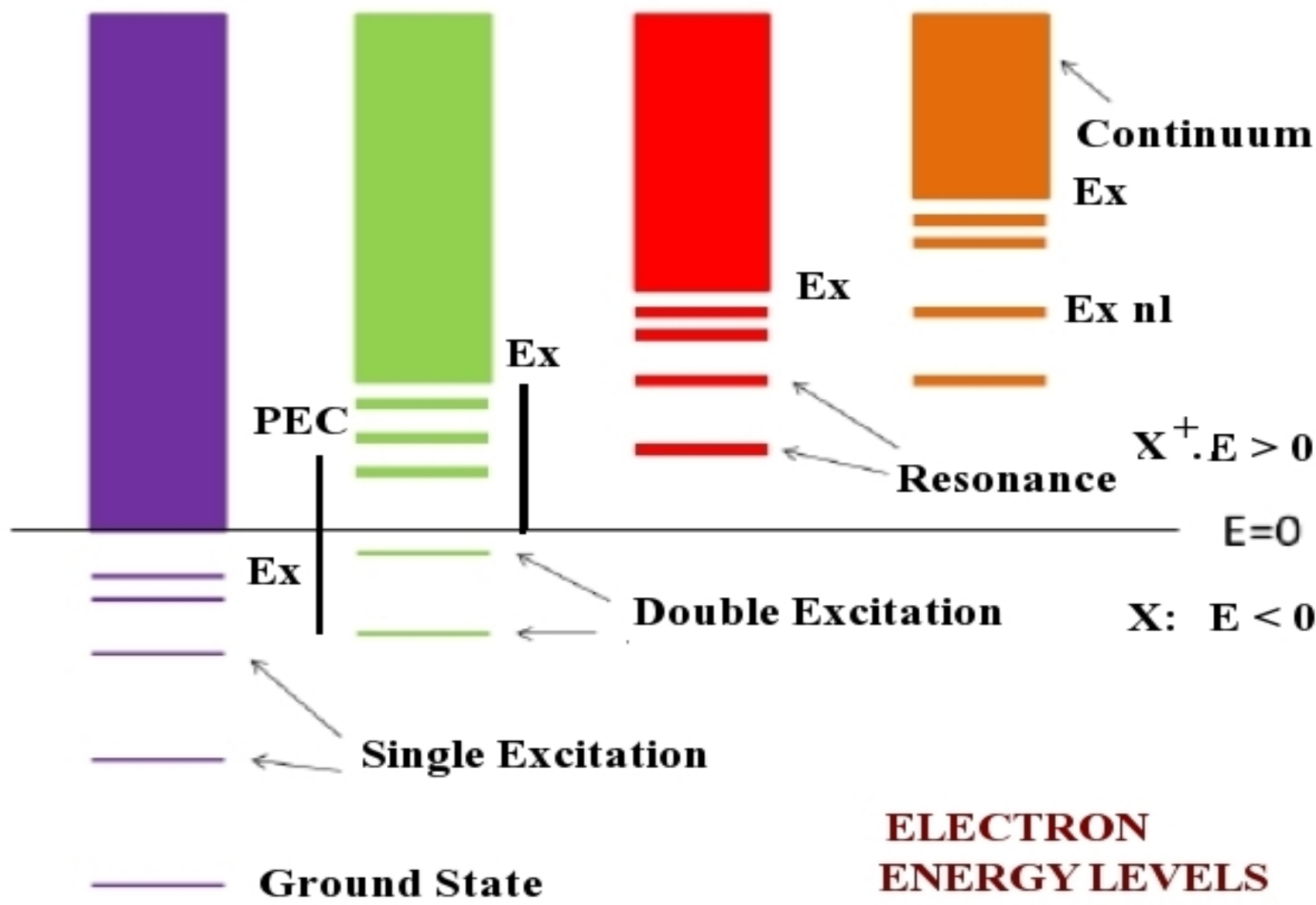
- RESONANT state: Electron at Rydberg state ($E_x nl > 0$)

$$E_x nl = E_{Res} = E^{**}(X^+ \nu l) = E_x - z^2/\nu^2$$

- PEC (Seaton) Resonance: $h\nu = Ex = Ei + Ee$

Close-Coupling (CC) Wave Function & R-matrix Method

- Details: "Atomic Astrophysics and Spectroscopy", A.K. Pradhan and S.N. Nahar (Cambridge press, 2011)

- CC approximation generates resoances naturally
- Wave Function expansion includes excited states of the residual ion which generate resonant states:

$$\Psi_E(e + ion) = A \sum_i^N \chi_i(ion)\theta_i + \sum_j c_j \Phi_j(e + ion)$$

- Resonances increase with increase of excited residual states
- Substitution of $\Psi_E(e + ion)$ in Schrodinger equation

$$H\Psi_E = E\Psi_E$$

results in a set of coupled euqations
- The equations are solved by the R-matrix method
- $E < 0 \rightarrow$ Bound (e+ion) states Ψ_B
- $E \geq 0 \rightarrow$ Continuum states Ψ_F
- Ψ_B & Ψ_F are used for parameters of the atomic processes

EIE OF O III (Palay et al 2012)

- Fig Resonanes in Ω (EIE): Top: $2p^2(^3P_0 - {}^3P_1)$ (88μm), Bottom: $2p^2(^3P_1 - {}^3P_2)$ (52μm) -IR)
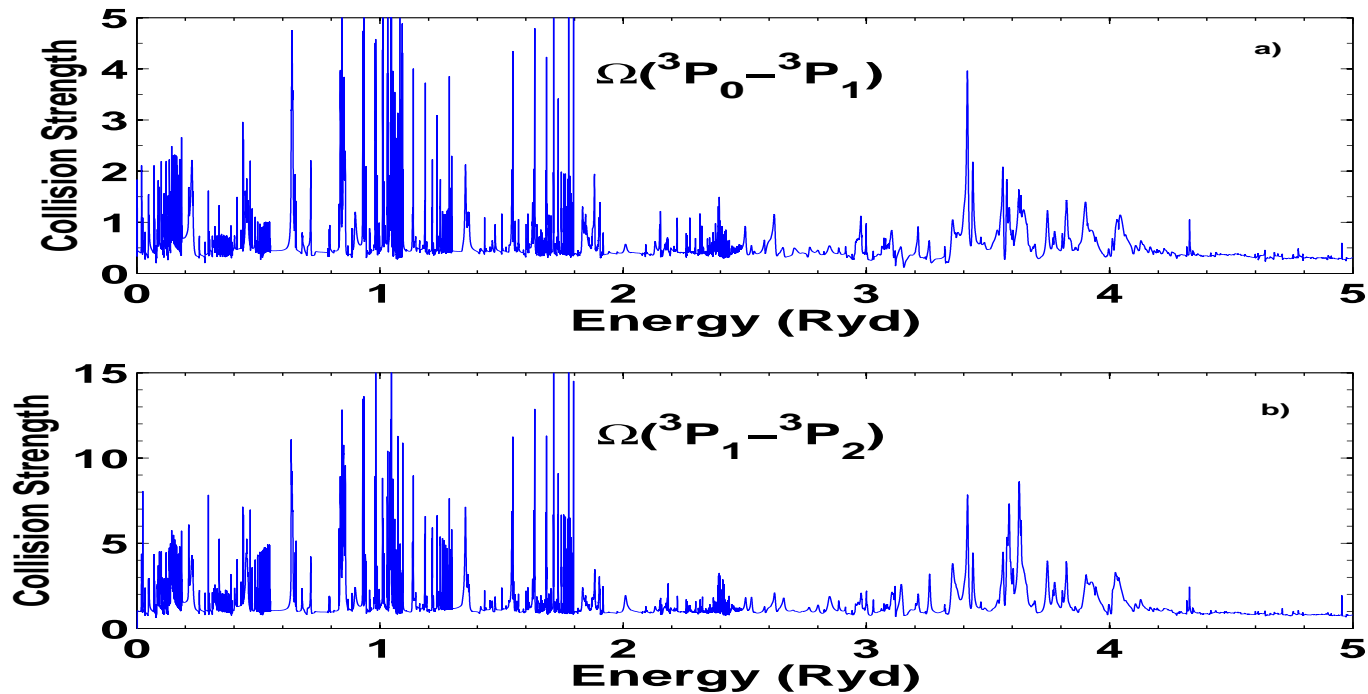
- Fig $\Gamma(T)$ of 3 optical lines; Solid: BPRM (present), Dashed: R-matrix(LS) (Aggarwal & Keenan) Differences affect T and ρ
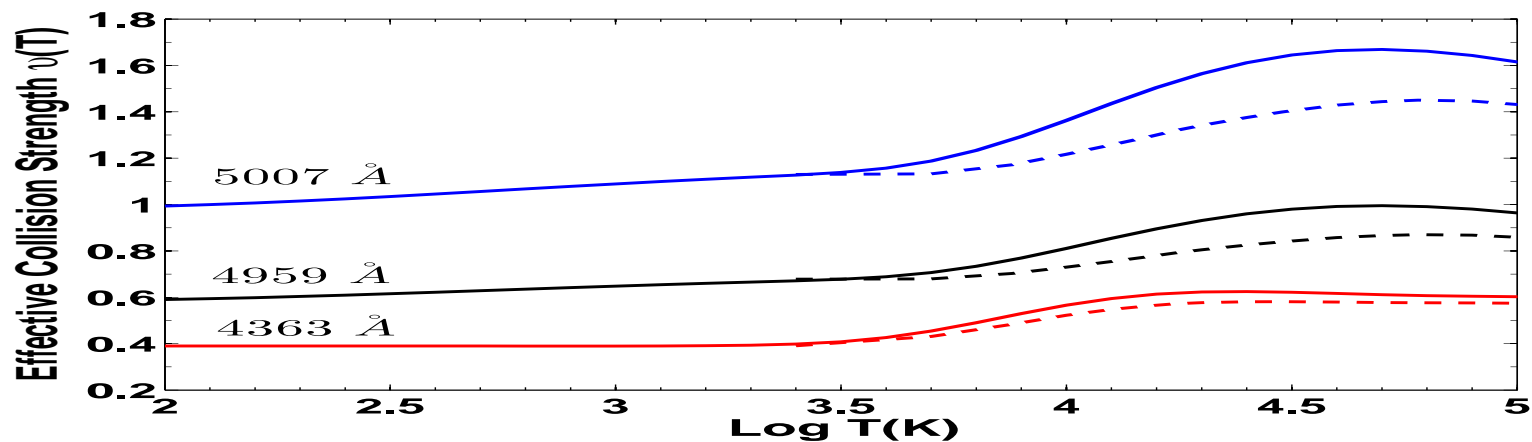
LINE RATIO DIAGNOSTICS

- Collisionally Excited Lines (CEL):

$$\mathrm{e} + \mathrm{X}^+ \to \mathrm{X}^{+*} \to \mathrm{X}^+ + \mathrm{h}\nu$$
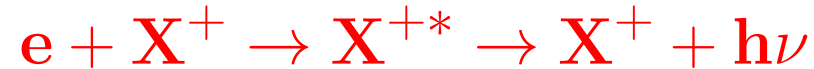
- The intensity of a CEL due to transition between a & b

$$\mathrm{I_{ba}(X^+, \lambda_{ba})} = \frac{\mathrm{h}\nu}{4\pi}\mathrm{n_e n_{ion} q_{ba}}$$

$\mathrm{q_{ba}}$ - EIE rate coeffcient in $\mathrm{cm}^3/\mathrm{sec}$.

- The ratio of intensities, mainly the emissivity ratio, of two different lines arising from the same level can be used for temperature and density diagnostics.
- The ratio depends on the level populations.
- Level populations depend on excitation rate coefficients and electron density.

$$\frac{\mathrm{I_{ji}(\lambda_{ji})}}{\mathrm{I_{lk}(\lambda_{lk})}} = \frac{\nu_{ji}\mathrm{n'_{ion}}}{\nu_{lk}\mathrm{n''_{ion}}}\frac{\mathrm{q_{ji}}}{\mathrm{q_{lk}}}$$

The density or T are varied for the line ratios to carry out the diagnostices of plasmas.

LINE RATIO: DENSITY ρ & T DIAGNOSTICS (Palay et al 2012)

• Intensity ratio of two observed lines can be compared to the calculated curves for density (ρ) & T diagnostics. Significant FS effect on ρ diagnostics, 100 - 10,000 K
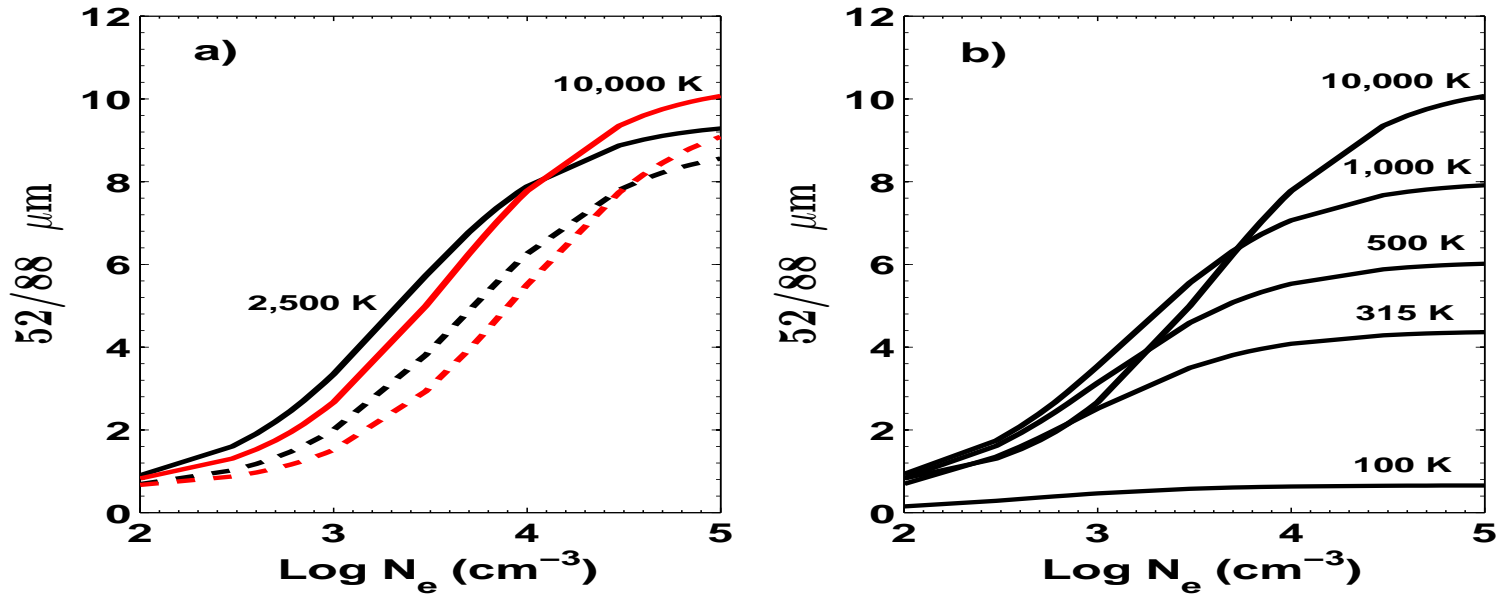
Blended line ratio with T at $N_e = 10^3 cm^{-3}$ indicates considerable rise in low T region
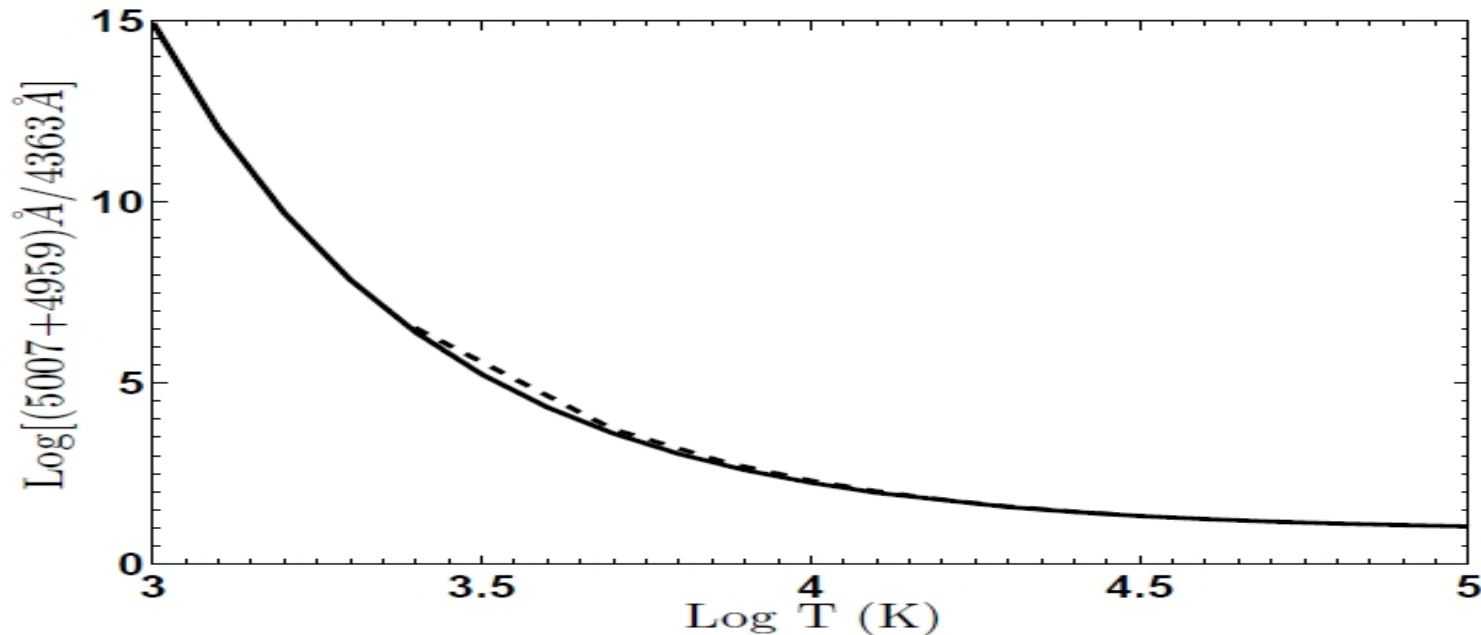
EIE: LINE RATIOS OF Ne V (Dance et al 2010)

- The intensity of a CEL of ion X_i: $\quad I_{ba}(X_i, \lambda_{ba}) = \left[\frac{h\nu}{4\pi} n_e n_{ion}\right] q_{ba}$
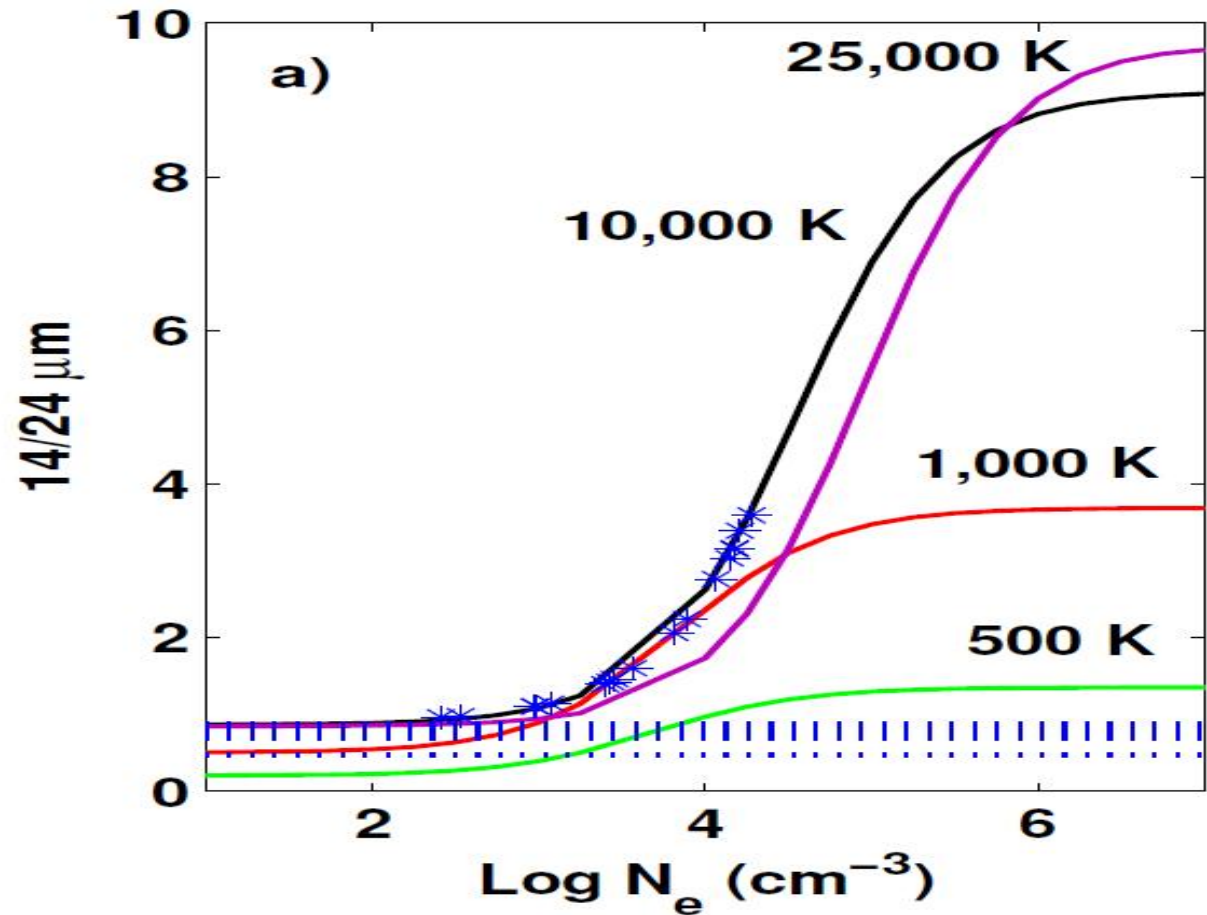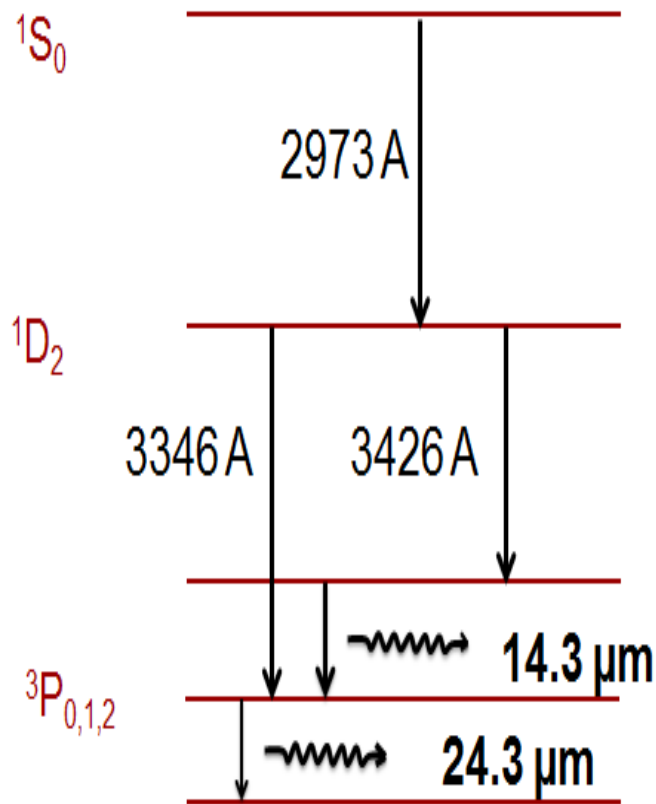
- **Comparison:** IR 14/24 μm line emissivity ratios: a) Present curves (solid) at different T, Asterisks (observed from PNe at T = 10,000 K with assigned densities, Rubin 2004), Dotted curves (observed line ratios, outside typical nebular T-ρ range except at low T, Rubin 2004), • Better agreement at T = 10,000 (10 PNe) and 500 K (anomalously

DETERMINATION OF ELEMENTAL ABUNDANCES

From the intensity of a line

$$I_{ba}(X^+, \lambda_{ba}) = \frac{h\nu}{4\pi} n_e n_{ion} q_{ba}$$

population of a level b can be written as

$$N(b) = n_{ion} q_{ba} = \frac{1}{n_e} \frac{4\pi}{h\nu} I_{ba}$$

Abundance of element X w.r.t. H, $n(X)/n(H)$, can be obtained from the intensity I of a collisional exited line of wavelength λ_{ba} from its ionization state X_i using several quantities. as

$$I(X^+, \lambda_{ba}) = \frac{h\nu}{4\pi} A_{ba} \frac{N(b)}{\sum_j N_j(X^+)} \frac{n(X^+)}{n(X)} \left[\frac{n(X)}{n(H)}\right] n(H)$$

A_{ba} = radiative decay rate, $\sum_j N_j$ = total populations of all excited levels, $N(b)/\sum_j N_j(X^+)$ = population fraction, $\frac{n(X^+)}{n(X)}$ - ionization fraction (from photoionization model)

Determination of Abundance of Elements Orion Nebula - Birthplace of Stars

- Orion Nebula ~ 1500 Lyr away, closest cosmic cloud to us. Center bright & yellow gas - illuminated ultraviolet (UV) radiation Images: Spitzer - Infrared (red & orange) C rich molecules - hydrocarbons, Hubble - optical & UV (swirl green) of H, S. Small dots - infant stars; over 1000 young stars
Detected lines of O II, O III

PLANETARY NEBULAE - Endpoint of a Star [PNe K 4-55 below]

- **Condensed central star: very high T $\sim$ 100,000 K ($>>$ T $\leq$ 40,000 K - typical star). Envelope: thin gas radiatively ejected & illuminated by central star radiation: red (N), blue (O). Lines of low ionization states - low ρ & low T**
- **Ionized gasous nebulae: associated with birth & endpoint of stellar evolution $\longrightarrow$ chemical enrichment is a chronometer of life of the universe itself** ● **Problem: OXYGEN Abundance - N_{oxygen}-**

PHOTOIONIZATION (PI):
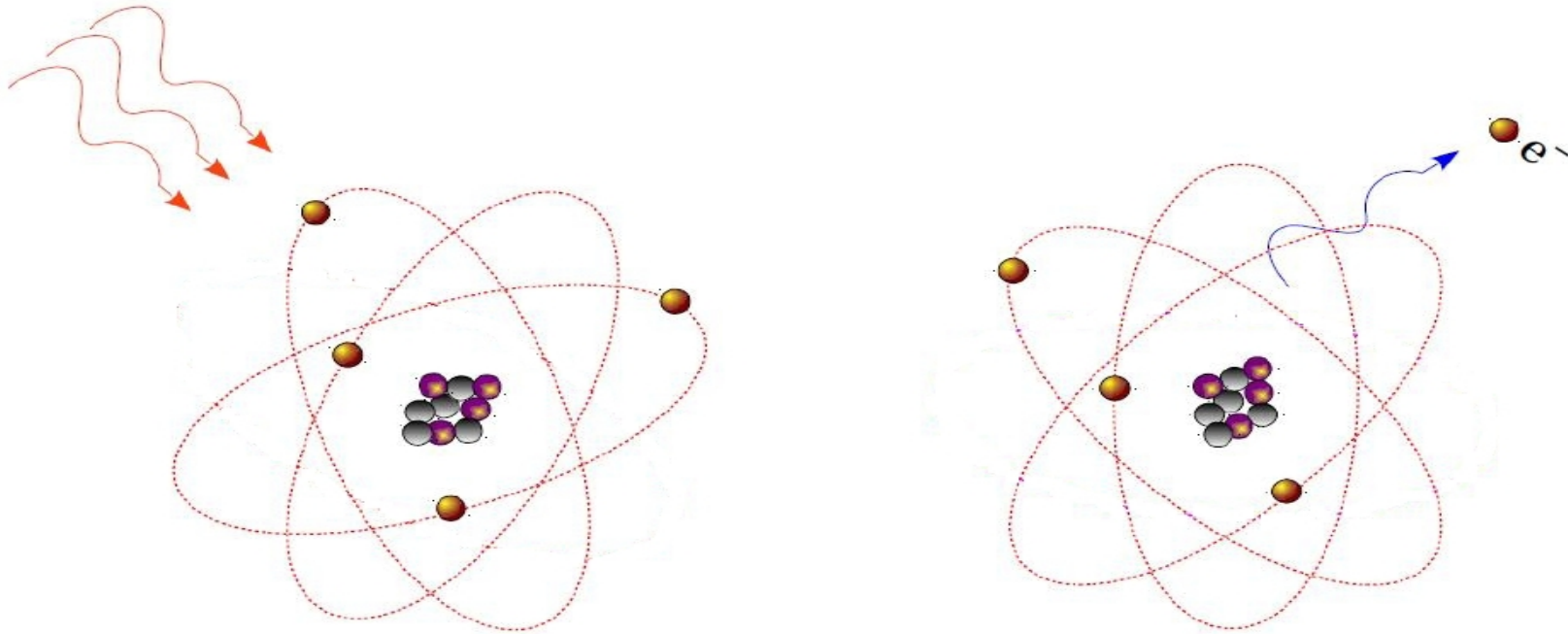
i) **Direct Photoionization (background):**

$$\mathbf{X^{+Z} + h\nu \rightleftharpoons X^{+Z+1} + \epsilon}$$

ii) **Resonant Photoionization: an intermediate state before ionization** → "Autoionizing state" → **RESONANCE**

$$\mathbf{X^{+Z} + h\nu \rightleftharpoons (X^{+Z})^{**} \rightleftharpoons X^{+Z+1} + \epsilon}$$

- κ_ν depends on photoionization cross section $\sigma_{\mathbf{PI}}$

$$\kappa_\nu = N_i \sigma_{\mathbf{PI}}(\nu)$$

PHOTOIONIZATION (PI) RECOMBINATION

- Quantities are:
- Photoionization cross section σ_{PI} and rates

Examples of observation:
- PI - in absorption & RC - in emission spectra
- Determine ionization fractions in astrophysical plasmas

Radiative Transition Matrix:

$$\mathbf{T_{BF}} = \; < \mathbf{\Psi_F \| D \| \Psi_B} >$$

$\mathbf{D} = \sum_n r_n$, $n = $ number of electrons

Matrix element is reduced to generalized line strength

$$\mathbf{S} = | < \mathbf{\Psi_j \| D \| \Psi_i} > |^2 = \left| \left\langle \Psi_f \left| \sum_{j=1}^{N+1} \mathbf{r_j} \right| \Psi_i \right\rangle \right|^2$$

Photoionization: The cross section is

$$\sigma_{\mathbf{PI}} = \frac{4\pi}{3c} \frac{1}{g_i} \omega \mathbf{S},$$

$\omega \rightarrow$ incident photon energy in Rydberg unit

PHOTOIONIZATION: H (1-electron), He (2-electrons)

- TOP FIG: PI of H - decays smoothly
- BOTTOM FIG: PI(g) of He - An atom with more than 1 electron will have resonances in σ_{PI} Resonance series: $2pn\ell$- the lowest one is $2s2p$ They become narrower & denser with ν, & converge on to the excited n = 2 core state

H I (ns ^{2}S) + hν -> H II + e
(Nahar 1996)

1s

2s

3s

4s

5s

He I (1s^2 ^{1}S) + hν -> He II + e
(Nahar 2010)

n=2 threshold
of the core

σ_{PI} (Mb)

Photon Energy (Ry)
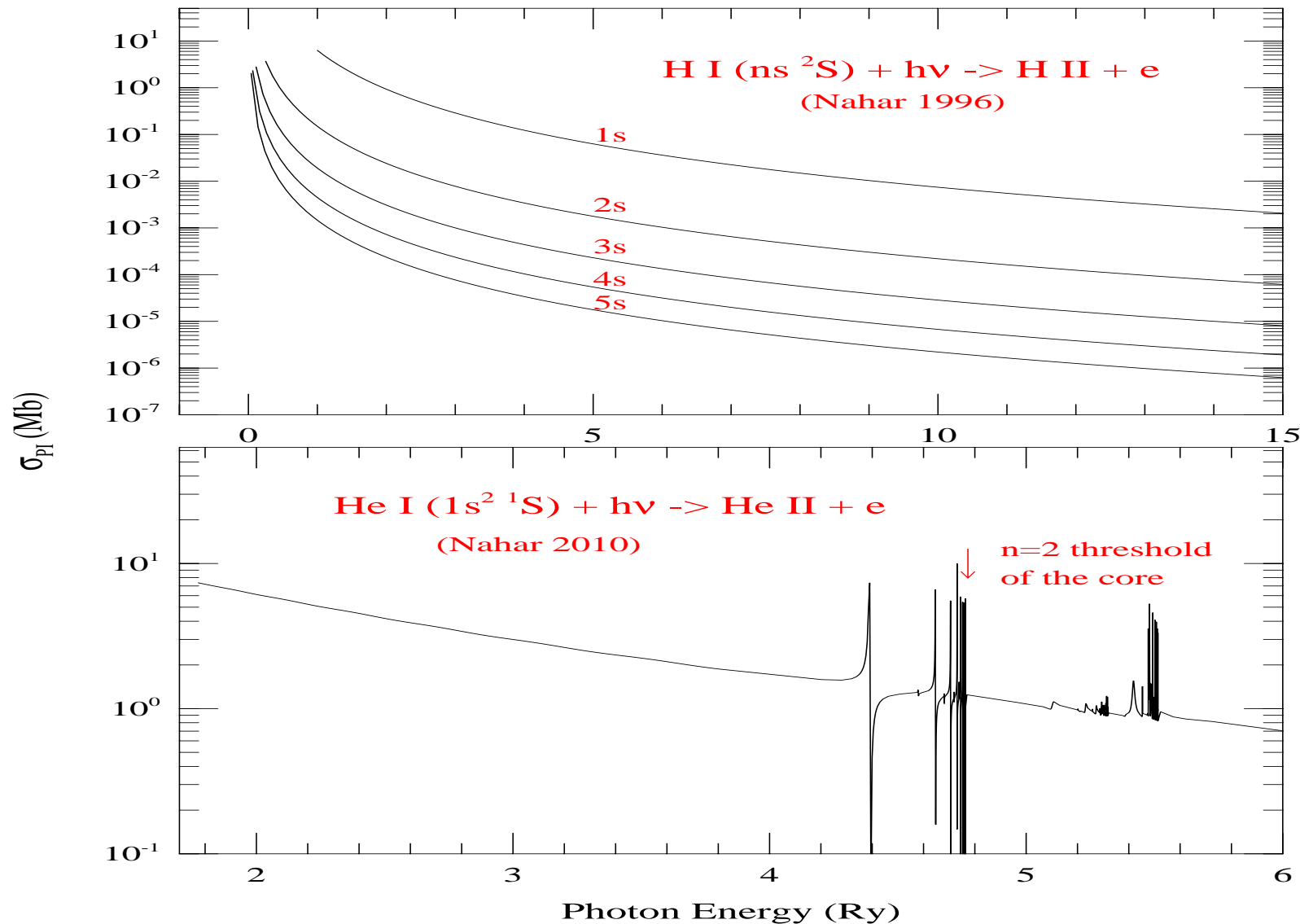
Photoioinization of N IV: Theory & Experiment

TOP: Measured at synchrotron facility BESSY II (Simon et al 2010)
BOTTOM: Comparison with NORAD-Atomic-Data (blue, Nahar & Pradhan 1997). MCDF (Orange drop lines)
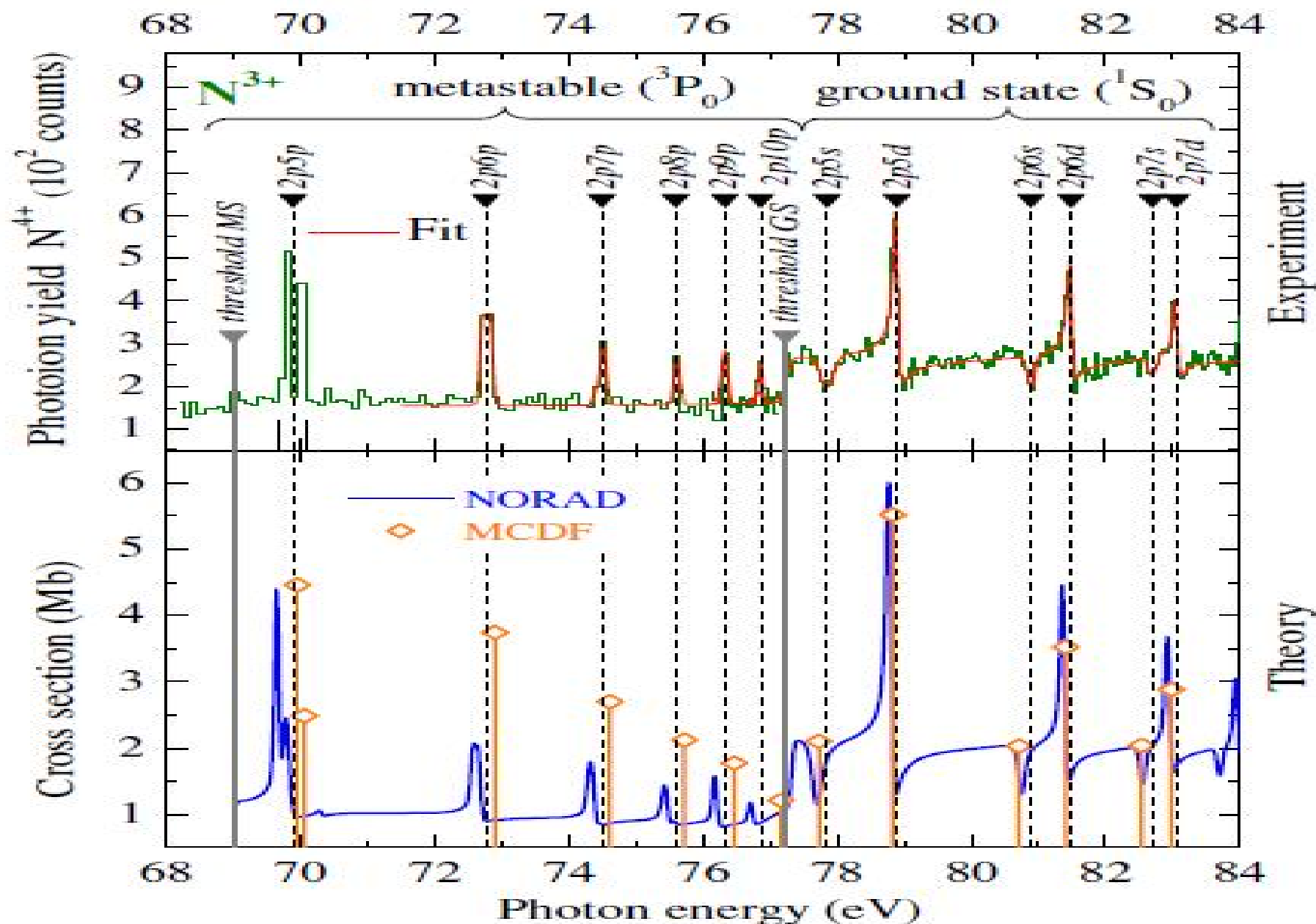
PHOTOIONIZATION RESONANCE CAN BE SEEN IN ABSORPTION SPECTRUM
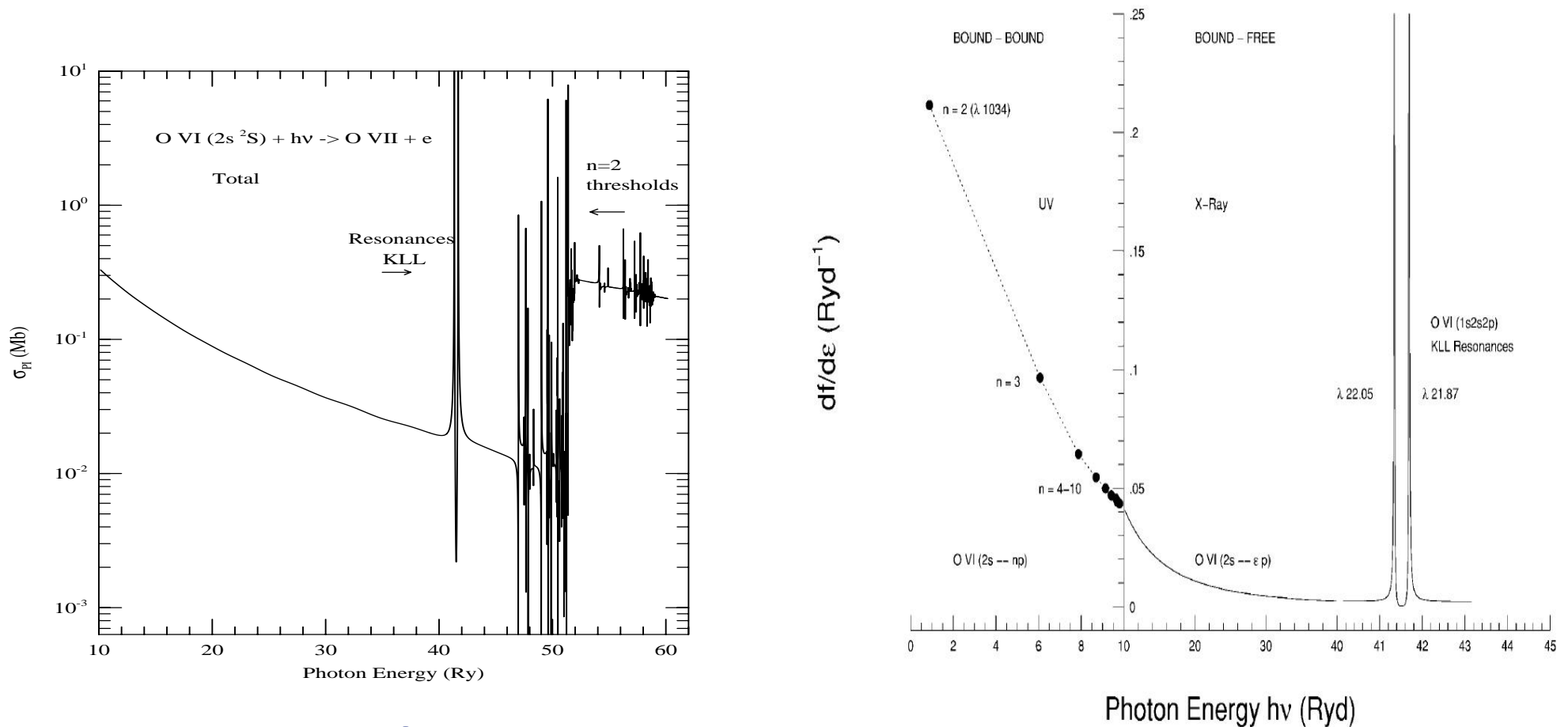
L) KLL ($1s^2 2s - 1s2s2p$) or Kα resonances in photoionization of Li-like O VI (Nahar 1998).

R) Pradhan (2000) calculated the resonant oscullator strength and predicted the presence of the absorption KLL lines at **22.05** and **21.87** $\mathring{A}$ between the two emission lines i and f of He-like O VII at **21.80** and **22.01** $\mathring{A}$

PHOTOIONIZATION RESONANCE SEEN IN ABSORPTION SPECTRUM
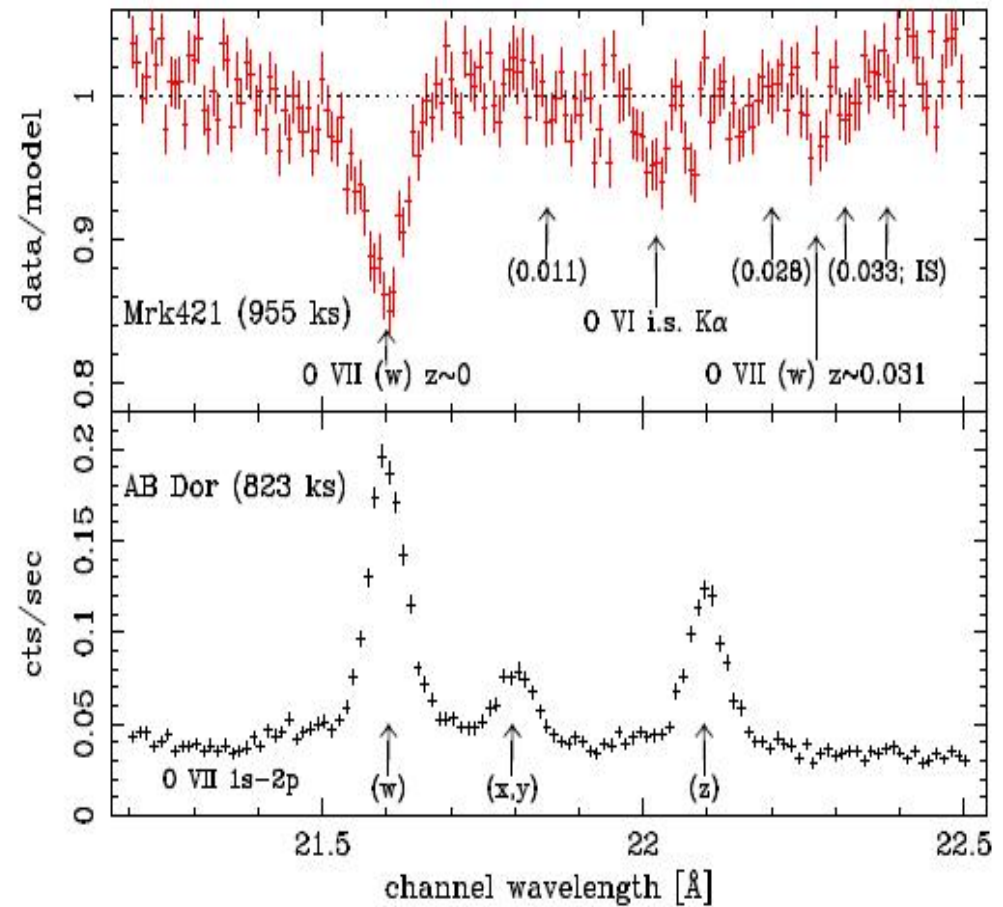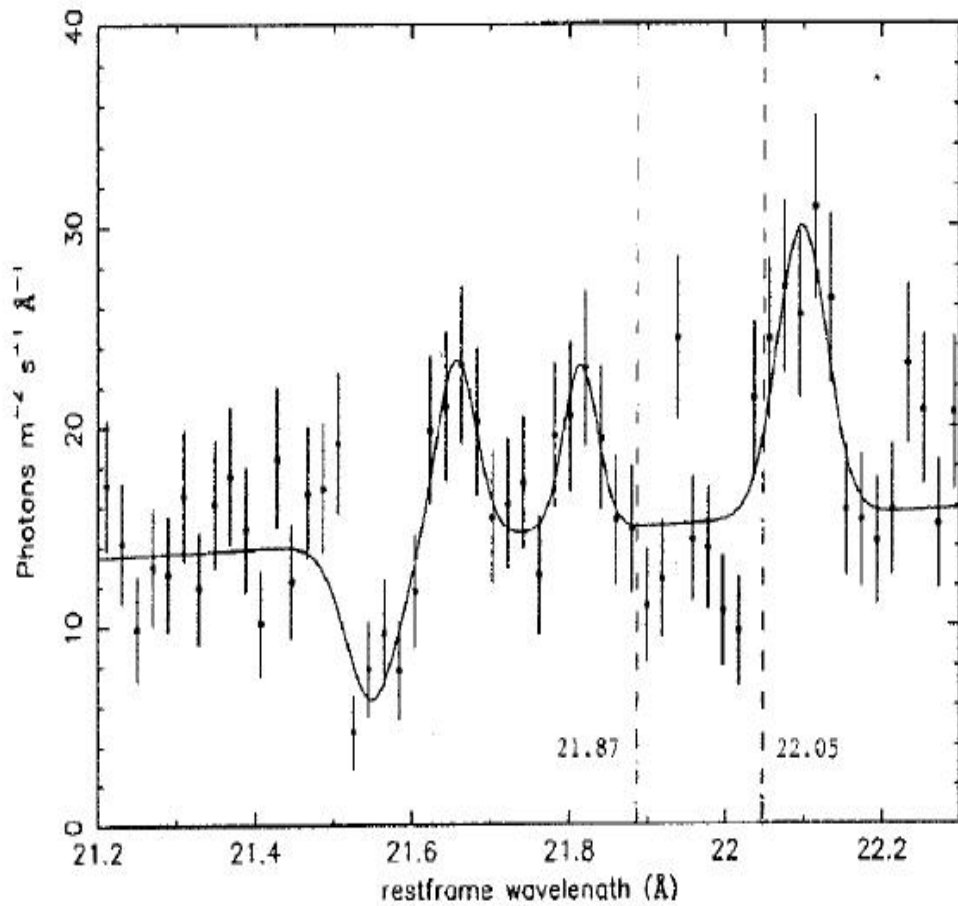
L) Pradhan (APJL 2000) identified the O VI absorption lines in between the two x-ray emission lines of O VII in the spctra of Seyfert galaxy NGC5548 (Kastra et al 2000). R) These lines were later detected in the X-ray spectra of Mrk 421 observed by XMM-Newton (Rasmussen et al 2007) and led to estimation of oxygen abundance

PHOTOIONIZATION OF P II: Experiment (ALS, Berkeley)
(Guillermo et al. 2015
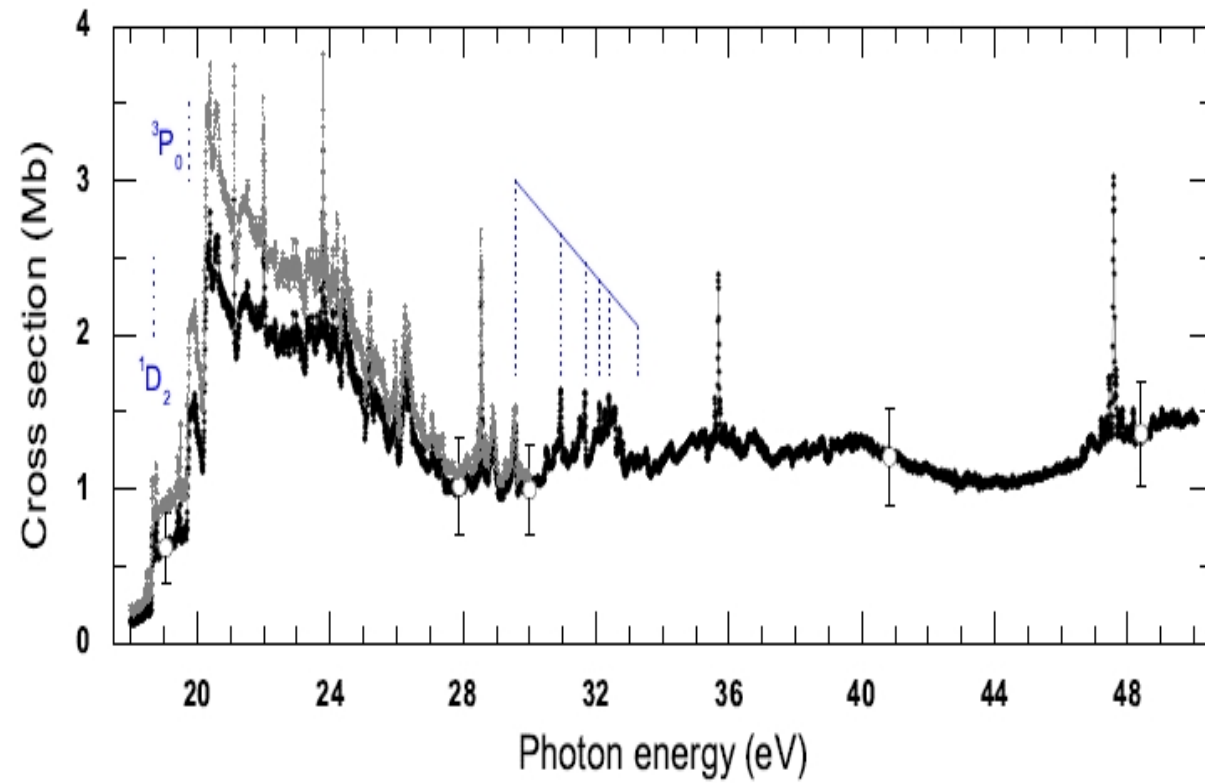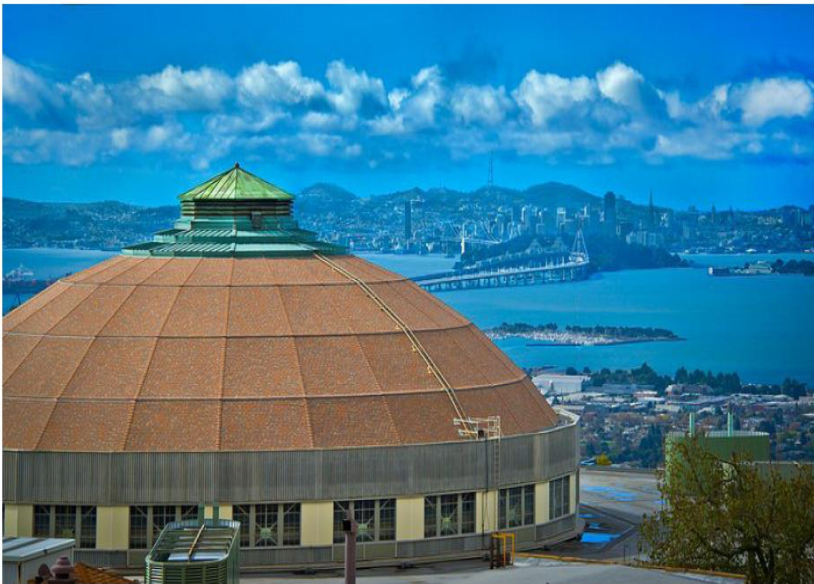
- Synchrotron based Advanced Light Source (ALS) produces high resolution photoionization spectra
- Figure shows combined features of states in target beam
- Needs theoretical spectral analysis for identification of features and abundance of states

MOTIVATION: P DETECTION IN SPACE

- P is a highly reactive element. It is used extensively in fertilizers, detergents, pesticides, plasticizers, etc
- It is also a basic element of evolution.
- Phosphorus, a constituent of DNA, cells, teeth, bone, has been searched in cosmos for a long time (Cartoon: "Our Cosmic Selves", New York Times, 2015, DNA Polymer)

THE NEW YORK TIMES, SUNDAY, APRIL 5, 2015

DNA Polymer

Atomic Key:
- Hydrogen
- Carbon
- Nitrogen
- Oxygen
- Phosporous
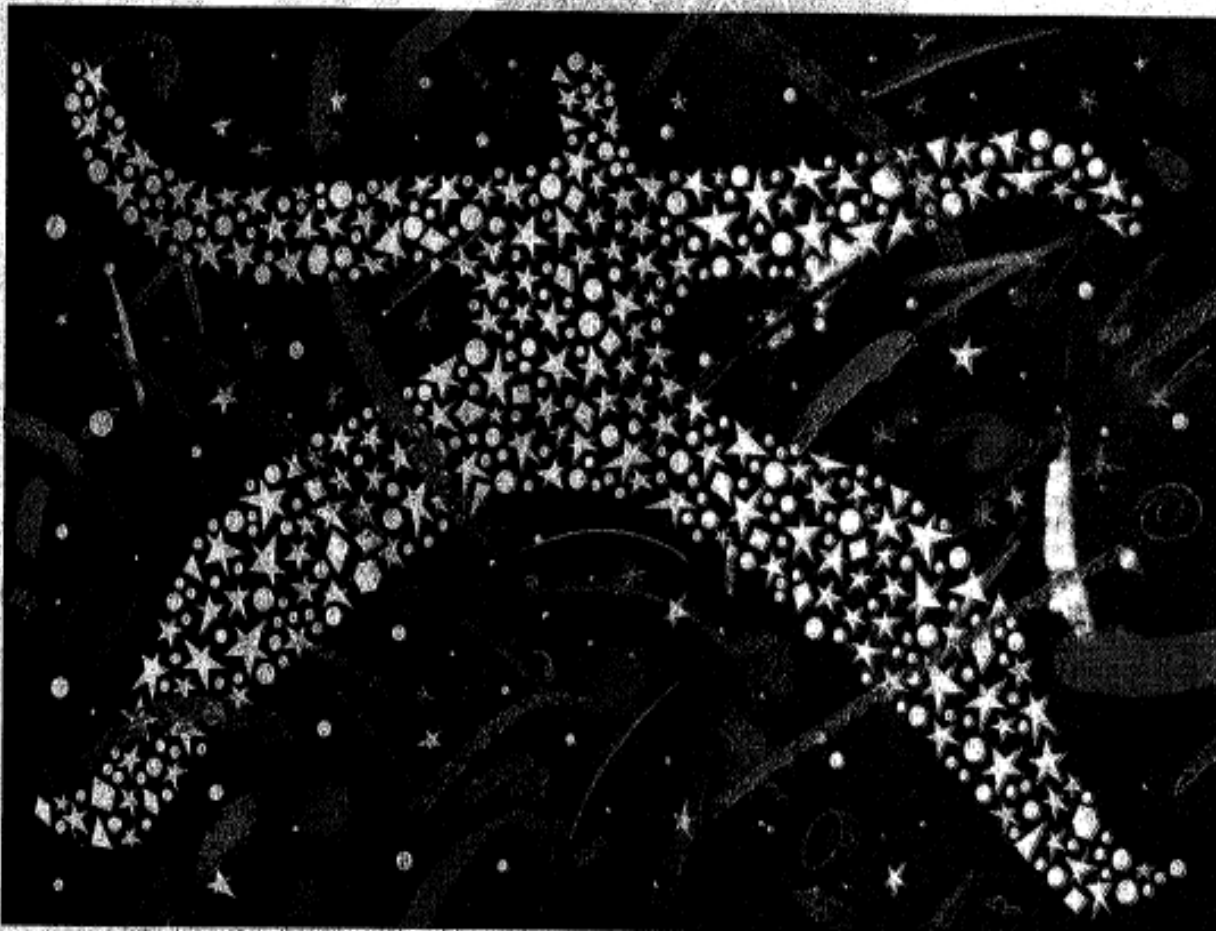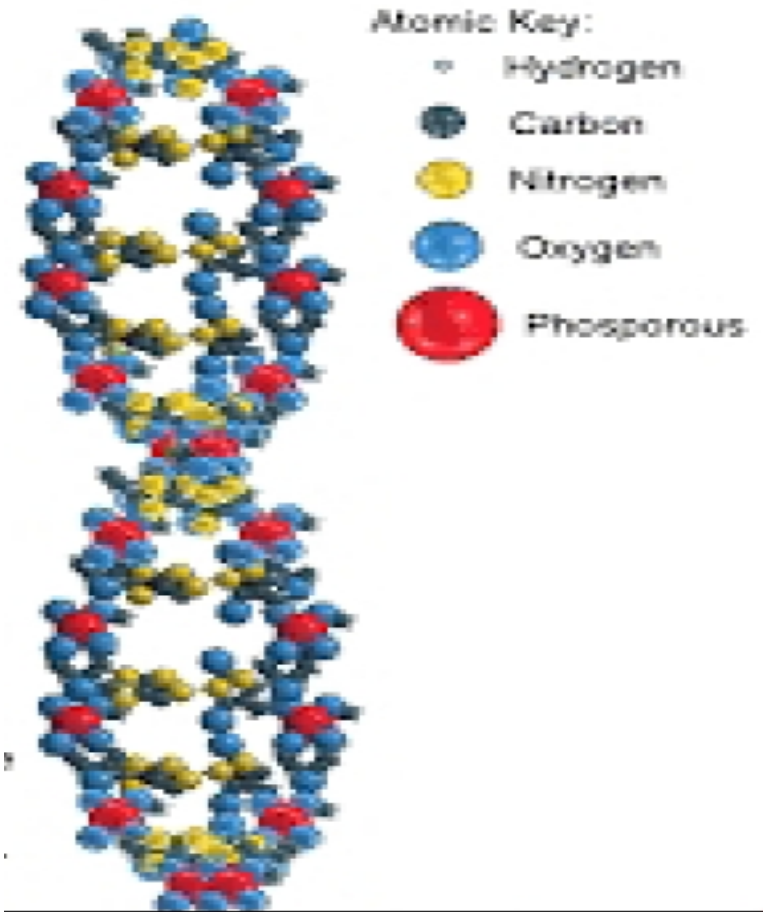
MEASURED PHOTOIONIZATION CROSS SECTIONS OF P II: BENCHMARK WITH R-MATRIX METHOD

- **TOP: Measured σ_{PI} - shows relativistic effects**
- **Panels (b-g): Calculated σ_{PI} of levels $(3s^23p^2)^3P_{0,1,2},{}^1D_2,{}^1S_0,(3s3p^3)^5S^o$**
- **Theory identifies the measured resonances Nahar et al 2016)**
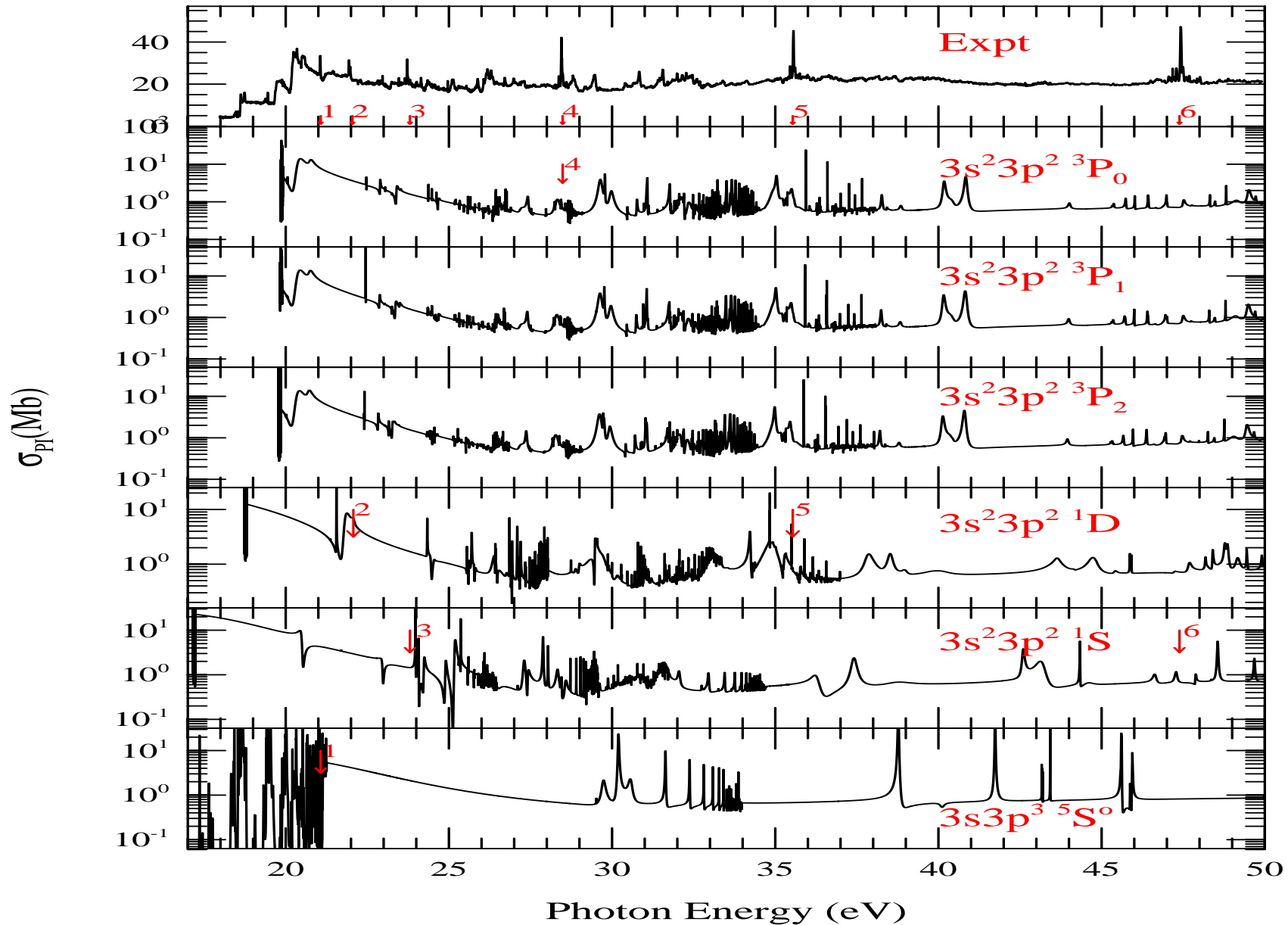
PHOTOIONIZATION OF Cr I & RROBE RATIO Fe/Cr

- **L: Abundance ratio [Cr/Fe] ratio** as probe of chemical evolution in metal-poor star in solar neighborhood (Bergemann 2010, WW95- Woosley & Weaver 1995)
- **R: The good agreement** between NLTE analysis of Cr I lines is obtained by using detailed photoionization cross sections (Nahar 2009)

ELECTRON-ION RECOMBINATION

Photoionization
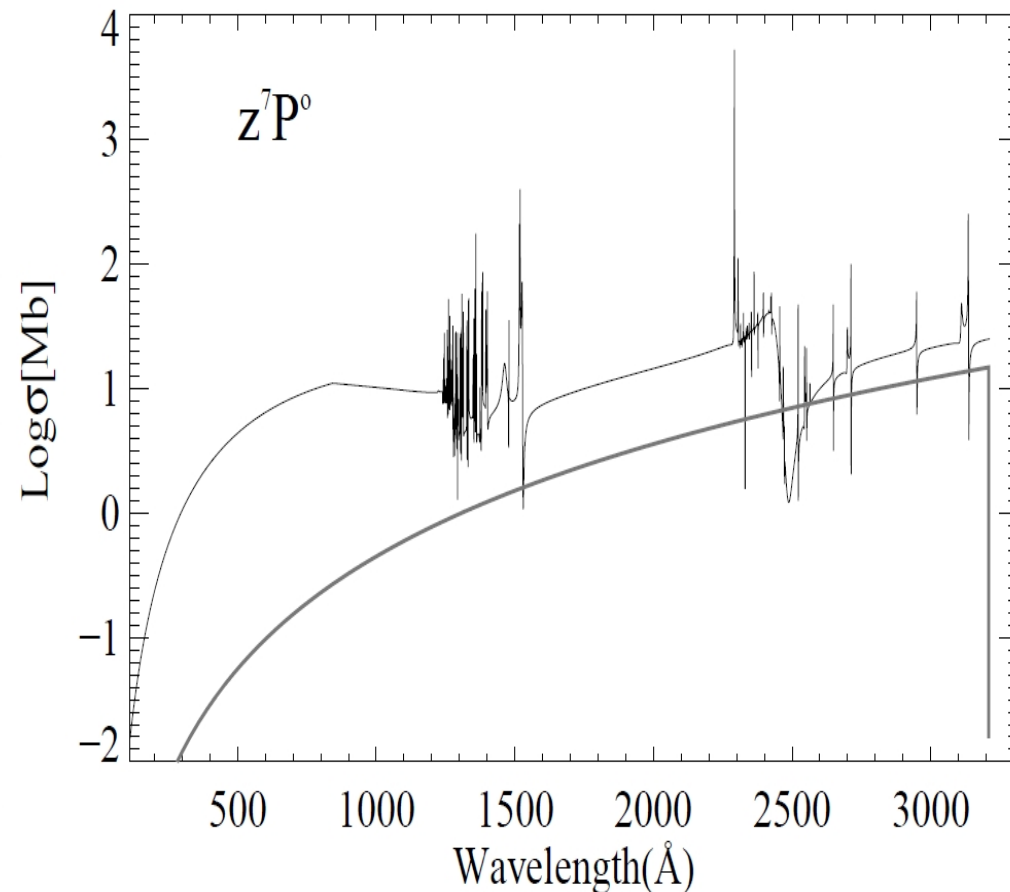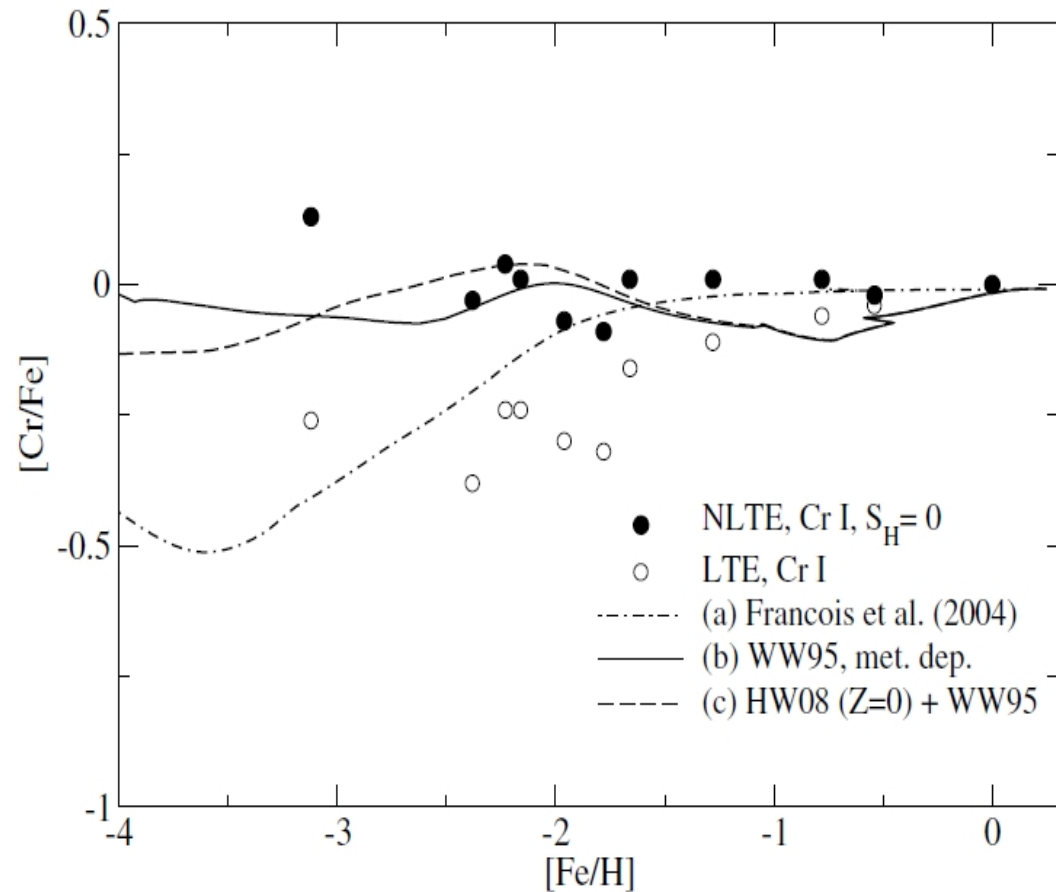
recombination
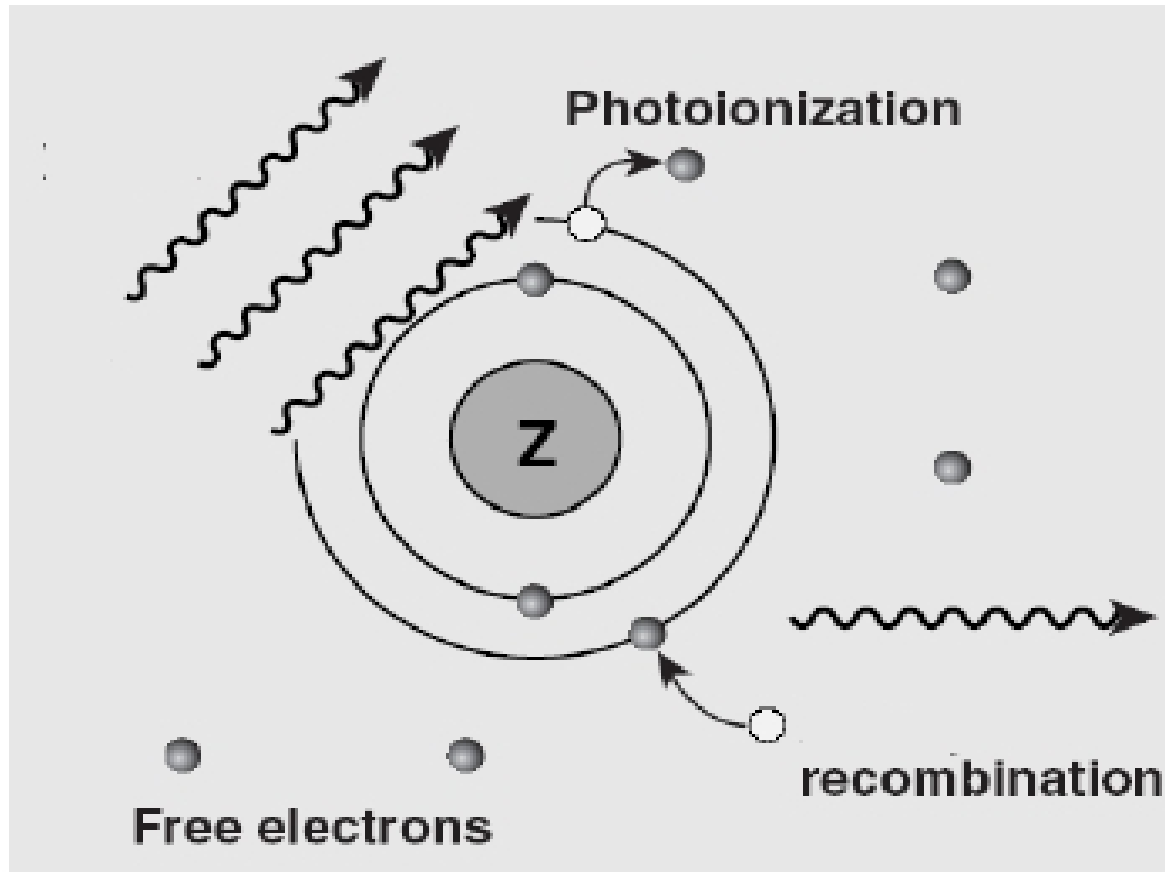
Free electrons

i) **Photoionization (PI) & Radiative Recombination (RR):**

$$\mathbf{X^{+Z} + h\nu \rightleftharpoons X^{+Z+1} + \epsilon}$$

ii) **Indirect PI & Dielectronic Recombination (DR) with intermediate autoionizing state $\rightarrow$ RESONANCE:**

$$\mathbf{X^{+Z} + h\nu \rightleftharpoons (X^{+Z})^{**} \rightleftharpoons X^{+Z+1} + \epsilon}$$

ELECTRON-ION RECOMBINATION: UNIFIED METHOD

(NAHAR & PRADHAN 1992)

Typical Approximation

- Separate calculations of Radiative Recombination (RR) rate & Dielectronic recombination (DR) rate
- Unified Method $\rightarrow$ total recombination

$$\alpha_{RC} = \alpha_{RR} + \alpha_{DR} \ \& \ \text{Interference!of RR} + \text{SR}$$

- Recombination cross section, σ_{RC}, from principle of detailed balance (Milne Relatation):

$$\sigma_{RC} = \sigma_{PI} \frac{g_i}{g_j} \frac{h^2 \omega^2}{4\pi^2 m^2 c^2 v^2}.$$

The recombination rate coefficient:

$$\alpha_{RC}(T) = \int_0^\infty v f(v) \sigma_{RC} dv,$$

$f(v, T) = \frac{4}{\sqrt{\pi}} \left(\frac{m}{2kT}\right)^{3/2} v^2 e^{-\frac{mv^2}{2kT}}$ = Maxwellian distribution function *Total α_{RC}: Contributions from infinite number of recombined states*

TOP: Calculated recombination cross sections
MIDDLE: Calculated recombination rate coefficients
BOTTOM: Measured recombination rate coefficients (TSR)
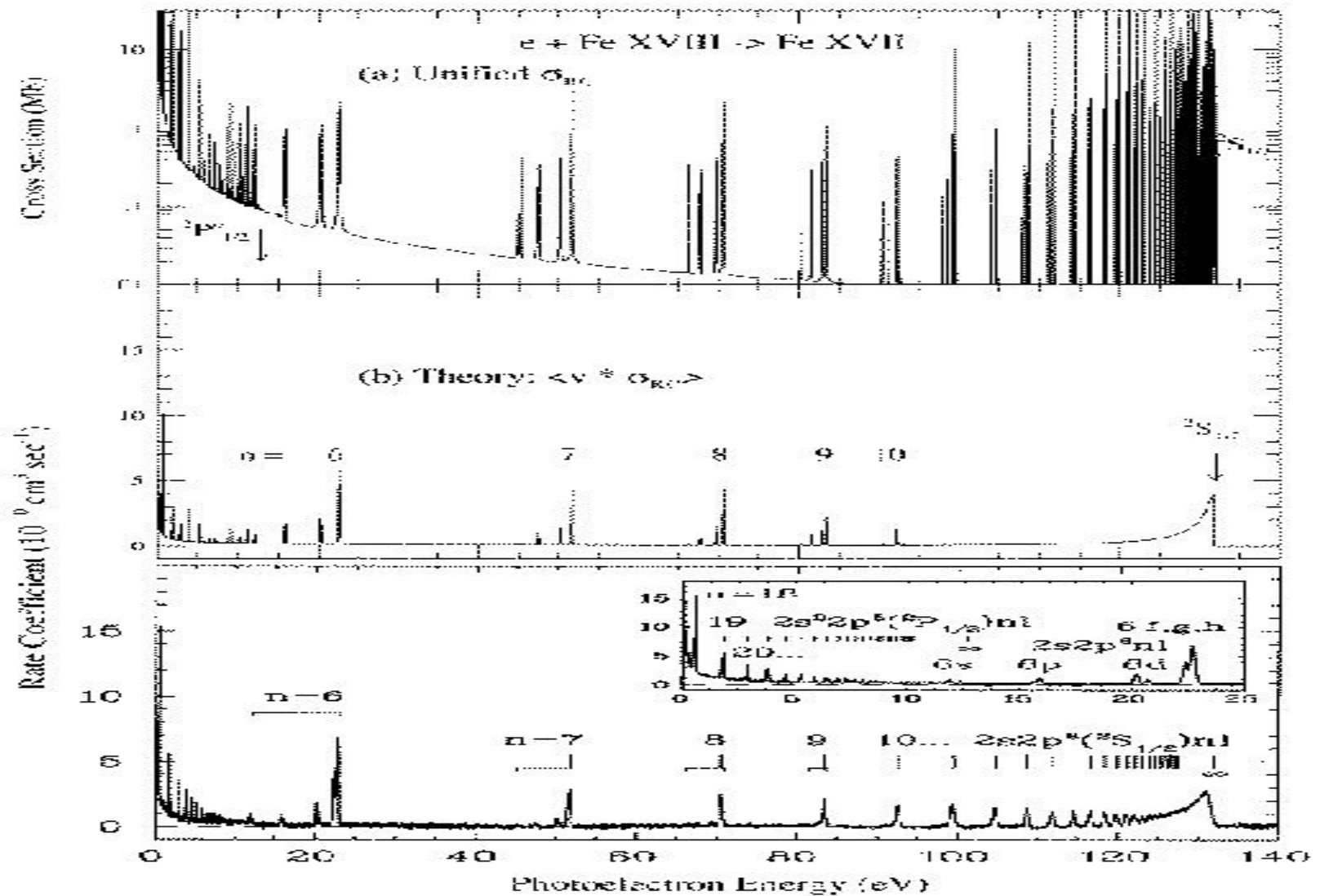
FEATURES OF THE TOTAL RRC OF P II (Nahar 2017)

- Curve around T = 330 K (arrow) due to low energy resonances
- Shoulder around T = 6700 K (arrow) due to interference between RR & DR,
- High T DR bump around T = 10^5 K (arrow)

Total Recombination Rates:
P III + e -> P II
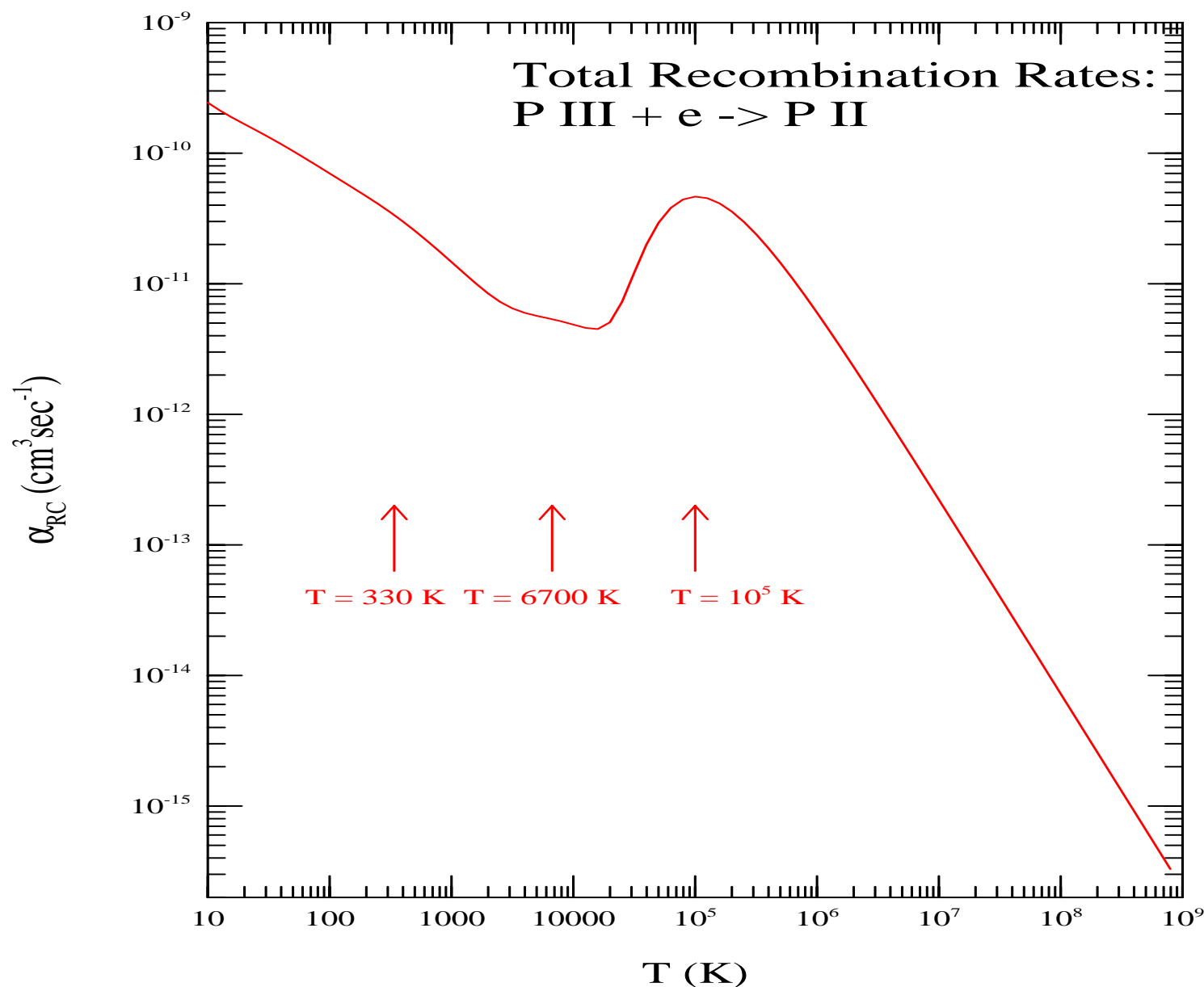
Dielectric Satellite Lines (DES): Fe XXV (Princeton U Expt)
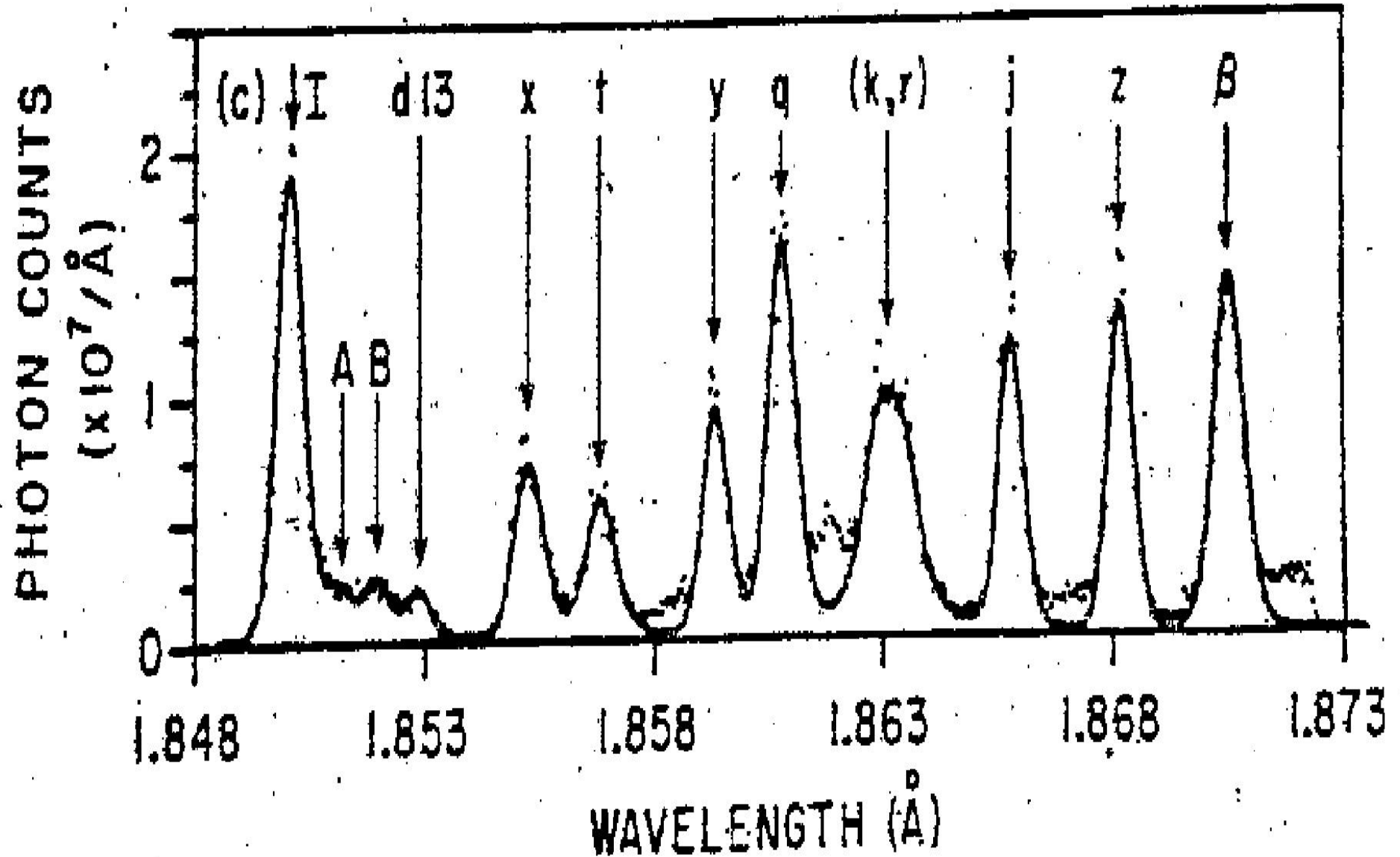
DES Lines in the narrow energy band - Below excitation

- 22 K_α DES lines named with alphabets a - v

SOLAR ACTIVITIES - Storms & Flares - "Halloween" Solar Storm (Oct 28, 2003) (Chandra, SOHO, SOXS)

X-Ray Modeling of Solar Corona and Flares: "Halloween" Solar Storm (Oct 28, 2003)

active region with big sunspot erupts ....

8 minutes later ... X-class Flare observed on the Earth

X-ray spectra of He-like Ca, Fe, Ni (SOXS Mission, PRL, India)

X-ray photons
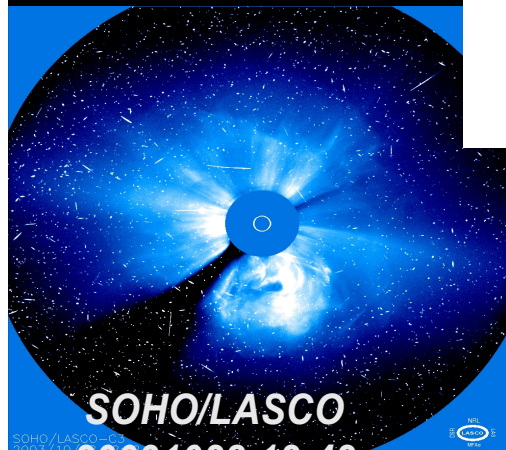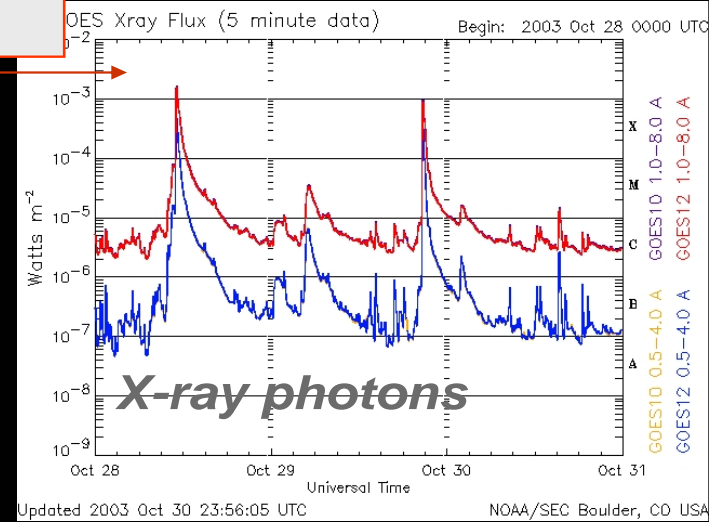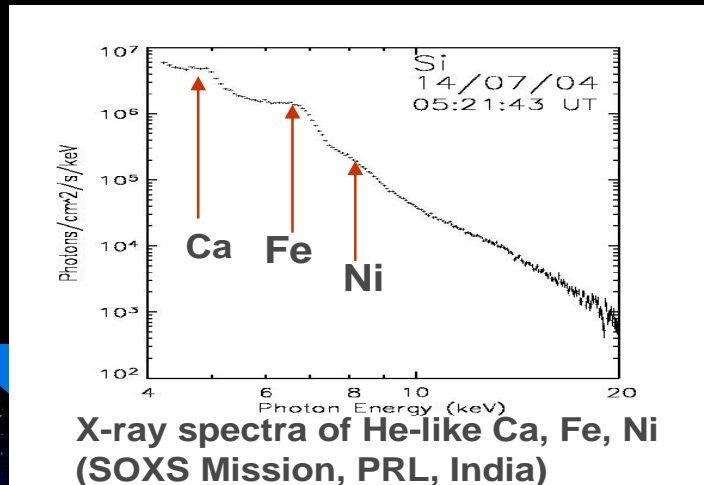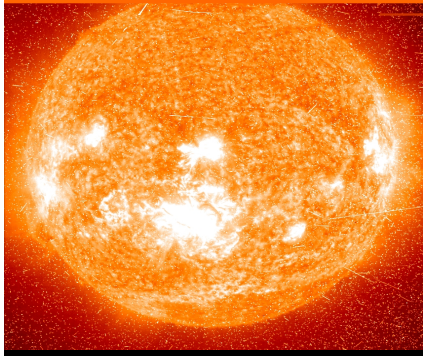
coronal mass ejection leaves the Sun ....

SOHO/LASCO 20031028 12:42 heliosphere ... at L1 20031028 20:49

30 R$_{sun}$

8 hours later... particles saturate SOHO/LASCO detector and reach the Earth ("proton shower")

NOAA National Weather Service

- Top Left: Sun spots are detected
- Lower Left: SOHO mass detector, LASCO, detects large coronal mass

STUDY OF SPECTRAL IRON (Fe XXV) LINES - DIELECTRONIC SATE (DES) LINES - IN SOLAR STROM (Nahar & Pradhan 2006)

Unified Spectrum of Dielectronic Satellite (DES) Lines

σ_{RC}(Mb)

e + Fe XXV -> Fe XXIV + hν: KLL satellite lines
a) Total

b) Jπ = (1/2)^e: 1s2s2p(SLJ) -> 1s^{2}2s(^{2}S$_{1/2}$) resonances

c) Jπ = (1/2)^o: 1s2p^2(SLJ) -> 1s^{2}2p(^{2}P$^o_{1/2}$) resonances

d) Jπ = (3/2)^o: 1s2p^2(SLJ) -> 1s^{2}2p(^{2}P$^o_{3/2}$) resonances

Photoelectron Energy (eV)
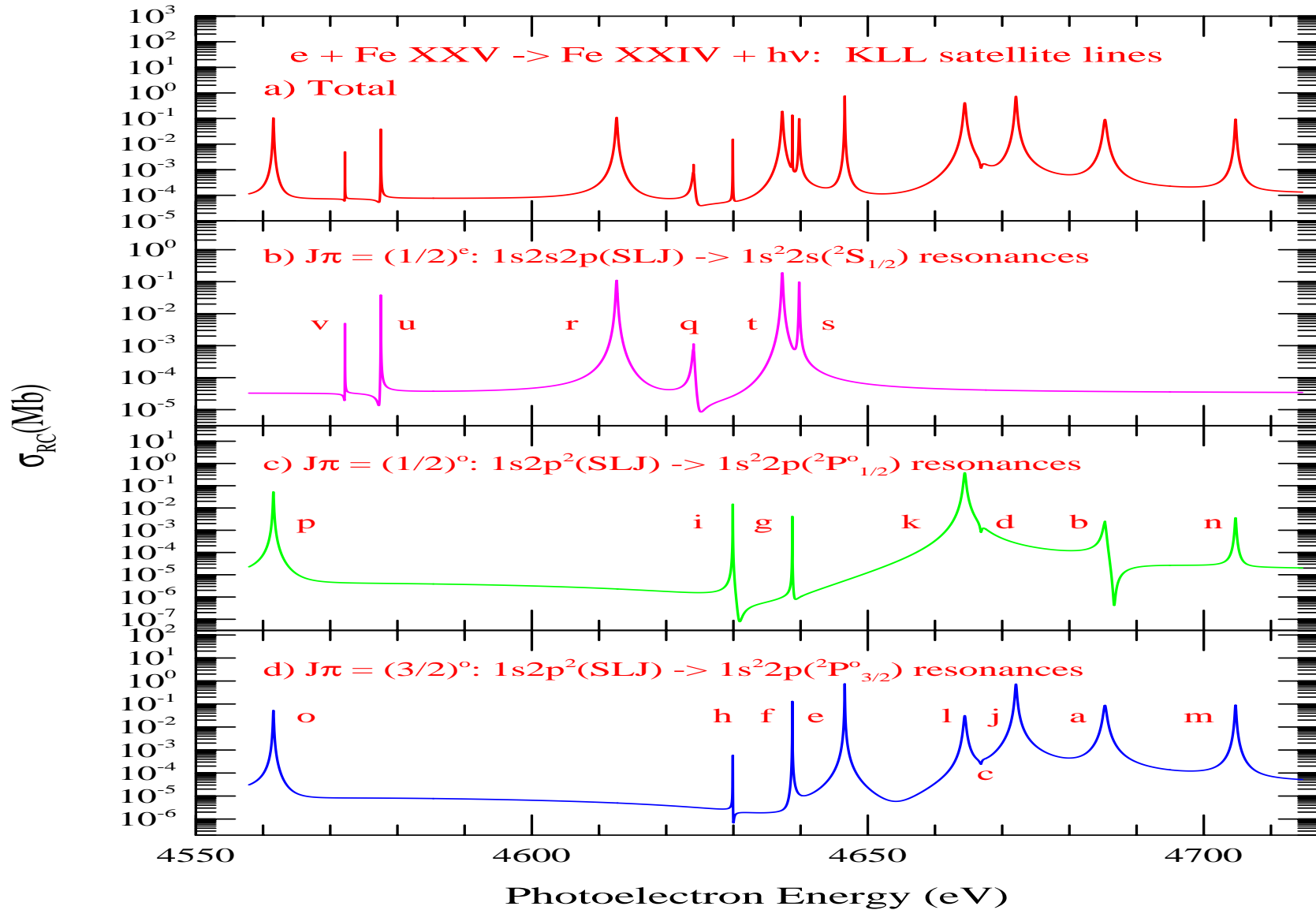
- Solar flare X-ray peaks are known to be from Di-electronic satellite lines
- Theoretical peaks in the DES plots correspond to high emission of the x

X-RAYS FROM A BLACK HOLE - CENTAURUS A GALAXY (Chandra)

- Photometric image: red - low, green - intermediate, blue - high energy X-rays. Dark green & blue bands - dust lanes that absorb X-rays
- Blasting from the black hole a jet of a billion solar-masses extending to 13,000 light years

SIGNATURE OF A BLACKHOLE
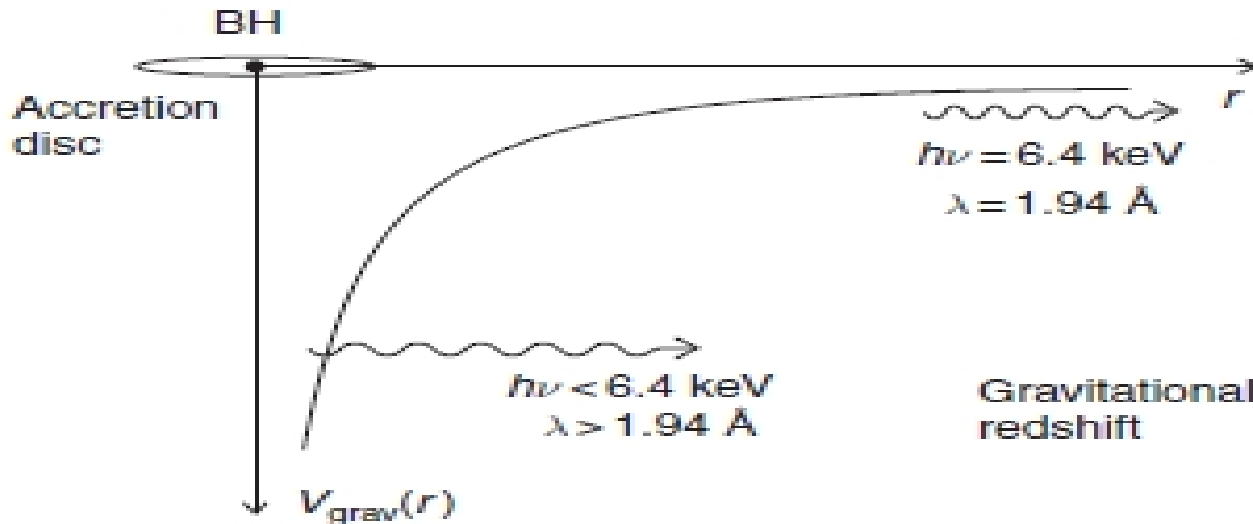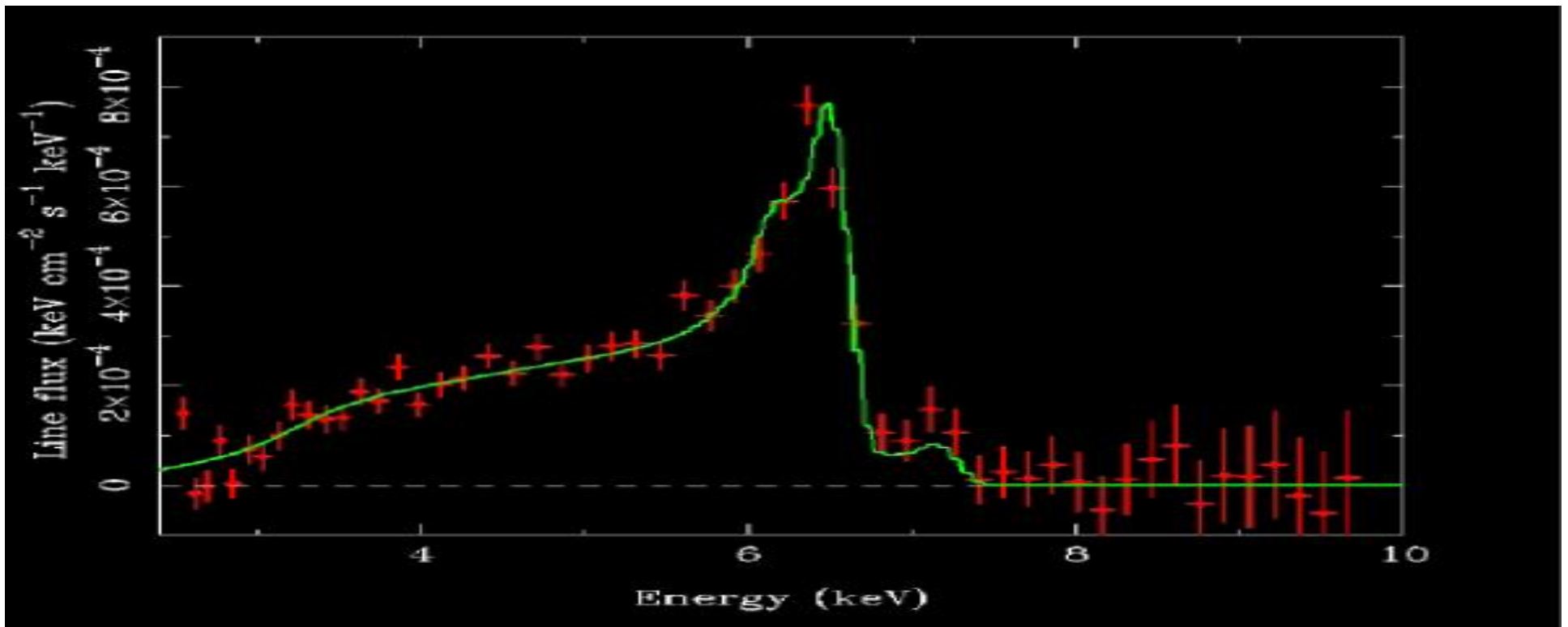
- **Top:** The well-known K_α (1s-2p) transition array lines of Fe XIV near a black hole in Seyfert I galaxy MCG-6-30-15 6 (ASCA & Chandra obs). Emax = 1s-2p transition in iron 6.4 keV. The large extension of the lines toward low energy means

STARS WITH PLANETS AND EXOPLANETS

2MASSWJ1207334-393254

778 mas
55 AU at 70 pc

N
E

© Nasa
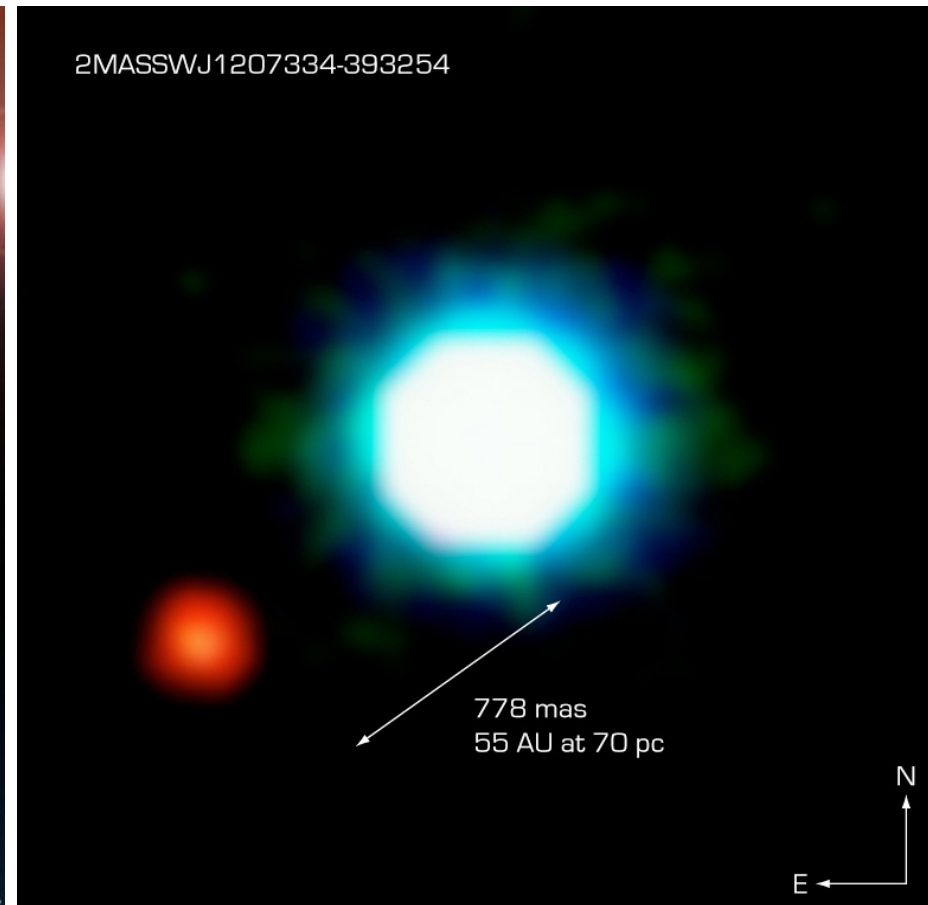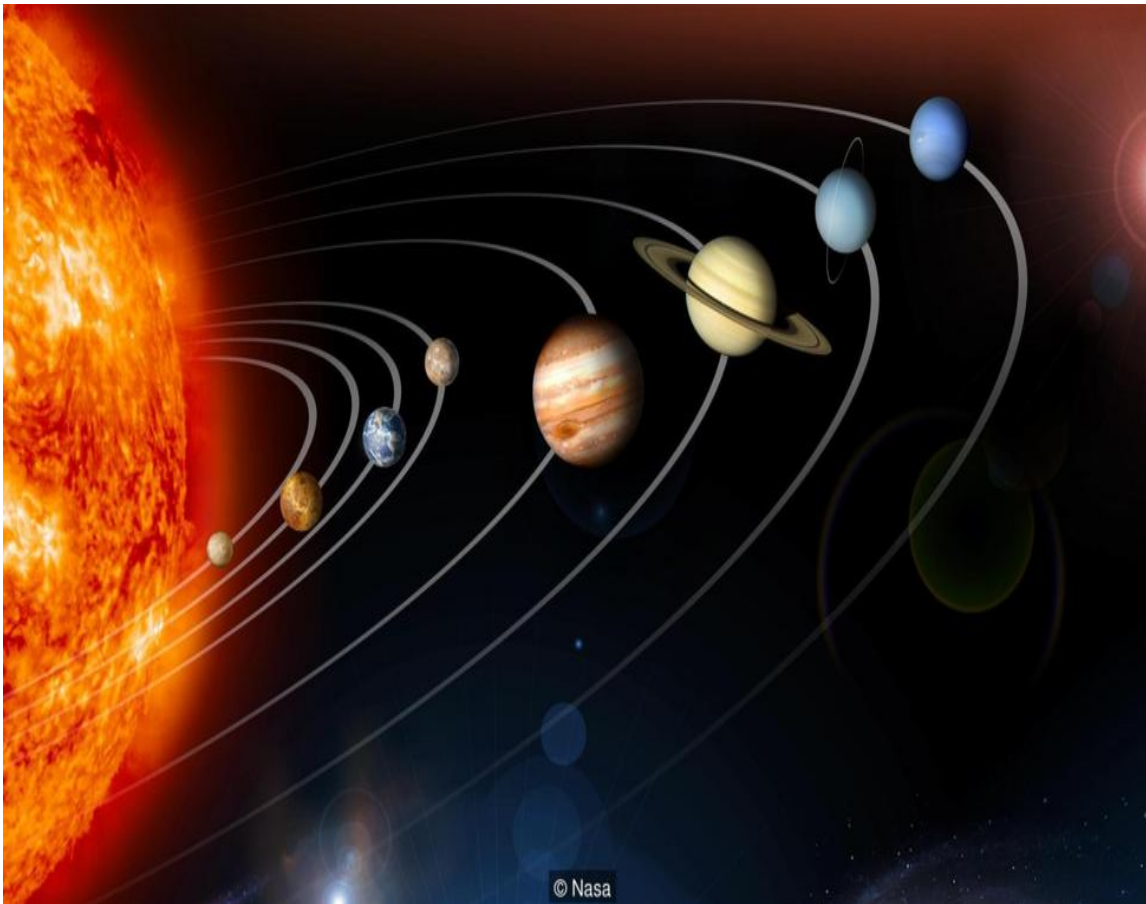
- **L: Solar planets:** Planets around our sun
- **R: Exoplanets:** Planets around a star except the sun - typically around cool red dwarfs
- The 1st exoplanet 2M120b-ESO2004, by HARPS in 2004
- 3545 expolanets detected during 1988 - Dec 2016, over 2000 by Kepler (space, NASA) & over a hundred by HARPS (Chile, ESO), others by HST, Spitzer etc

KEPLER'S CANDIDATES: EXOPLANETARY HOST STARS

New Kepler Planet Candidates
As of July 23, 2015
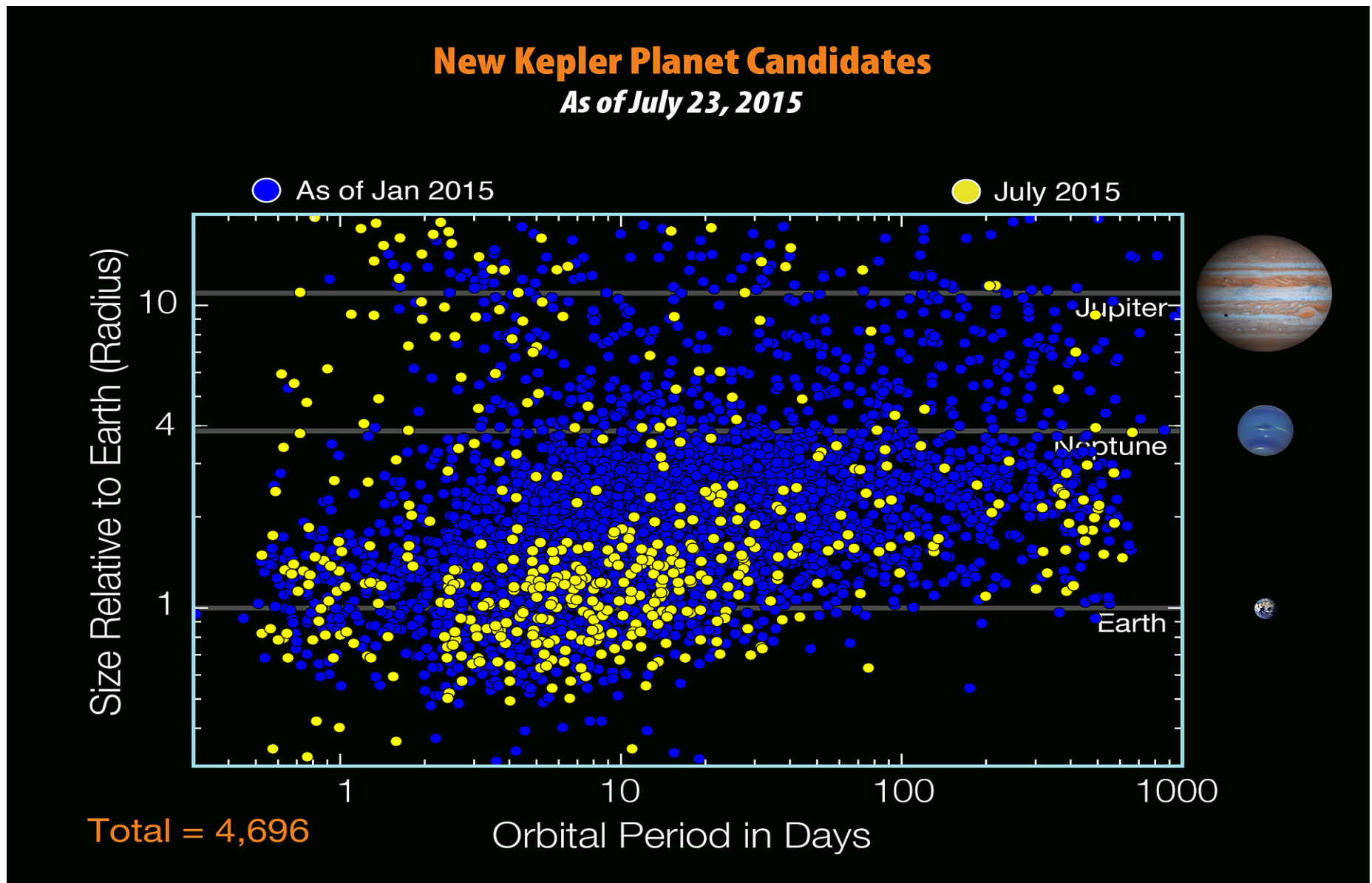
- Kepler detected 4696 host cadidates in 2015
- Size varying < Earth to > Jupitar
- Considering 200 billion stars and number of red dwarfs in the Milky Way, there could be 40 billion planets

OUR INTEREST: HABITABLE EXOPLANETS
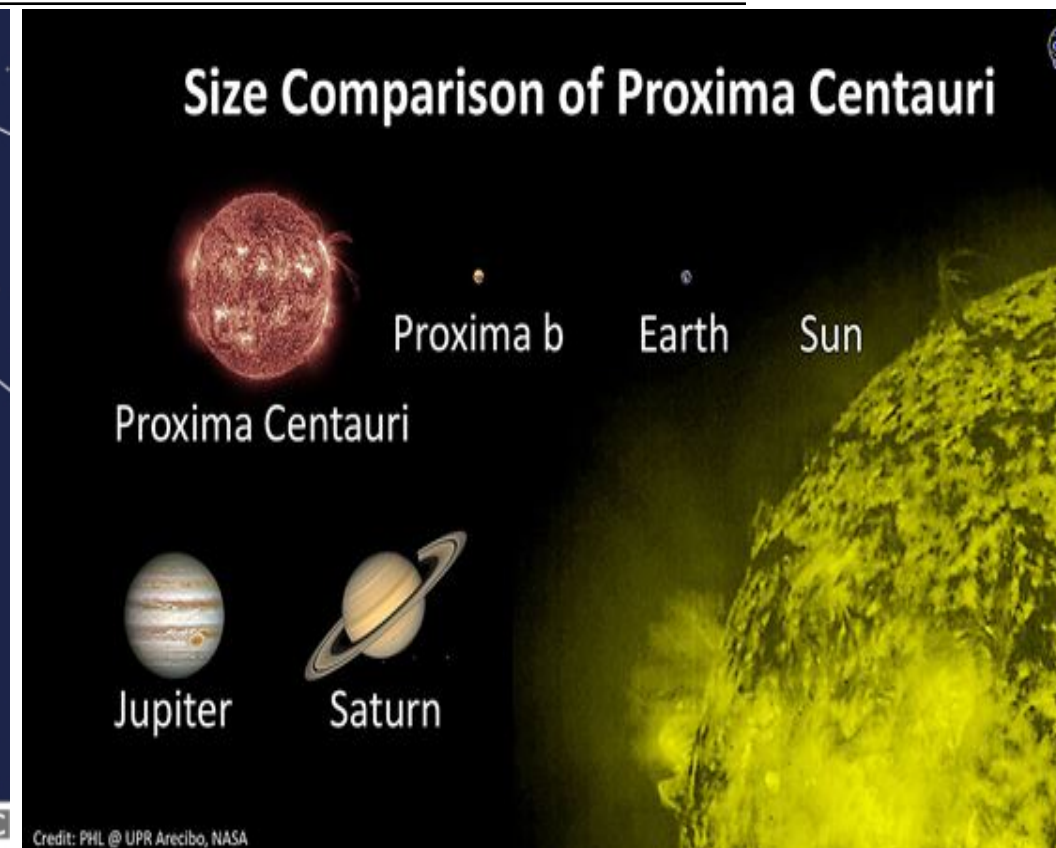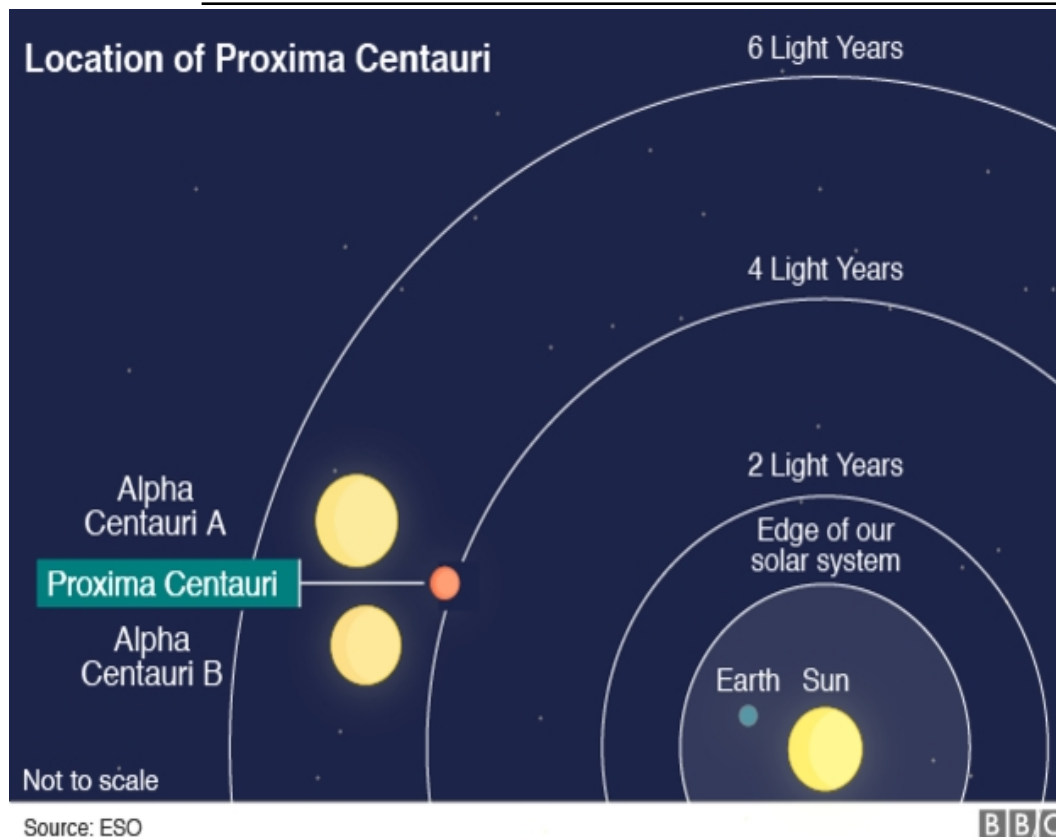
- Habitable planets where liquid water may exist
- Proxima b, exoplanet to our closest star Alpha Centauri (4 ly away: Earth-like in size, hard & rocky surface, possibility of liquid water & temperature similar to us
- But a spacecraft using current technology will take 18 thousands of years to reach it → New idea for 20 years
- 1 in 5 sun-like stars have an earth-sized planet in the habitable zone → potentially 11B planets exist in Milky Way

DETECTION SPECTROSCOPY OF EXOPLANETS

planetary transit
in the star HD 209458

HOST STAR

EXOPLANET
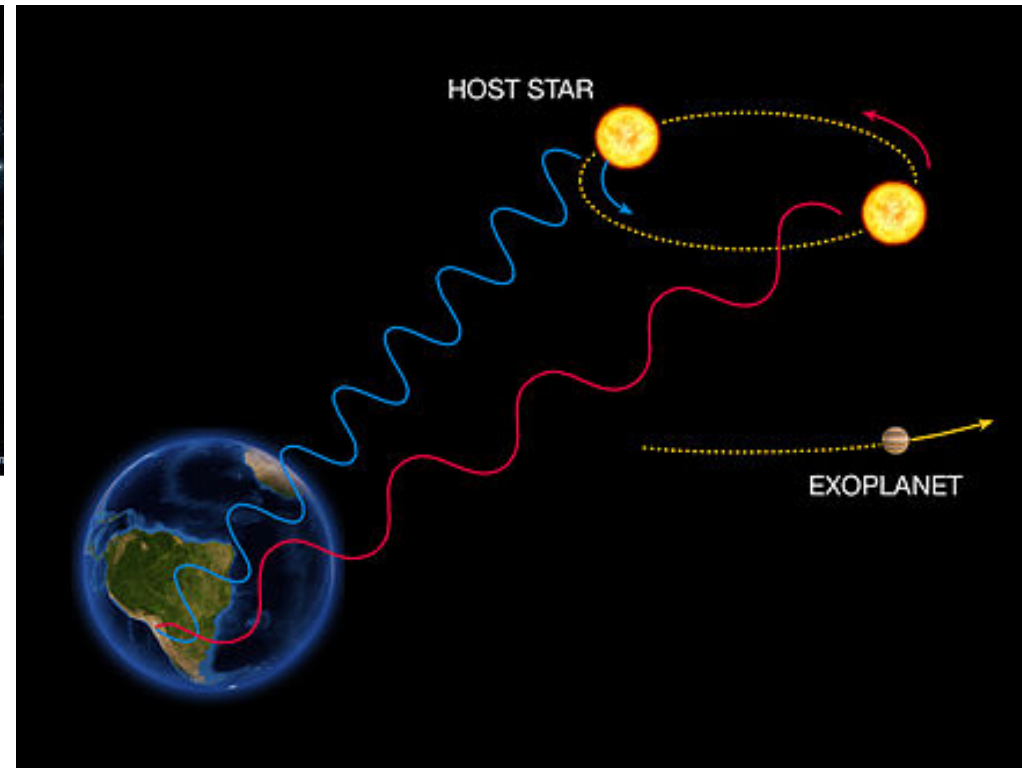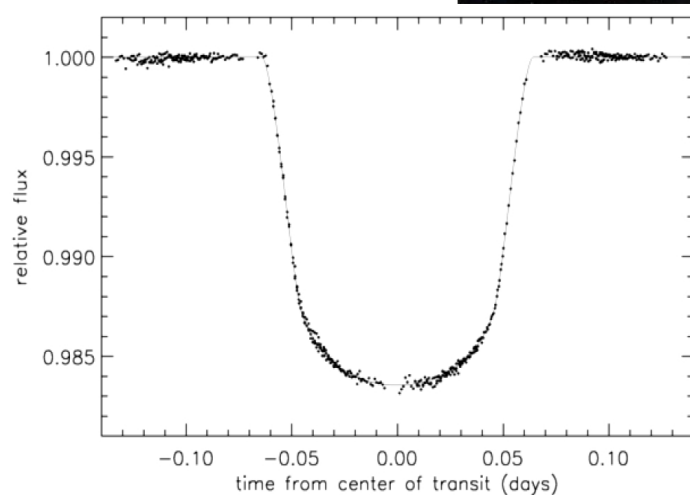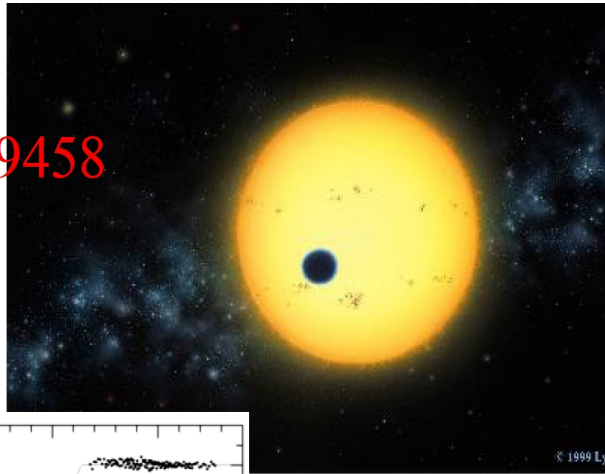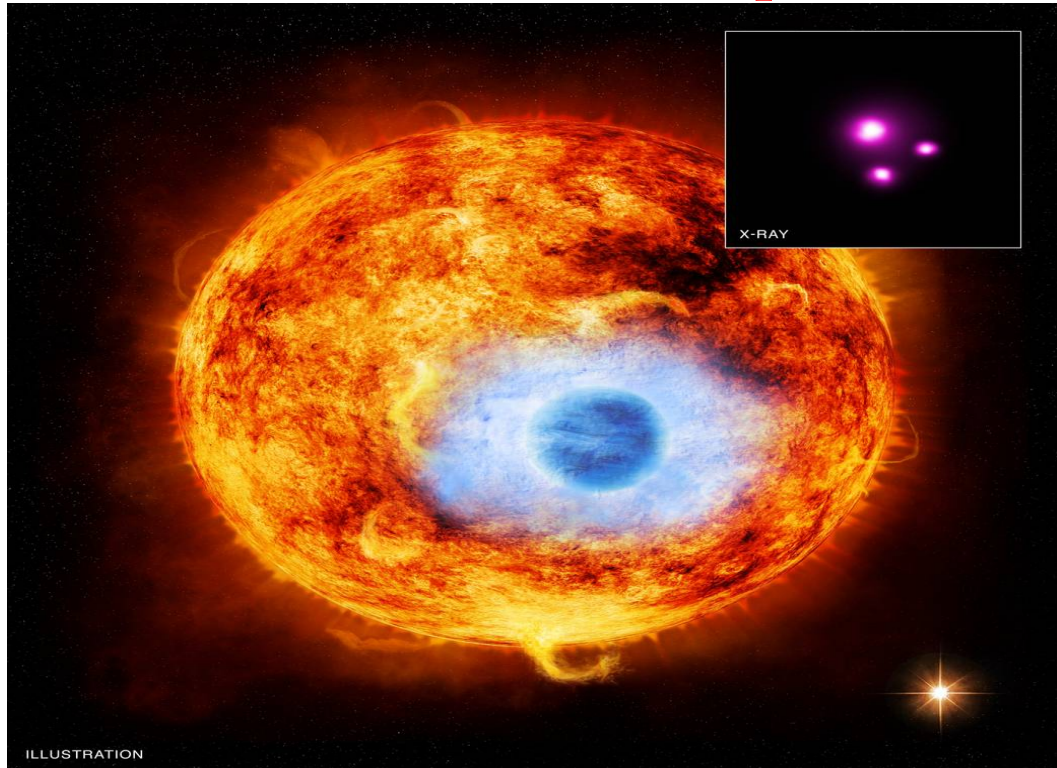
The Radial Velocity Method

ESO Press Photo 22e/07 (25 April 2007)
This image is copyright © ESO. It is released in connection with an ESO press release and may be used by the press on the condition that the source is clearly indicated in the caption.
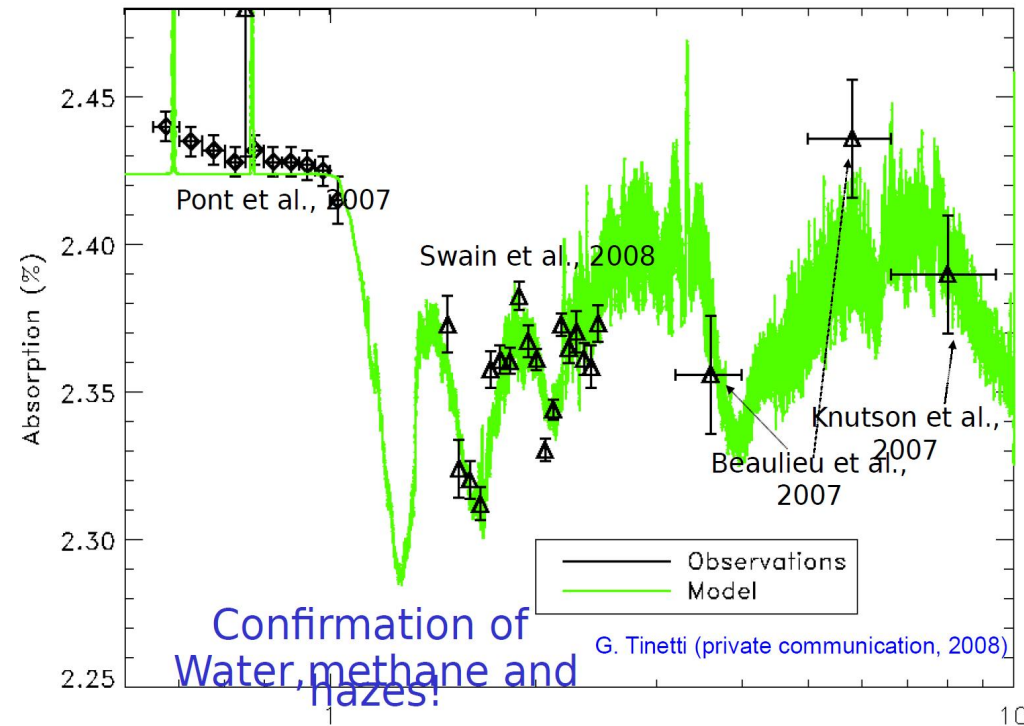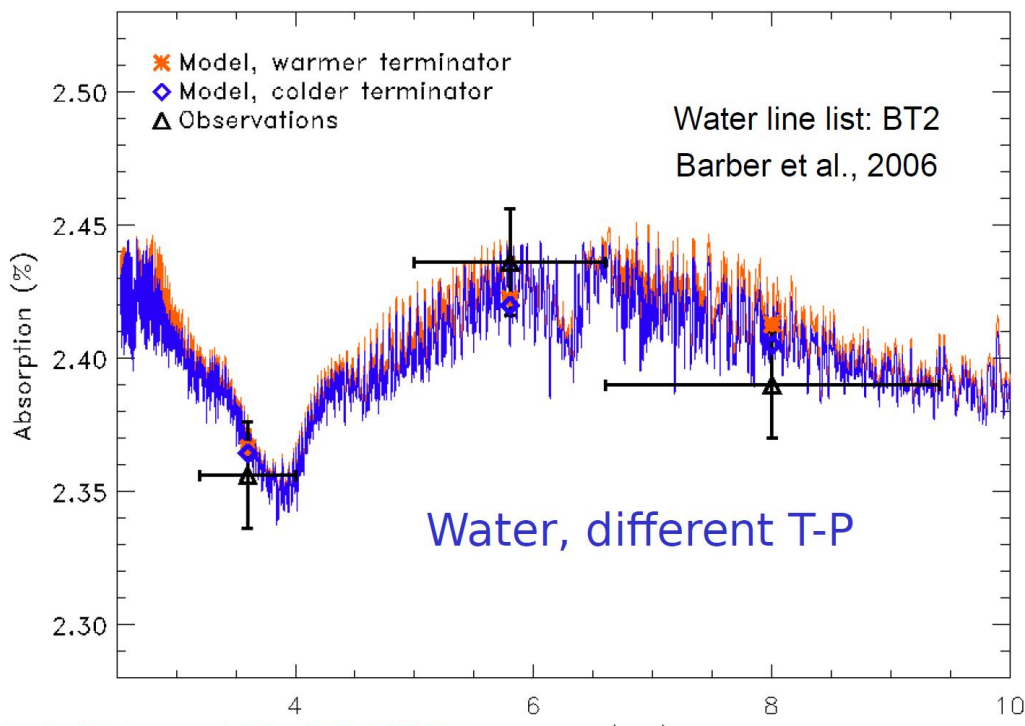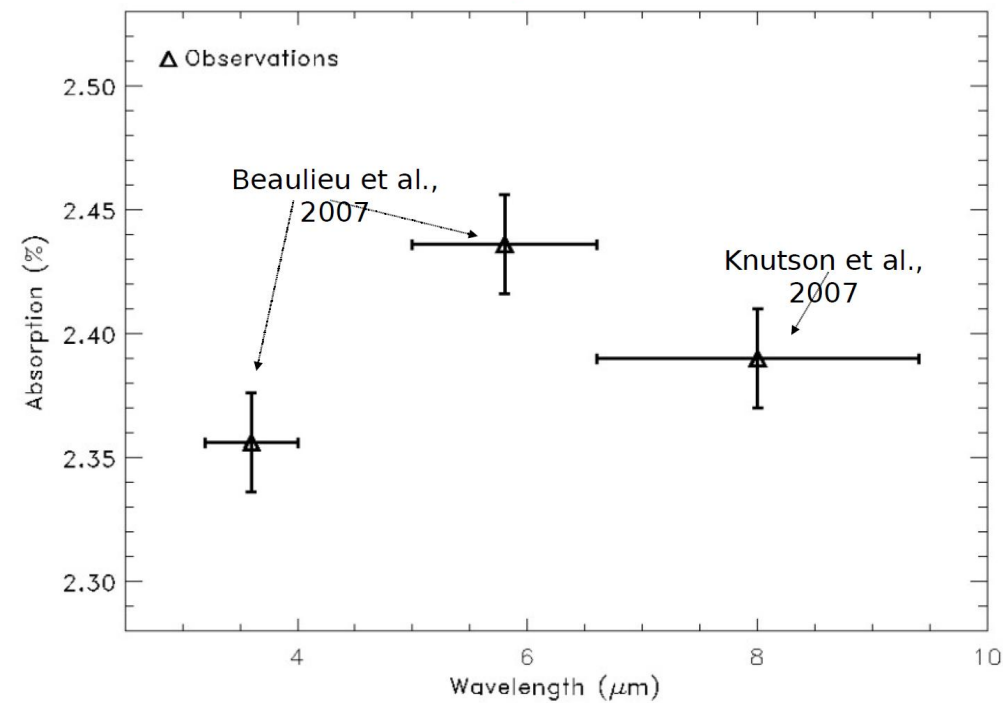
- **L: Transit method:** Most common, via photometry as intensity varies up to of a few percent
- **R: Radial-velocity method:** Use of Doppler spectroscopy of periodic red- and blueshifts in radial velocity due to gravitational force of the exoplanet on the host star
  - Ex: Simply identifying "Proxima b", was a considerable challenge
- **Direct image:** By, e.g., 200-in mirror Hale telescopes
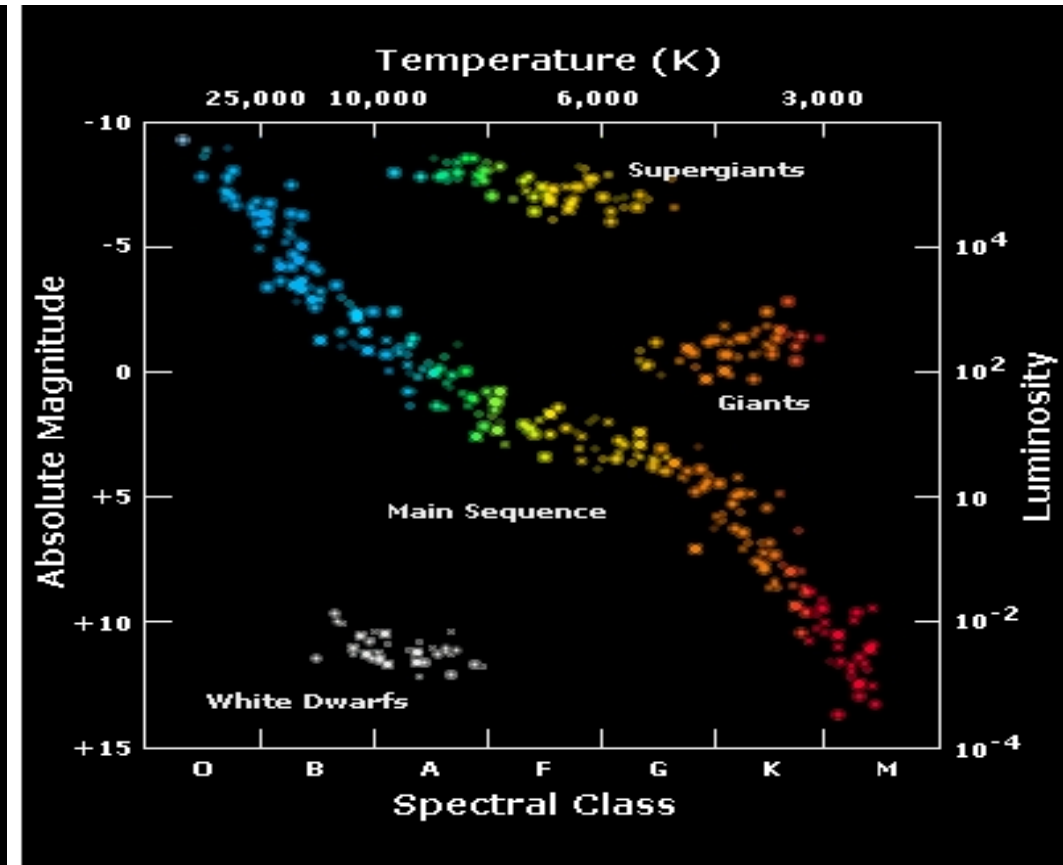- **Gravitational microlensing**
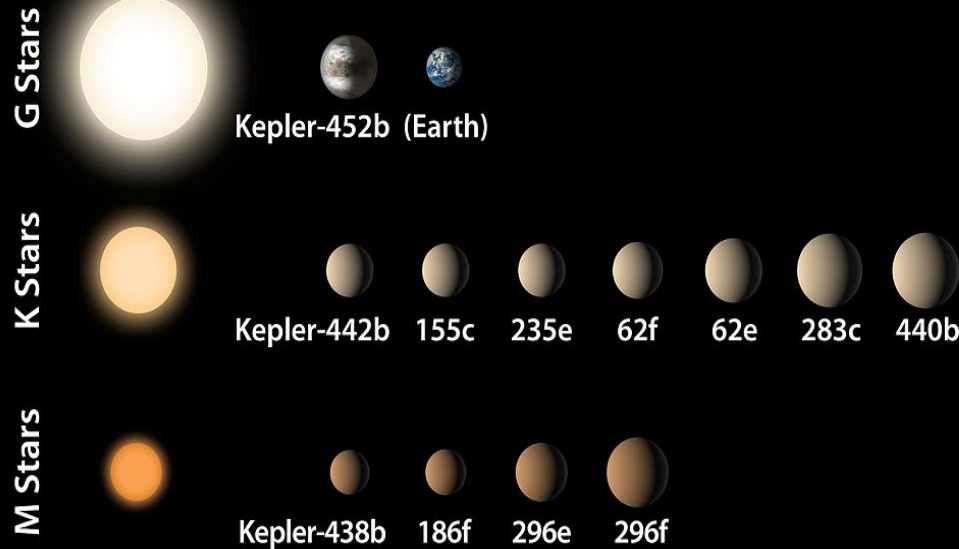
HD18933 and its planet: BIO-SIGNATURES

HD189733b: Primary transit with Spitzer

Beaulieu et al., 2007

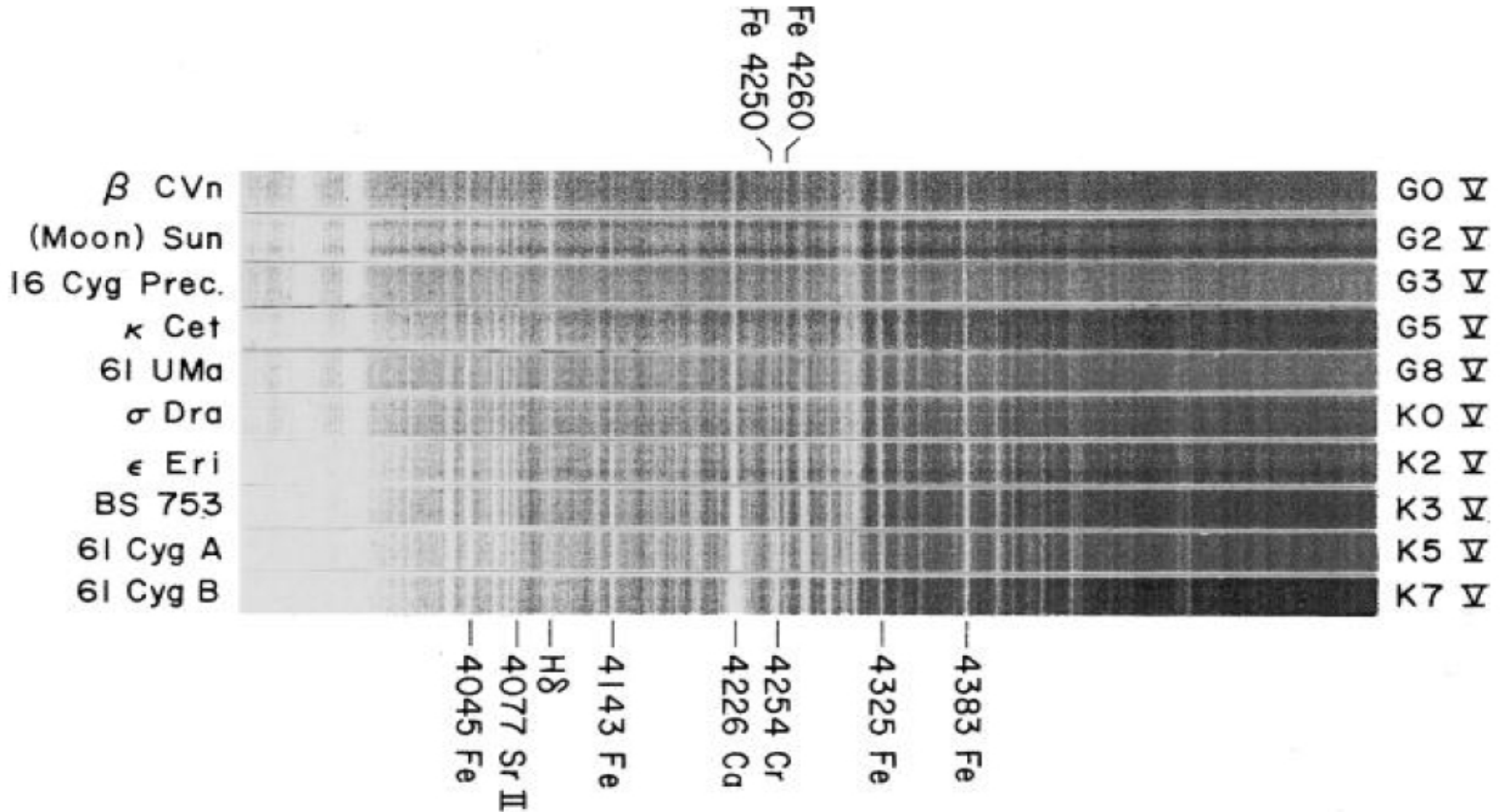Knutson et al., 2007

Model, warmer terminator
Model, colder terminator
Observations

Water line list: BT2
Barber et al., 2006

Water, different T-P

Confirmation of Water, methane and hazes!

Pont et al., 2007

Swain et al., 2008

Knutson et al., 2007

Beaulieu et al., 2007

Observations
Model

G. Tinetti (private communication, 2008)

HR DIAGRAM FOR EXOPLANETARY HOST STARS

- L: All habitable planets are largely G, K, & F, M stars
- R: Mainly cool stars yellow to red in the HR diagram
- Transit Method: The measurement of variation in stellar flux is extremely slight, and interpretation of observation requires precise knowledge of stellar atmospheres and of emitted spectrum.
- In particular, the predicted near-UV flux is important since Earth-like life forms are highly sensitive to it.
- However, current model spectra of cool stars do not accurately reproduce observed fluxes even for the Sun. The problem lies in the attenuation of transmitted flux due to the opacity of the stellar plasma

SPECTRUM OF G AND K-STARS (Keenan and Morgan)

Fe 4260
Fe 4250

β CVn	G0 V
(Moon) Sun	G2 V
16 Cyg Prec.	G3 V
κ Cet	G5 V
61 UMa	G8 V
σ Dra	K0 V
ε Eri	K2 V
BS 753	K3 V
61 Cyg A	K5 V
61 Cyg B	K7 V

4045 Fe
4077 Sr II
Hδ
4143 Fe
4226 Ca
4254 Cr
4325 Fe
4383 Fe

• Progression of stellar spectra from G to K spectral types - luminosity Class V stars in the lower main sequence. The legends on the left refer to the (abbreviated) name of the constellation and star. The similarities in the spectra imply near-solar composition.

• Requires precise study of the sun

PLASMA OPACITY - ELEMENTAL ABUNDANCES

Transmission
$T = I(\nu) / I_0(\nu) = \exp\{-\tau(\nu)\}$

Optical depth
$\tau(\nu) = \kappa(\nu)\rho x$
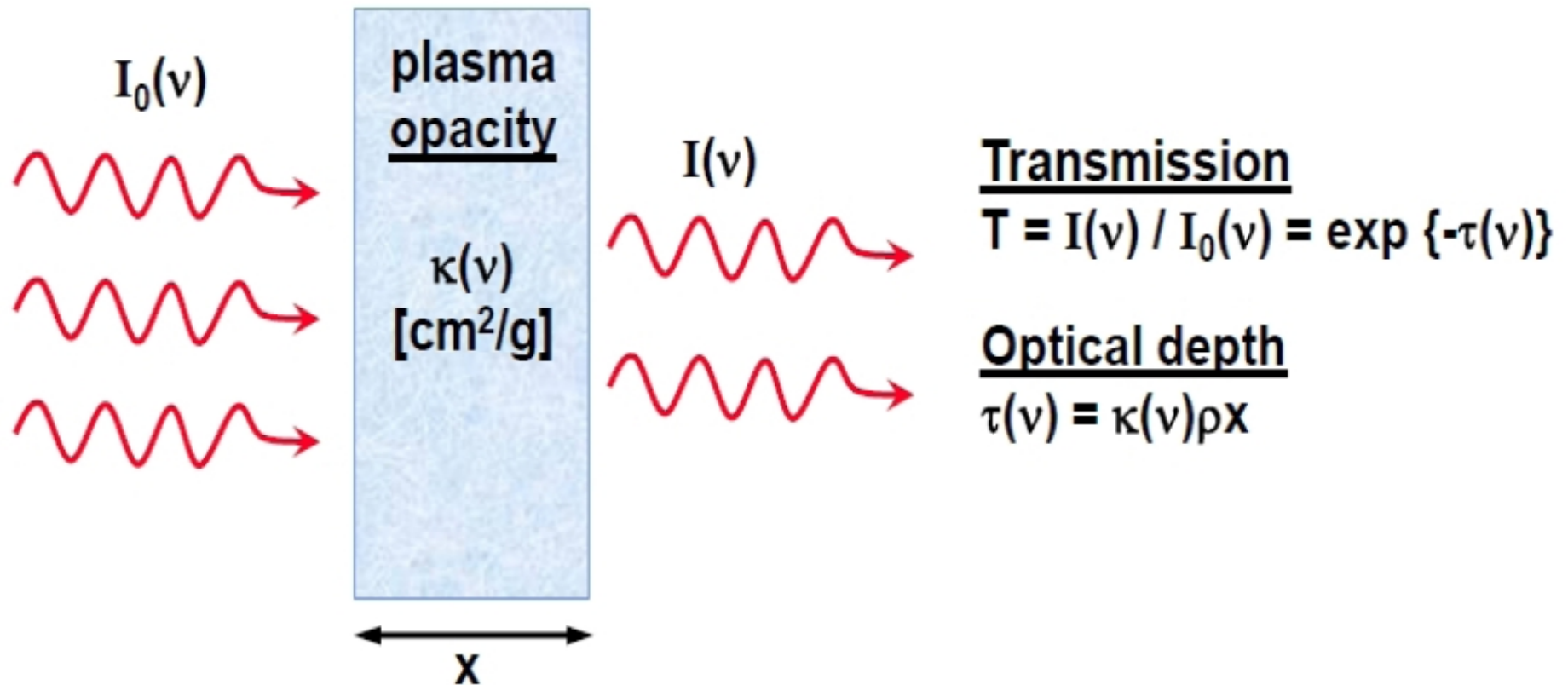
- Opacity is a fundamental quantity of radiation absorption during transmission in plasmas. It is caused by repeated absorption and emission of radiation by the constituent plasma elements.
- Microscopically monochromatic opacity $\kappa(\nu)$ depends on two radiative processes: 1. Photoexcitation -

$$\kappa_\nu(\mathbf{i} \to \mathbf{j}) = \frac{\pi e^2}{mc}N_i f_{ij}\phi_\nu$$

2. Photoionization -

$$\kappa_\nu = N_i \sigma_{PI}(\nu)$$

Through N_i, κ_ν depends on the plasma density

κ_ν DEPENDS ALSO ON FOLLOWING PROCESSES

- **Inverse Bremstrahlung free-free Scattering:**

$$h\nu + [X_1^+ + e(\epsilon)] \rightarrow X_2^+ + e(\epsilon'),$$

An approximate expression for the free-free opacity is

$$\kappa_\nu^{ff}(1,2) = 3.7 \times 10^8 N_e N_i g_{ff} Z^2/(T^{1/2}\nu^3)$$

where g_{ff} is a Gaunt factor

- **Photon-Electron scattering:**

a) Thomson scattering when the electron is free

$$\kappa(sc) = N_e \sigma_{Th} = N_e \frac{8\pi e^4}{3m^2 c^4} = 6.65 \times 10^{-25} \text{ cm}^2/\text{g}$$

b) Rayleigh scattering when the electron is bound

$$\kappa_\nu^R = n_i \sigma_\nu^R \approx n_i f_t \, \sigma_{Th}(\nu/\nu_I)^4$$

$h\nu_I$ = binding energy, f_t = total oscillator strength
The total monochromatic opacity is then given by

$$\kappa_\nu = \kappa_\nu(bb) + \kappa_\nu(bf) + \kappa_\nu(ff) + \kappa_\nu(sc)$$

Rosseland mean $\kappa_R(T, \rho)$:

Harmonic mean opacity averaged over the Planck function, ρ is the mass density (g/cc),

$$\frac{1}{\kappa_R} = \frac{\int_0^\infty \frac{1}{\kappa_\nu} g(u) du}{\int_0^\infty g(u) du},$$

where $g(u)$ is the Planck weighting function

$$g(u) = \frac{15}{4\pi^4} \frac{u^4 e^{-u}}{(1 - e^{-u})^2}, \quad u = \frac{h\nu}{kT}$$

$g(u)$, for an astrophysical state is calculated with different chemical compositions H (X), He (Y) and metals (Z), such that

$$X + Y + Z = 1$$

Solar abundaces: X=0.7, Y=0.28, Z=0.02

• Opacities can be calculated with the programs and opacity data at

OPserver at OSC: http://opacities.osc.edu/

NUMBER DENSITY N_i: THE EQUATION OF STATE (EOS)

- Requires (AAS, Pradhan & Nahar 2011):

i) ionization fractions and ii) level populations of non-negligible occupation probability

- Saha equation for ionization fraction at thermal equilibrium

$$\frac{n_S(X^i)}{n(X^+)} = \frac{g_i}{2g_s}\frac{h^3}{(2\pi m_e kT)^{\frac{3}{2}}}\exp\left(-\frac{E_{gi}}{kT}\right)n_e \tag{46}$$

Boltzmann equation for the level populations at LTE,

$$\frac{N_i}{N_j} = \frac{g_i}{g_j}\,e^{-h\nu/kT} \tag{47}$$

The Equation-of-state (EOS) in LTE can be expressed as the combination of the Saha-Boltzmann equations with inclusion of the plasma interactions as

$$N_{ij} = \frac{N_j g_{ij} w_{ij} e^{-E_{ij}/kT}}{U_j}, \quad U_j = \sum_i g_{ij} w_{ij} e^{(-E_{ij}/kT)}$$

where U_j is the partition function

SOLAR ABUNDANCES

Solar abundances (A_k, usually in log scale):
- H > 90 % (by number), 70% (by mass fraction)
- He > 7 % (by number), 28 % (by mass)
- Metals - 2%.
- By mass. O (highest), C, N, Ne, Mg, Si, S, Ar, Fe
- Traditionally H abundance: $\log(A_H) = 12$, other elements are scaled relative to it
- Table: "Standard" solar abundances (10% uncertainties, Seaton et al. 1994)

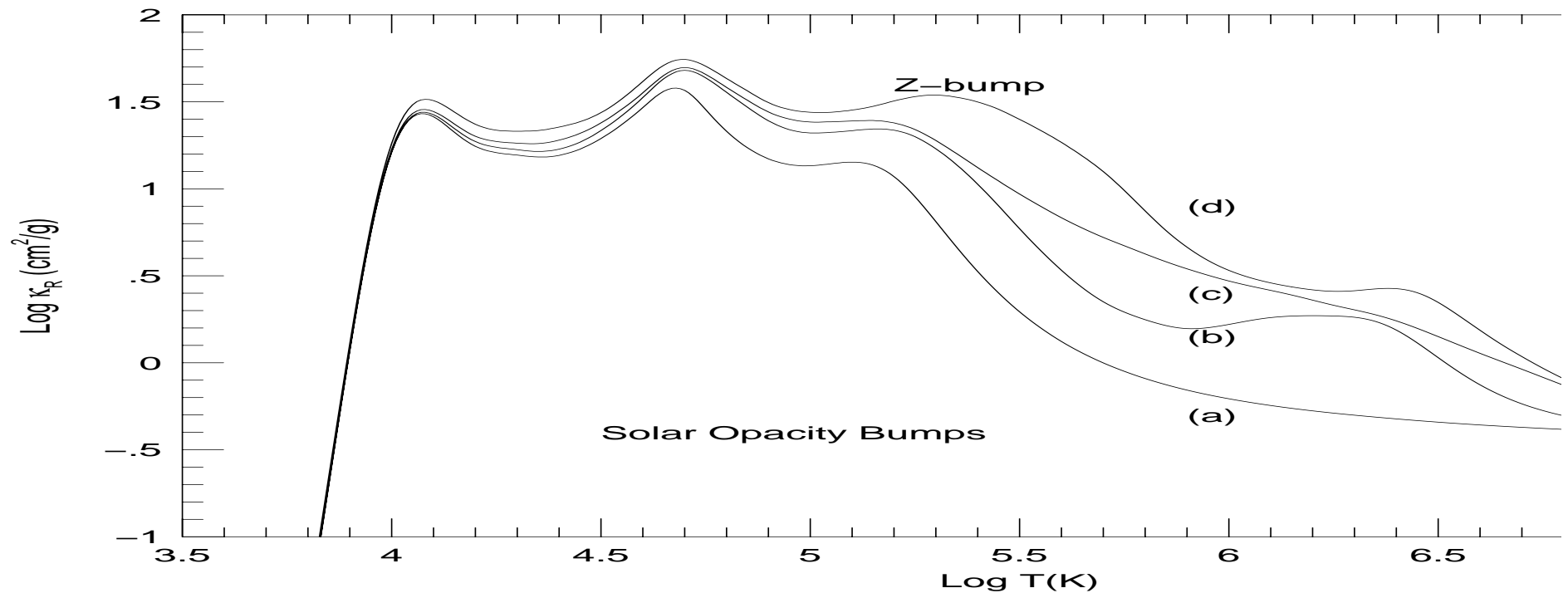| Element (k)	Log A_k	A_k/A_H
H	12.0	1.0
He	11.0	1.00(-1)
C	8.55	3.55(-4)
N	7.97	9.33(-5)
O	8.87	7.41(-4)
Ne	8.07	1.18(-4)
Na	6.33	2.14(-6)
Mg	7.58	3.80(-5)
Al	6.47	2.95(-6)
Si	7.55	3.55(-5)
S	7.21	1.62(-5)
Ar	6.52	3.31(-6)
Ca	6.36	2.29(-6)
Cr	5.67	4.68(-7)

SOLAR OPACITY: UNDER THE OPACITY PROJECT
(Seaton, Yan, Mihalas, Pradhan 1993)
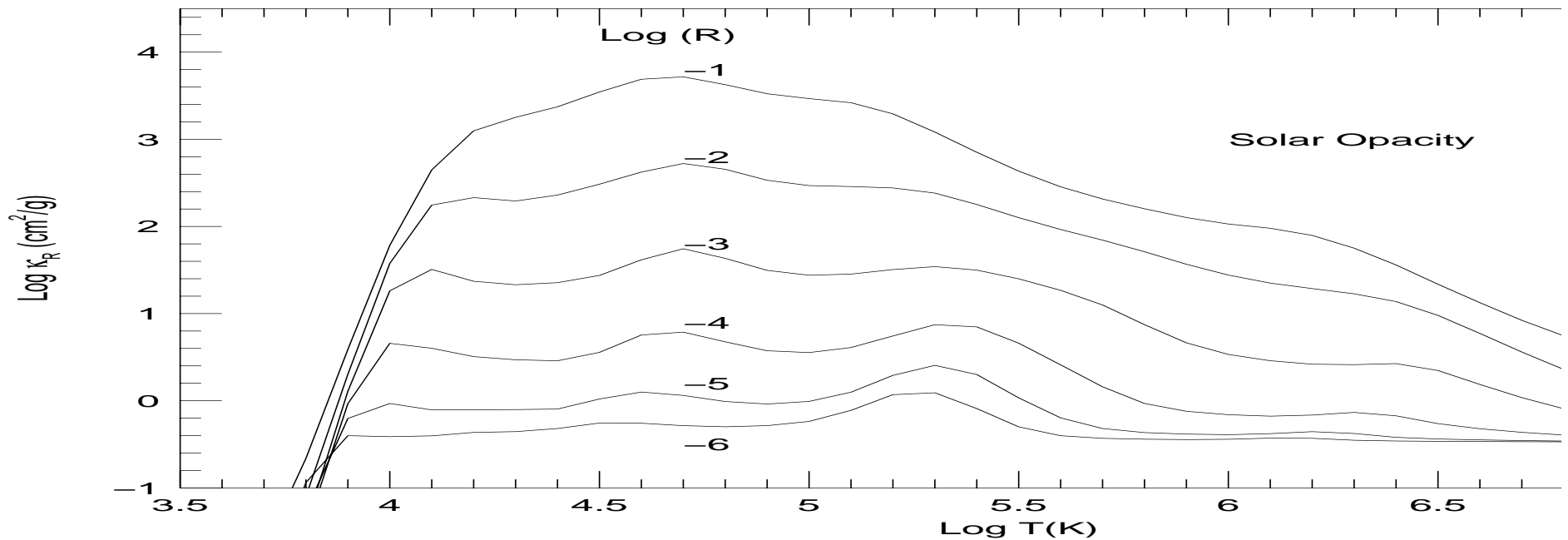
- Rosseland mean opacity κ_R in various temeprature-density regimes throughout the solar interior characterized by the distance parameter R (density decreases with T)
$$\mathbf{R} = \rho(\mathbf{g/cc})/\mathbf{T_6^3}, \quad \mathbf{T_6} = \mathbf{T} * \mathbf{10^{-6}}$$
- For the sun, $-6 \leq R \leq -1$
- The bumps and kinks in the curves represent higher opacities due to excitation/ionization of different atomic species at those temperatures (H-, He-, Z-, and inner-shell bumps)

Z-BUMP IN SOLAR OPACITY
## (Using OPserver, Pradhan and Nahar 2011)

Figure: plot of $\log \kappa_R$ (cm^2/g) versus $\log T(K)$, showing curves labelled (a), (b), (c), (d), with "Z-bump" and "Solar Opacity Bumps" annotations.

- Increment of Rosseland mean opacity κ_R with elements at R=-3
- a) H and He, b) H to Ne, c) H to Ca, d) H to Ni
- d) shows maximum increment in κ_R above logT=4.0 giving a Z-bump
- Iron contributes most to Z-bump

# DISCREPANCY IN UV OPACITY (Valenti et al 2015)
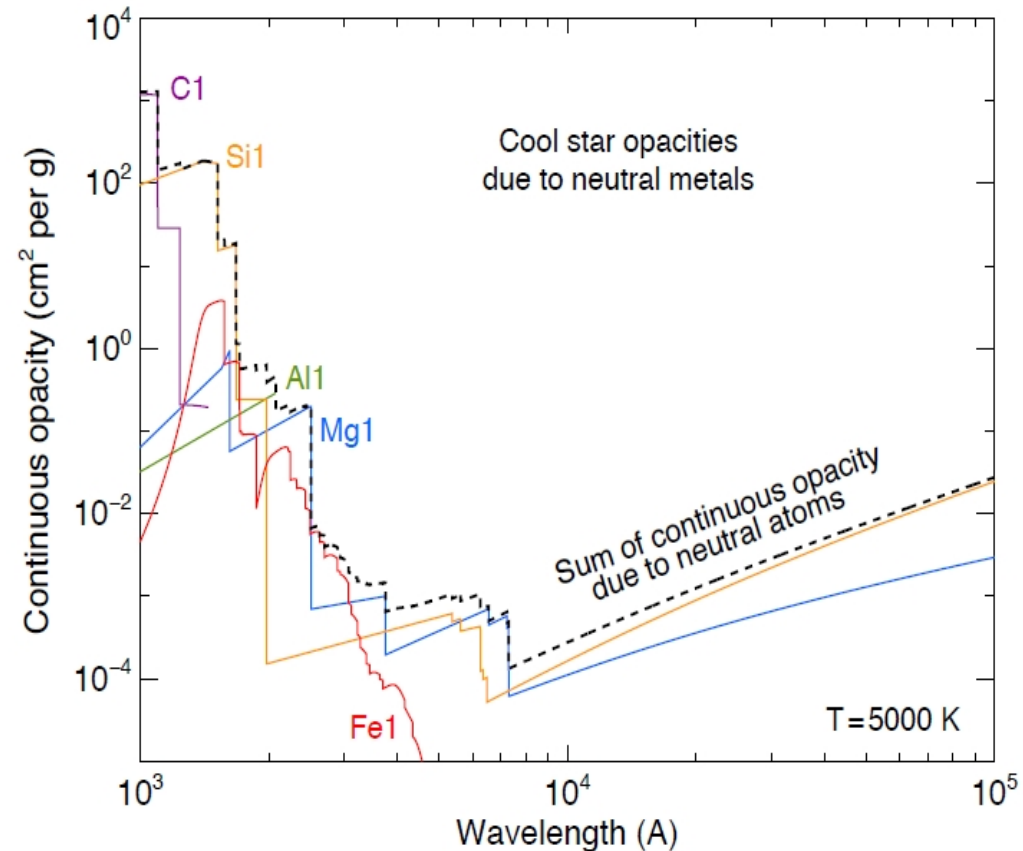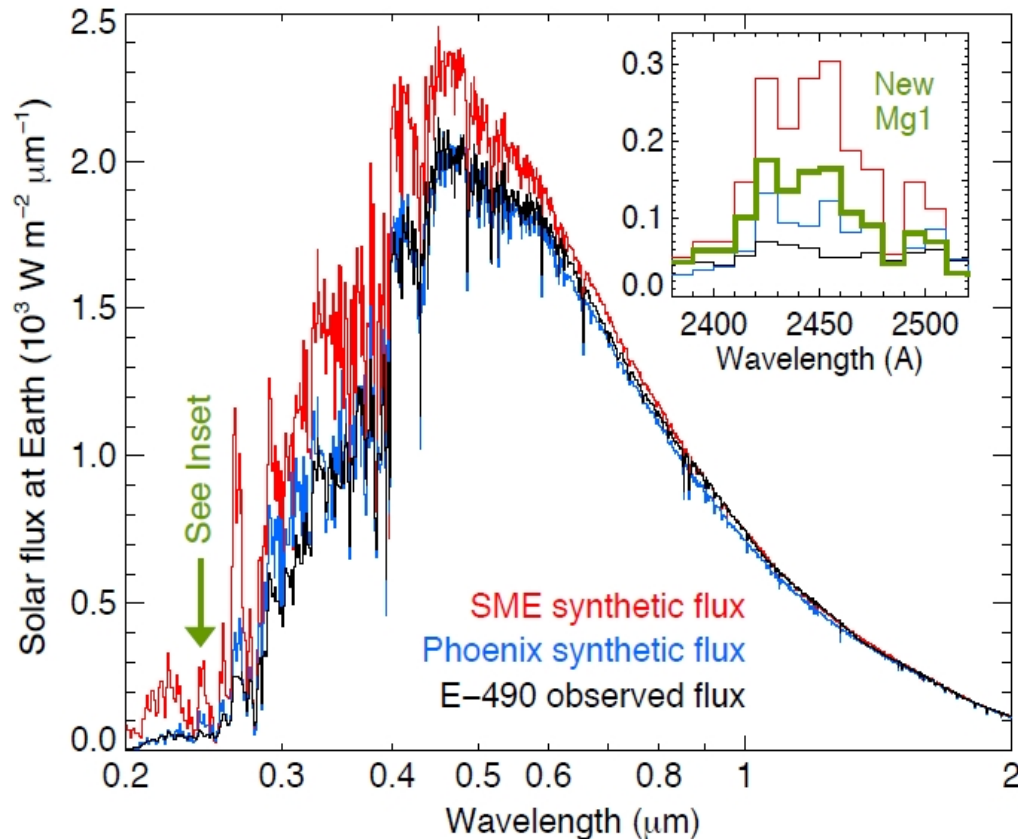
- L: Synthetic flux spectra of the Sun - Models (Red, Blue) fail to account for the underlying observed (Black) continuum opacity over a large wavelength region, near-UV to optical in the 0.2-0.5 micron range
- R: The bound-free & free-free opacity in the UV for neutral C, Si, Al, Mg and Fe in the atomspheres of cool stars, that needs to be considered in the models

SOLAR OPACITY AND ELEMENTAL ABUNDANCES
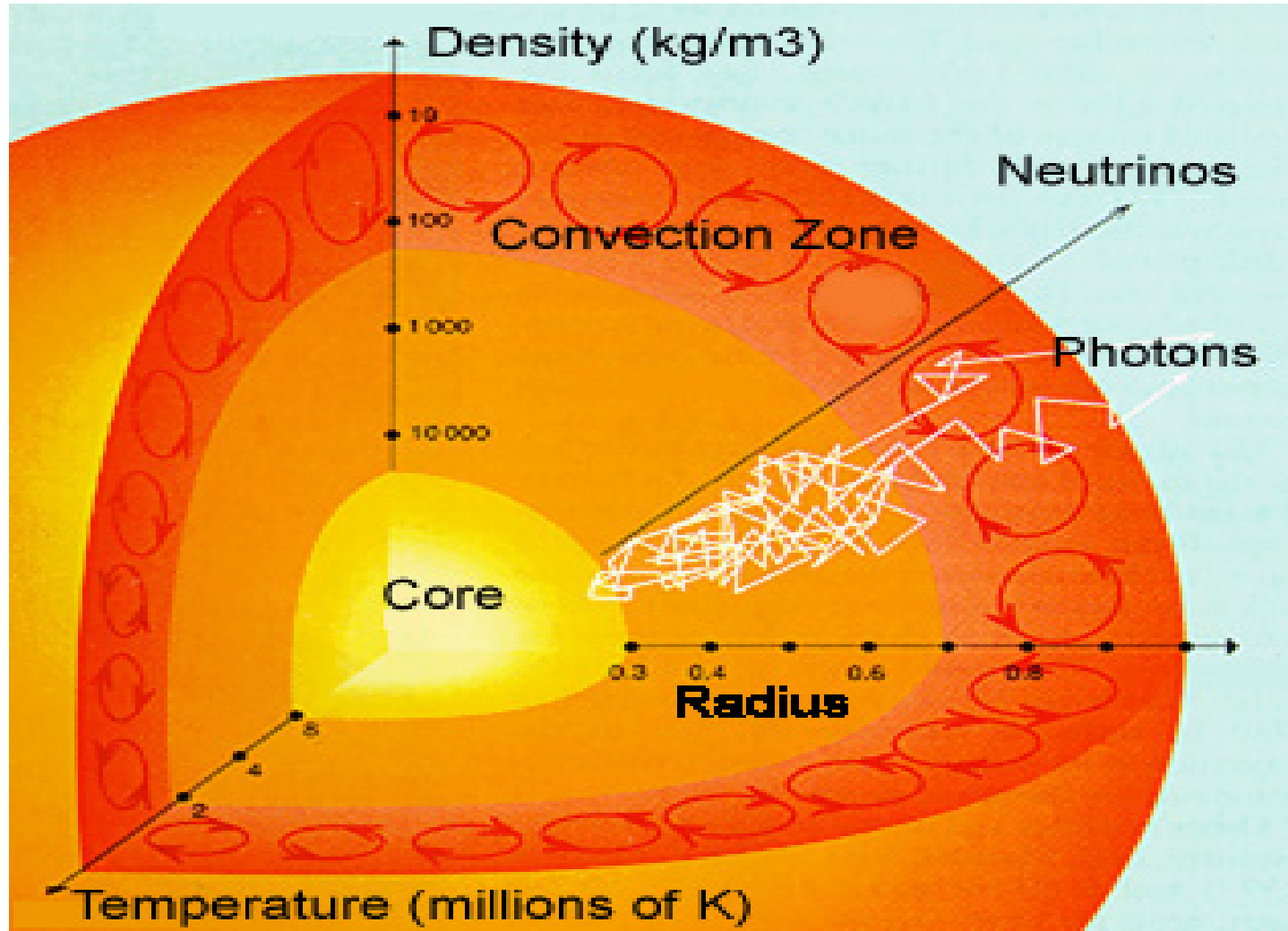
- **Opacity, a fundamental quantity for plasmas, determines radiation absorption and transport in plasmas**
- **Solar opacity: Study amount of radiation traveling out**
- **Microscopically opacity (κ) depends on**
i) photo-excitation (bound-bound transition)
ii) photoionization (bound-free transition)

DISCREPANCY IN SOLAR RADIATIVE AND CONVECTION ZONES BOUNDARY (R_{CZ})
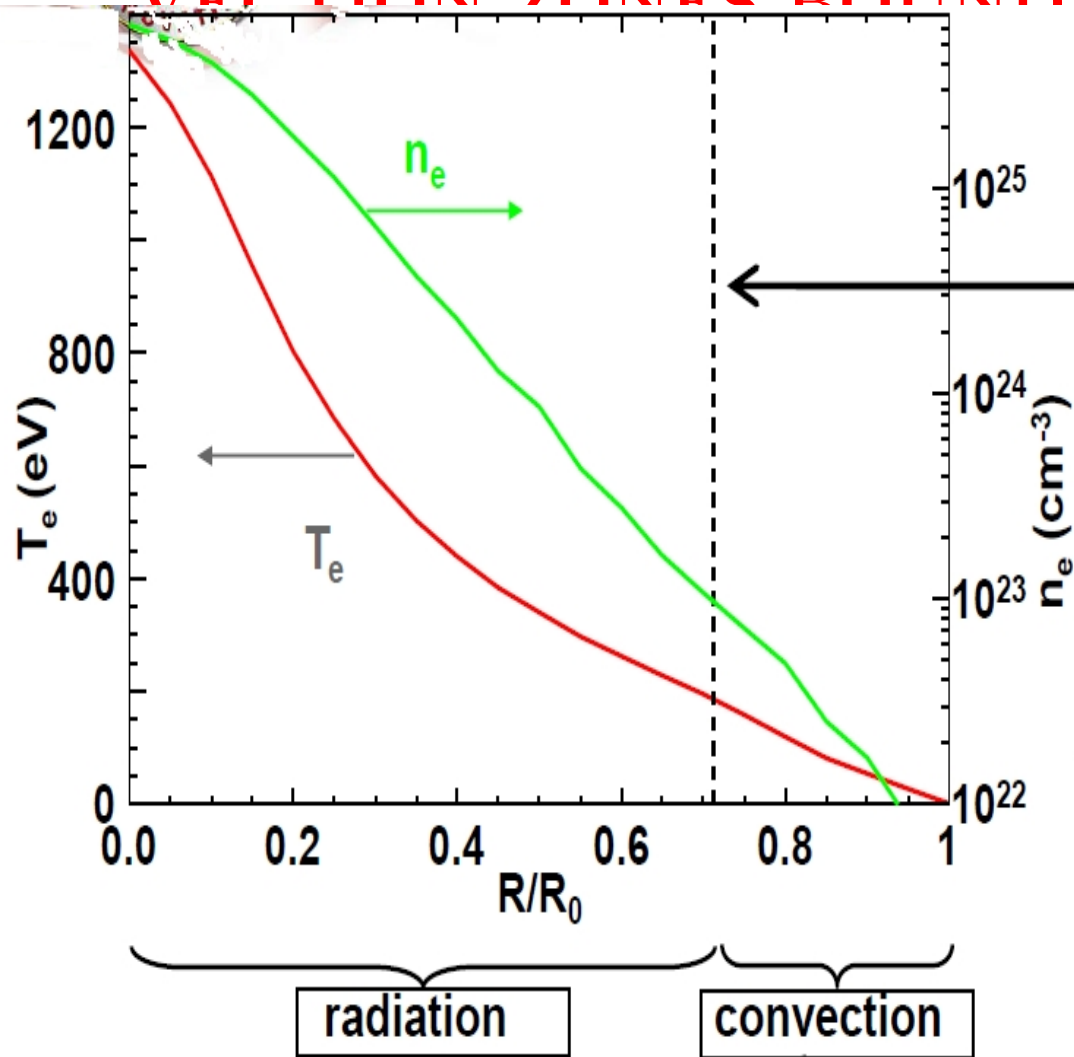
- measured boundary $R_{CZ} = 0.713 \pm 0.001$
- Predicted $R_{CZ} = 0.726$
- Thirteen σ difference

Bahcall et al, ApJ (2004)
Basu & Antia Physics Reports 2008

Asplund et al Ann Rev AA (2009)
Christensen-Dalsgaard et al A&A (2009)

• Calculated, using current atomic data, $R_{CZ} = 0.726$ - large (over 5600 mi difference) → changes solar structure
• Recent 3D model finds C, N & O, up to 40-50% lower
• Less elements, but increase in 10-15% opacity to resolve the discrepancy → MISSING PHYSICS

Z PINCH SET-UP, SANDIA NATL LAB

● Created plasma at T=190 eV ~ 2 MK, $\rho = 2.8 \times 10^{22}/\text{cm}^3$ at same condition as inside the Sun
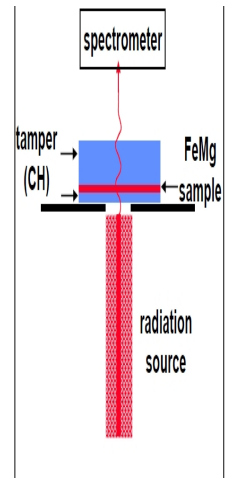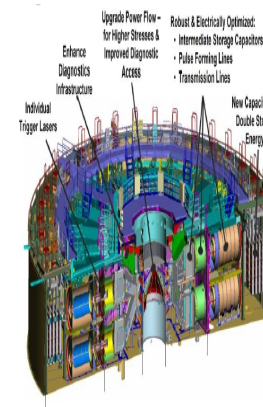
The 20million Amp current provided by the Z accelerator enables this research
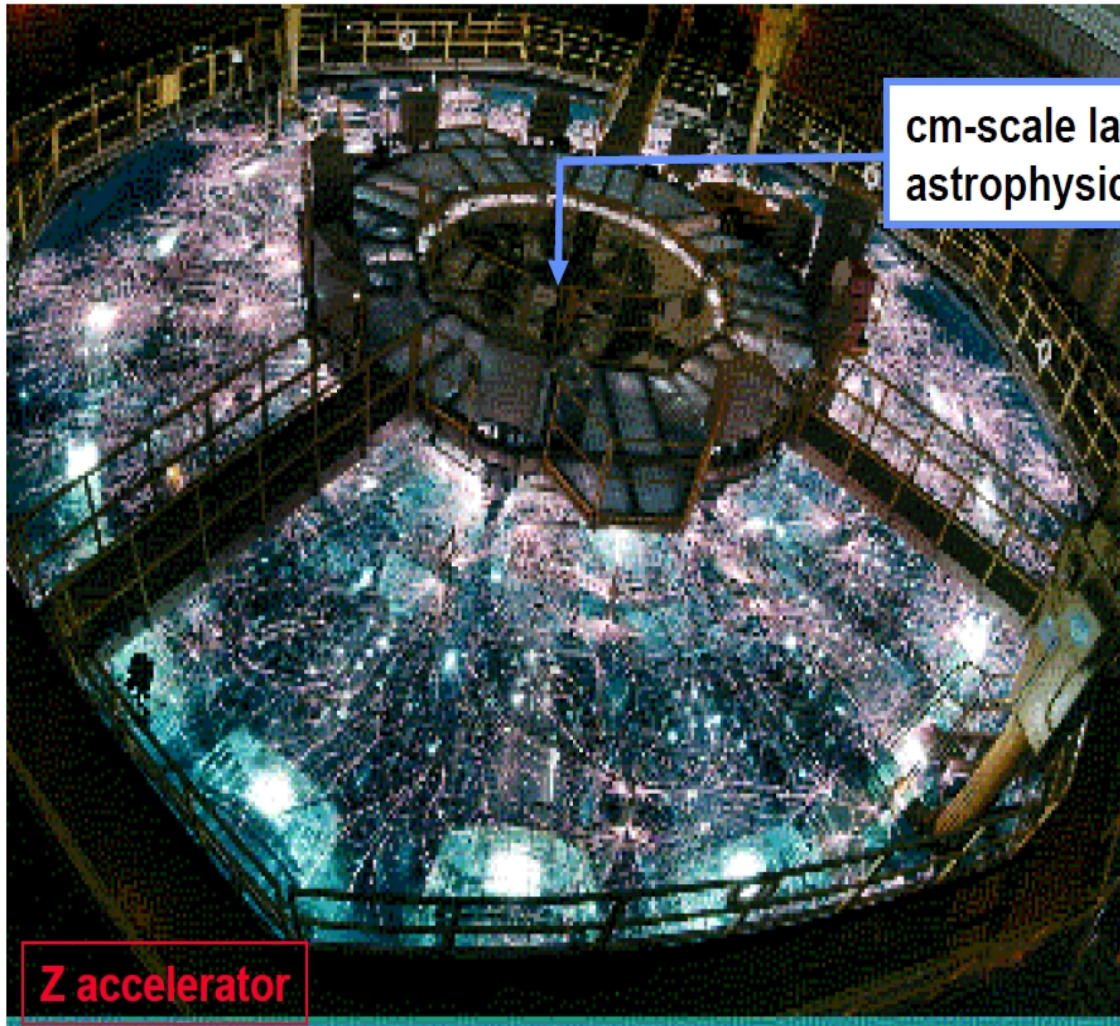
cm-scale laboratory astrophysics experiment

Z accelerator

40 m

spectrometer

tamper (CH)
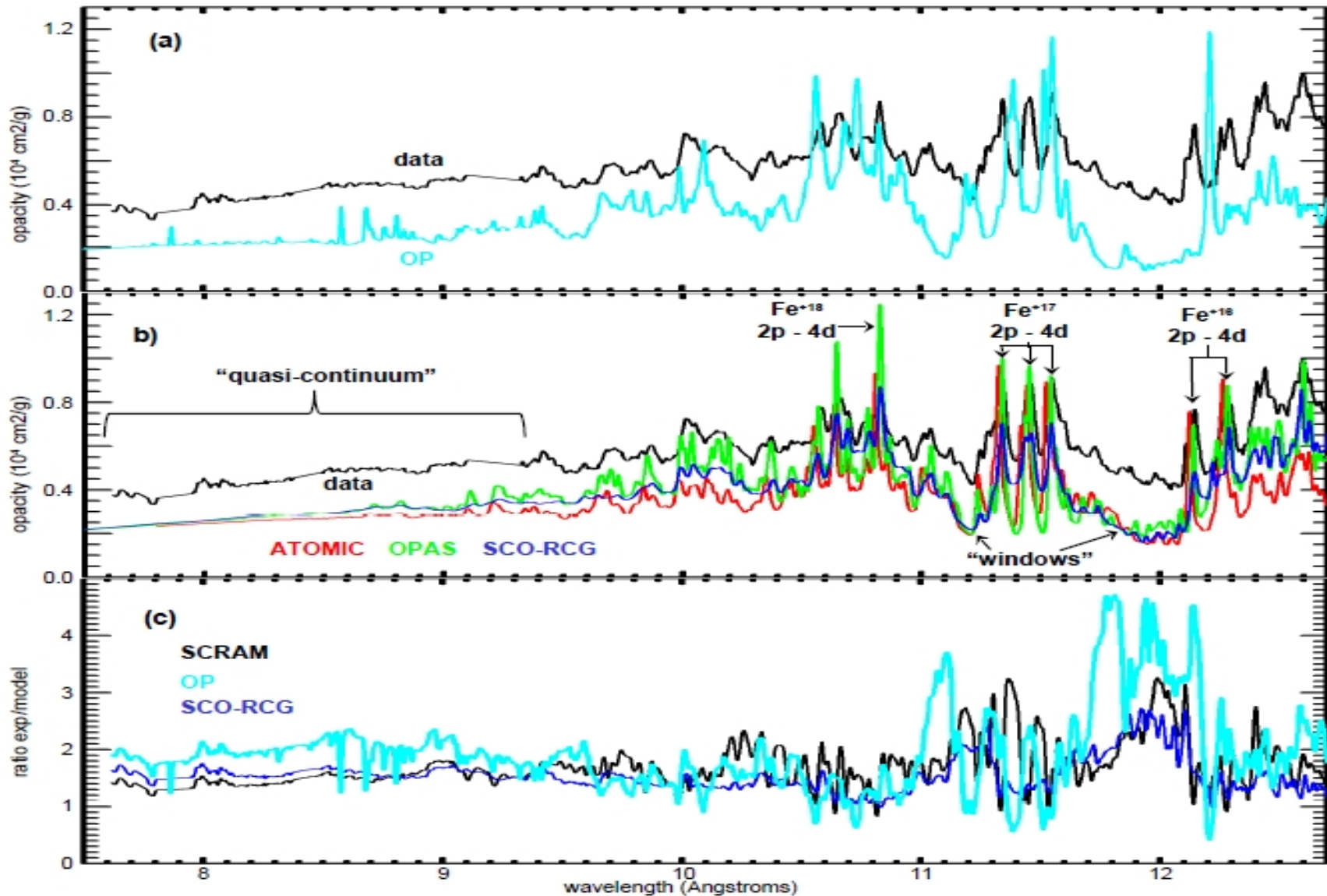
FeMg

sample

radiation source

New Z
The refurbished Z delivers 24 million Amps to the load
50% increase in electrical energy for present day experiments

New sample design
Increasing the rear tamper thickness delays expansion onset
This leads to higher density and higher temperature

COMPARISON OF IRON OPACITY: Experiment & Theory
## (Bailey et al, Nature Lett 2015)

- Present models use photoionization data - no resonances, except those in TOPbase database

Problems (theory): i) Deep windows, ii) lower background

COMPARISON: RESONANT EFFECT ON Fe XVII PHO-TOIONIZATION (Red - New, Blue - OP, Black - 2011):

<u>TOP:</u> a) Measured Fe opacity (Bailey et al 2015)

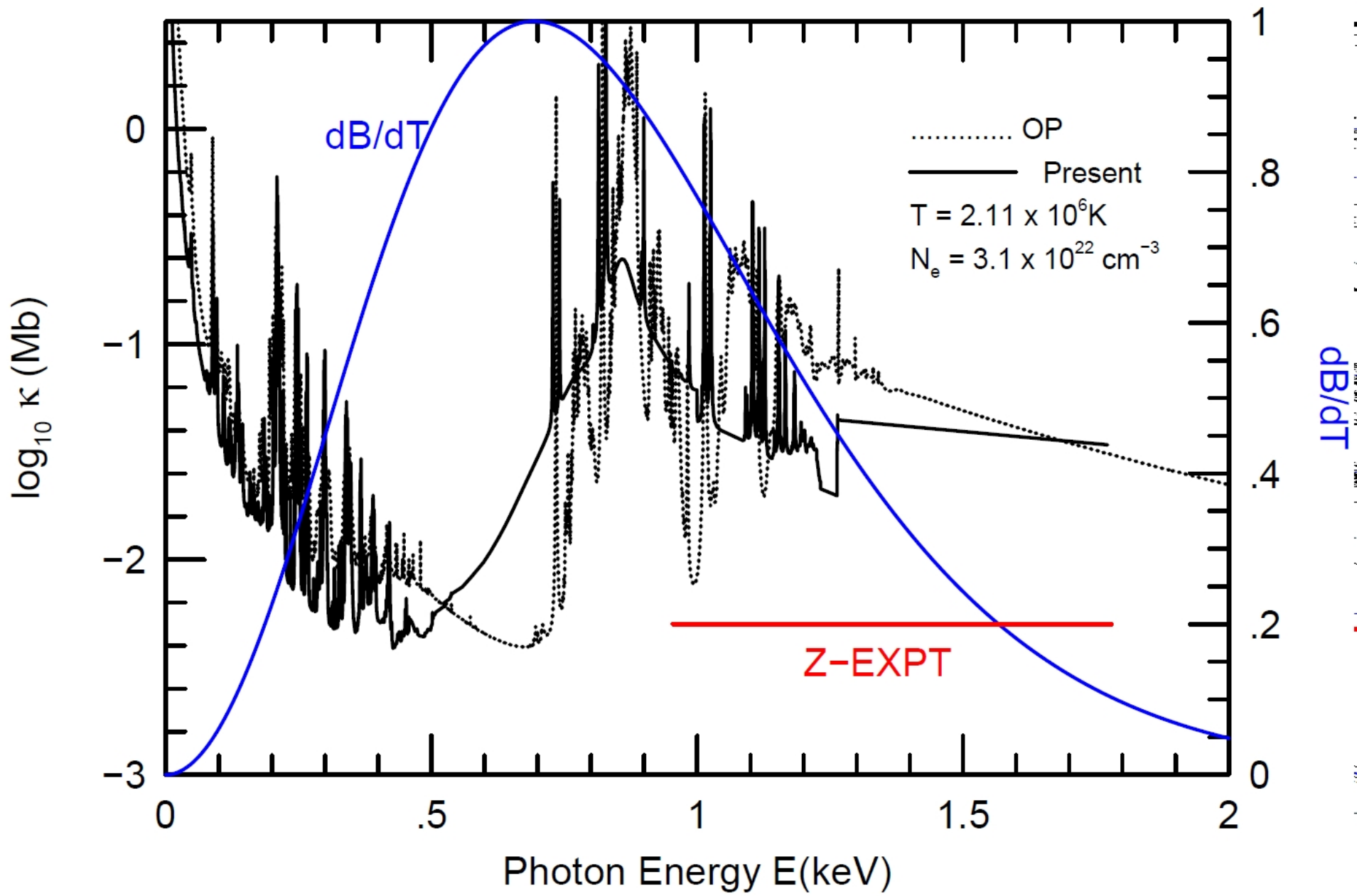<u>LOWER TWO:</u> Photoionization cross sections of Fe XVII (Nahar & Pradhan, Phys.Rev.Lett 2016)

Achieved: i) Resonant convergence, ii) κ_R increment by 35%
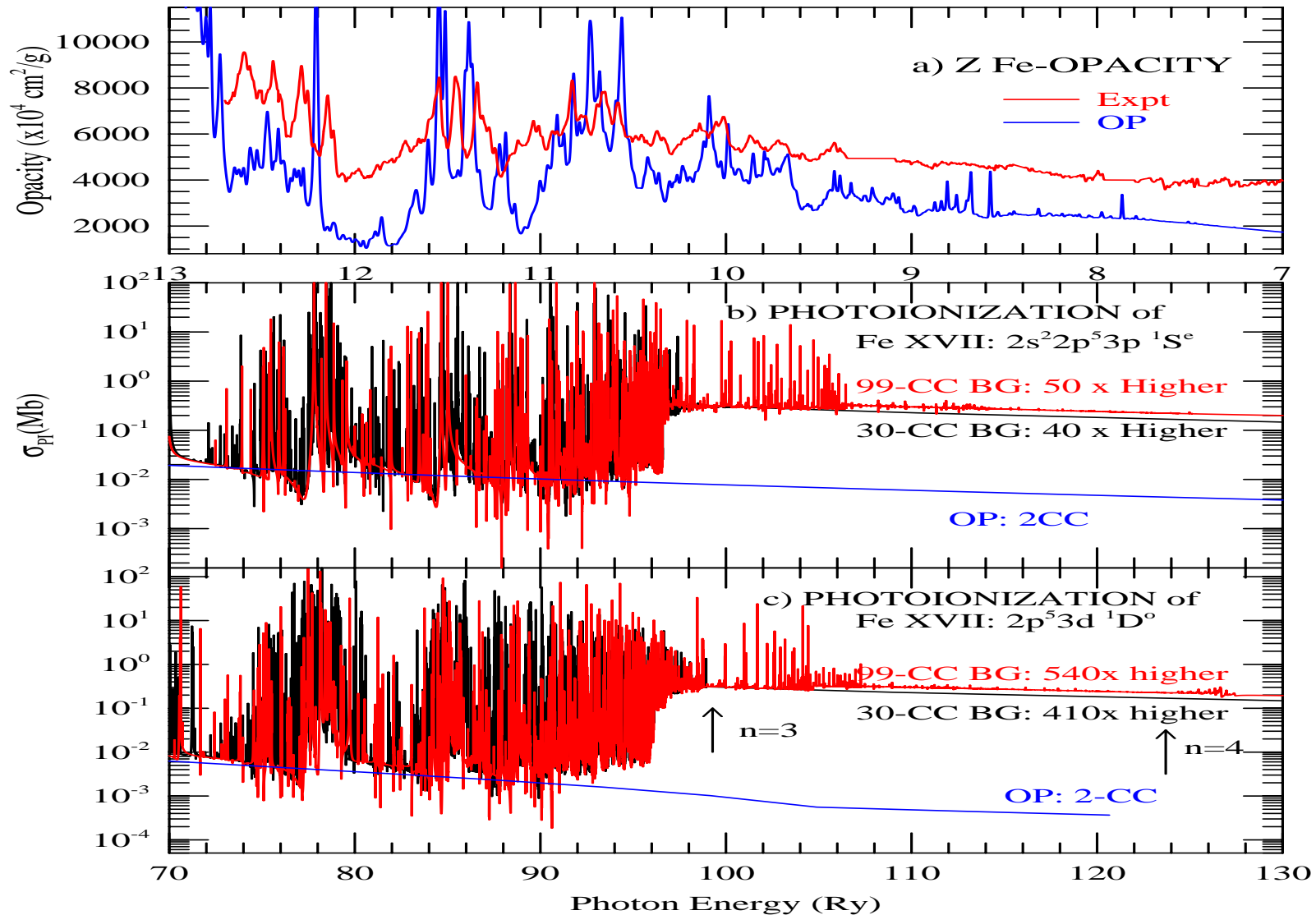
Fe XVII OPACITY SPECTRUM IN SOLAR INTERIOR

Latest Fe XVII spectrum (Pradhan, Nahar, Lianshui, Orban, Werner, in progress)
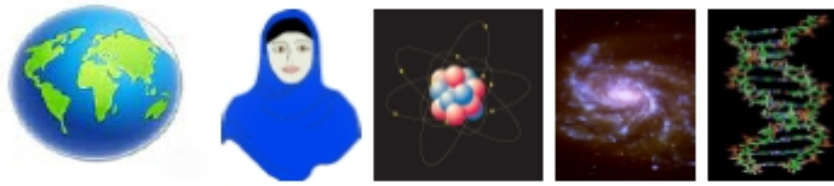
- Mean opacity increment by 35%

The OPACITY Project & The IRON Project

<u>AIM:</u> Accurate Study of Atoms & Ions, Applications to Astronomy

- International Collaborations: France, Germany, U.K., U.S., Venezuela, Canada, Belgium
- Earlier opacities were incorrect by factors of 2 to 5 $\rightarrow$ inaccurate stellar models $\rightarrow$ initiation of the Opacity Project in 1981
- **THE OPACITY PROJECT - OP (1981 - 2006):**
- Studied radiative atomic processes for (E, f, σ_{PI})
- Elements: H to Fe
- Calculated opacities of astrophysical plasmas

- **THE IRON PROJECT - IP (1993 -):** collisional & radiative processes of Fe & Fe peak elements
- **RMAX:** Under IP, study X-ray atomic astrophysics

- **Atomic & Opacity Databases (from OP & IP)**
- TOPbase (OP) at CDS: http://vizier.u-strasbg.fr/topbase/topbase.html
- TIPbase (IP) at CDS: http://cdsweb.u-strasbg.fr/tipbase/home.html
- OPserver for opacities at the OSC: http://opacities.osc.edu/
- Latest data at NORAD-Atomic-Data at OSU: http://norad.astronomy.ohio-state.edu

بسم الله الرحمن الرحيم

INTERNATIONAL SOCIETY OF MUSLIM WOMEN IN SCIENCE (ISMWS)

ISMWS CHARTER

Founder: Dr. Sultana N. Nahar
The Ohio State University, Columbus, Ohio, USA
April 19, 2010

- **AIM:** - encourage Muslim women in science profession, form a network for various support
- **Objective:** Stay in Science (basic or applied)
- **Motto:** Out of 24 hours a day, we keep some hours for our intellectual nourishment
- **Members:** Over 200 from 28 countries

Web: http://www.astronomy.ohio-state.edu/ ~nahar/ismws.html
For membership (free) - Email: nahar.1@osu.edu